This is to certify that the

dissertation entitled

ADHESION MECHANISMS OF POLYURETHANES
TO GLASS SURFACES

presented by

RAJ K. Agrawal

has been accepted towards fulfillment
of the requirements for

Ph.D. degree in Chemical Engineering

Laurence T. Drzal
Major professor

Date October 28, 1994

ADHESION MECHANISMS OF POLYURETHANES TO GLASS SURFACES

By

Raj K. Agrawal

A DISSERTATION

Submitted to
Michigan State University
in partial fulfillment of the requirements
for the degree of

DOCTOR OF PHILOSOPHY

Department of Chemical Engineering

1994

ABSTRACT

ADHESION MECHANISMS OF POLYURETHANES TO GLASS SURFACES

By

Raj K. Agrawal

Adhesion mechanisms of segmented polyurethanes to glass surfaces were investigated in this study. Polyurethanes were prepared from caprolactone based polyols and toluene diisocyanate with 1,4 butanediol as the chain extender. A model based on hard and soft segment miscibility was developed to predict phase separation in these polyurethanes. The model was compared with experimentally determined phase separation data from near-infrared, fourier transform infrared, differential scanning calorimetry, dynamic mechanical analysis, and mechanical characterizations.

Adhesion of various polyurethanes to glass surfaces was evaluated using "block-shear" adhesion test method. It was found that phase separation in polyurethanes significantly affects their adhesion. Polyurethanes with higher modulus showed better adhesion, but in polyurethanes with the same modulus, phase separated samples showed better adhesion than the phase mixed samples. Scanning electron microscopy and x-ray photoelectron spectroscopy of the fractured surfaces revealed the formation of a 20Å - 100Å thick interphase region. Composition and thickness of this interphase region was found to be dependent on the matrix phase separation. It was determined that phase separation in the matrix could cause preferential segregation of butanediol to the interphase region.

The possibility of chemical bonding between the polyurethanes and the glass surfaces was explored by making the glass surface chemically inert through methyltrimethoxy silane and trimethyl chlorosilane treatments. Chemical bonding was found not to be an important factor in glass/polyurethane adhesion. The effect of increased modulus of the BDO rich interphase region, due to BDO enrichment, was detected but was concluded to be a minor factor in adhesion of the phase-separated polyurethanes to glass.

The surface free energies of the various polyurethanes were evaluated using the molar parachors and contact angle measurements. The work of adhesion was calculated from the surface energetics and compared to the experimentally determined adhesion data. A linear correlation was found between the polar surface free energy (γ^P) of the polyurethanes and their adhesion values; adhesion being higher for higher γ^P polyurethanes.

An adhesion experiment with butanediol coated glass plaques and the various polyurethanes demonstrated that adhesion of these polyurethanes can be significantly improved by creating an interphase region rich in butanediol type species. Hydrogen bonding between the constituents of the interphase region and the glass surface was concluded to be the primary mechanism of adhesion. A model of the interphase region is proposed with various possible hydrogen bonding mechanisms.

To my parents

ACKNOWLEDGEMENTS

I would like to express my sincere appreciation to Dr. Lawrence T. Drzal for his guidance, support, encouragement and mentoring throughout this project. It has been a real pleasure to work with him and I have certainly learned a great deal during my past nine years of association with him.

I also wish to thank my fellow engineering students at the composite center past and present - Shri, Tesh, Javad, Brent, Ed, Sanjay, Murty, Venkat, Rik and many others for their assistance and friendship. In addition, I wish to thank Dan Hook, Henjen Ho, Brian Rook and Mike Rich for their help in equipment operation, experimental analysis as well as their friendship. I am thankful to the other members of my committee - Dr. J. Jackson, Dr. K. Jayaraman, Dr. R. Narayan, Dr. W. Mungall and Dr. A. Scranton for the time they dedicated to this dissertation. I am also thankful to Niall Lynam, Anoop Agrawal, Desaraju Varaprasad and Hamid Habibi, all of Donnelly Corporation, for their help, encouragement and thoughtful discussion throughout this project. I thank the Donnelly Corporation, the office of Naval Research and the Automotive Composites Consortium for supporting this work.

I thank my parents and family for their emotional and financial support and their never ending encouragement through out my educational career. Finally I thank my wife Sunita for her love, constant support, encouragement and help, without which I would not have been able to complete this work.

TABLE OF CONTENTS

LIST OF TABLES

LIST OF FIGURES

NOMENCLATURE

ADXPS	Angular dependent x-ray photoelectron spectroscopy
BDO	Butanediol
DABCO	1,4-diazabicyclo[1.1.1]octane
DBTDL	Dibutyl tin dilaurate
DETDA	Diethyl toluene diamine
DMA	Dynamic mechanical analyzer
DSC	Differential scanning calorimetry
E'	Elastic storage modulus
E"	Loss modulus
E_{coh}	Cohesive energy
e_{coh}	Cohesive energy density
EG	Ethylene glycol
ESCA	Electron spectroscopy for chemical analysis
F	Molar attraction constant
FTIR	Fourier transform infrared spectroscopy
IM	Injection molding
IMC	In-mold coating
M	Molecular weight
M_C	Molecular weight per cross-link
MDI	4,4'-diphenylmethane diisocyanate
N_H	Number of monomer units in the hard segment
N_s	Number of monomer units in the soft segment
NIR	Near-infrared spectroscopy
P_s	Molar parachor
PPO	Polypropylene oxide
PVC	Polyvinyl chloride
R	Universal gas constant
RIM	Reaction injection molding

RRIM	Reinforced reaction injection molding
SEM	Scanning electron microscope
SIMS	Secondary ion mass spectroscopy
SRIM	Structural reaction injection molding
T	Temperature
T_g	Glass transition temperature
TDI	Toluene diisocyanate
V	Molar volume
V_R	Reference volume
V_W	Van der Waals volume
WAXD	Wide angle x-ray diffraction
W_{adh}	Work of adhesion
W^P_{adh}	Polar work of adhesion
W^D_{adh}	Dispersive work of adhesion
XPS	X-ray photoelectron spectroscopy

GREEK SYMBOLS

γ	Surface free energy
γ^P	Polar surface free energy
γ^D	Dispersive surface free energy
γ_G	Surface free energy of glass
γ_H	Surface free energy of hard segment
γ_L	Surface free energy of liquid
γ_S	Surface free energy of soft segment
γ_U	Surface free energy of polyurethane
δ	Solubility parameter
δ_S	Solubility parameter of soft segment
δ_H	Solubility parameter of hard segment

θ	Contact angle
ρ	Specific gravity
χ	Interaction parameter
χ_C	Critical interaction parameter
χ_{HS}	Hard and soft segment interaction parameter
$\chi_{(\Delta S)}$	Interaction parameter due to entropy change

CHAPTER 1

INTRODUCTION AND BACKGROUND

Glass/polymer adhesion in general has become very important due to the popularity of glass fiber reinforced composite materials. Good adhesion between the polymer matrix and the glass reinforcement is shown to be an important factor in determining the overall mechanical properties of these composite materials (Dawson et al, 1982; Dau et al, 1989; Yang and Lee, 1987; Schwarz, 1979). Among the wide variety of polymers for composites manufacturing, polyurethanes are becoming increasingly important due to their fast molding cycles. Reinforced reaction injection molding (RRIM) and structural reaction injection molding (SRIM) of polyurethanes are widely used in the automotive industry to make body panels, fascias, bumper beams, etc. In addition to these, glass/polyurethane combinations can be found in a variety of applications such as reaction injection molded modular windows for automobiles, laminated windshields, and fiber optic cables. Also the use of polyurethane coating on the inside surface of windshields is being investigated for making these antilacerative. In all of these applications, good adhesion between the glass and the polyurethane is imperative for their viability and effectiveness.

1.1 BACKGROUND ON POLYURETHANES

Polyurethanes are commonly processed by liquid molding process such as reaction injection molding (RIM). The RIM process is quite different from the injection molding process commonly used for thermoplastics, and can have a significant effect on urethane

to glass adhesion. The RIM process, RIM urethane chemistry and encapsulated modular windows are discussed below.

1.1.1 Reaction Injection Molding (RIM)

RIM is a process for rapid production of complex polyurethane plastic parts from the combination and rapid reaction of low viscosity monomers and oligomers. These liquids are combined by impingement mixing just as they enter the mold. Mold pressures are very low. The solid polymer forms by cross-linking or phase separation and parts can often be demolded in less than one minute.

Figure 1.1 shows a schematic of a RIM machine. Two or more chemical streams flow at high pressures (around 2,000 psi) into a mixing chamber. In the mixhead the streams impinge at high velocity, mix, and begin to polymerize as they flow out into the mold cavity. Because the mixture is initially at a low viscosity, a lower pressure of around 50 psi is needed to fill the mold cavity.

The RIM process consists of eight unit operations which are illustrated in Figure 1.2. Supply tanks are used to store and blend components. They maintain the level in the conditioning tank in the machine. The conditioning tanks control temperature and degree of dispersion of the reactants by low pressure recirculation. An important step in RIM is high pressure metering of the reactants to the mixhead at sufficient flow rate for good mixing and at the proper ratio for complete polymerization. From the impingement chamber, the reacting mixture flows into the mold, filling it in typically less than five

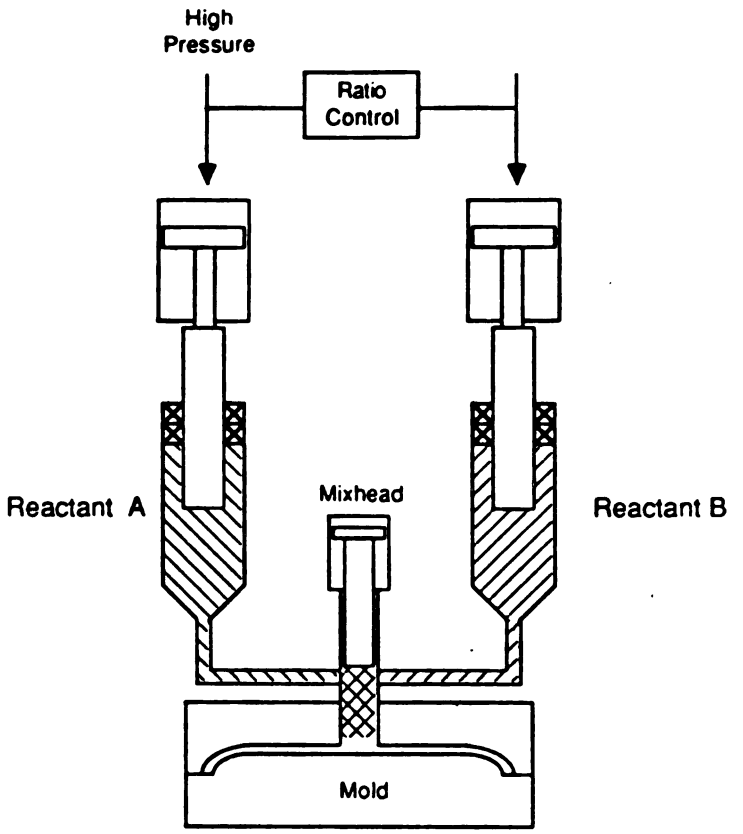

FIGURE 1.1 Schematic of a RIM Machine

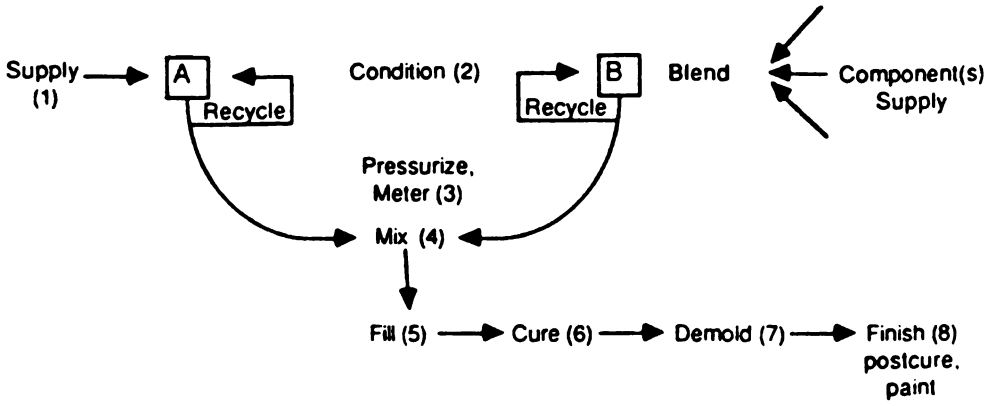

FIGURE 1.2 The Eight Unit Operations for RIM

seconds. There it polymerizes and solidifies sufficiently to take the stresses of demolding. The final operation consists of various finishing steps including trimming of flash and cleanings.

RIM has three processing characteristics which make it especially attractive for high-volume production of large parts. These are the low pressures required, the low processing temperatures involved, and the use of reactive liquid intermediates.

The RIM process requires material to be metered at around 2,000 psi. This pressure requirement is much lower than that involved in other high-volume plastic fabrication processes. For example, injection molding machines generate barrel pressures from 8,000-40,000 psi to force high viscosity resin into the mold. The low viscosity of the injected fluids in RIM make it possible to fill molds completely at pressures below 50 psi. This leads to much smaller and less expensive mold clamps for large parts.

Low viscosity and low pressure during filling also translates into lighter weight and lower cost molds. Complex shape parts with multiple inserts can readily be fabricated with the RIM process. The low viscosity involved in the process also opens many options for reinforcements. One is to place long fiber mats into the mold and then inject reactive monomers into them in a second step (Gonzalez and Macosko, 1983; Eckles and Wilkinson, 1986; Carleton et al, 1986). Thus RIM can be used for high-speed resin transfer molding. This process is generally called structural RIM (S-RIM).

RIM urethane systems are also filled/reinforced with glass for achieving high stiffness, low thermal expansion coefficient and better dimensional stability. In one approach, glass fillers (chopped glass, milled glass, and flake glass) are added to the reactants of the urethane formulation and the process is referred as reinforced RIM (R-RIM).

Temperatures utilized in RIM processing are also low when compared with thermoplastic injection molding process. In RIM urethane processing, the reactive liquid streams are maintained at temperatures between 75° and 140°F with specific temperature depending on the chemical stream being processed. The mold is kept at a temperature between 130° to 170°F. Since the urethane polymerization is highly exothermic, minimal heat input is required to maintain tooling temperature during production.

RIM's use of liquid intermediates has additional benefits beyond the low pressures and temperatures involved. A tremendous amount of design flexibility is possible with RIM. Since the mold is filled with a low viscosity liquid, very large parts with complex designs can be produced.

These process advantages have allowed the designer to take full advantage of the remarkable versatility that is possible with urethane chemistry. By selecting from a wide range of intermediates, the formulator can develop a polymer which will meet a specified set of physical property requirements (Gillis et al, 1983). The material can range from very flexible elastomers to very stiff plastic. It can be modified with a variety of

fillers/reinforcements. Since the intermediates are liquid, this compounding can be done economically in relatively small batches.

RIM has a relatively short history of about 20 years since their first major commercial use for producing automotive bumpers and fascias in flexible polyurethane in 1974. About 95% of all the RIM production is in polyurethanes or urethanes (Macosko, 1989). Several other chemical systems suitable for RIM process, for example, Nylon 6 (Hedrick et al, 1985) and dicyclopentadiene (Geer, 1983) are also currently in use.

1.1.2 RIM Urethane Chemistry

In the RIM urethane process, two chemical streams, one of diisocyanate and the other of polyol, are impingement mixed. Isocyanate reacts with polyol to form a urethane linkage.

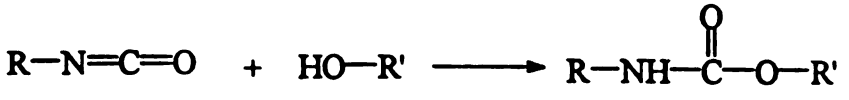

Several diisocyanates can be used to form the polyurethane elastomer, but the majority of RIM formulations are built on derivations of 4,4'-diphenylmethane diisocyanate (MDI).

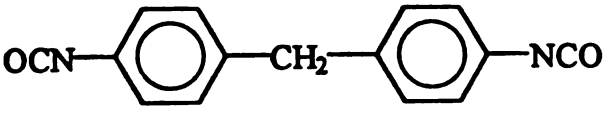

Popular derivatives include use of polymeric MDI and uretonimines.

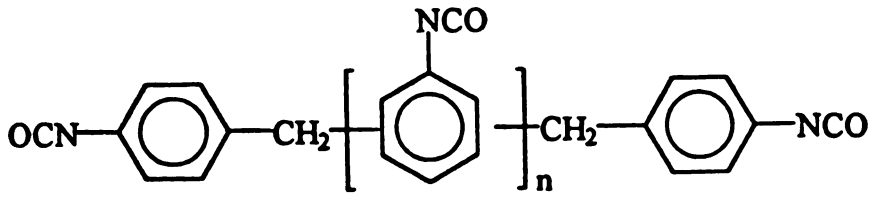

POLYMERIC MDI

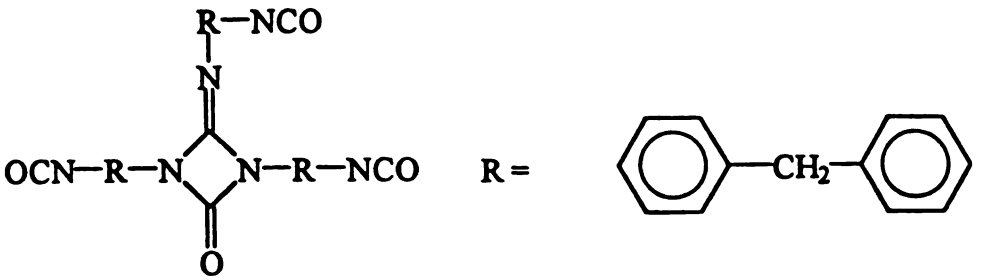

MONOMERIC URETONIMINE

Prepolymers obtained by the reaction of low molecular weight diols with excess MDI are also used in some urethane formulations.

The second chemical stream is of a hydroxyl terminated flexible chain oligomer. Most popular oligomers are based on polypropylene oxide (Speckhard and Cooper, 1986). Ethylene oxide capped, polypropylene oxide diols and triols with molecular weights between 3,000 and 7,000 are the main oligomers used today in RIM urethane formulations.

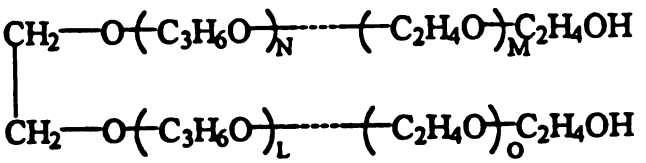

ETHYLENE OXIDE CAPPED POLYPROPYLENE OXIDE BASED POLYOL

The polyol stream also contains chain extenders, catalysts, and other additives such as fillers, pigments, surfactants, and internal mold release agents.

Chain extenders are added to form a segmented block copolymer (hard segment) when it reacts with diisocyanates. The most common chain extenders in use today are ethylene glycol and isomeric mixture of 2,4 and 2,6 diamine isomers of 3,5 diethyltoluene diamine (DETDA) (Pannone and Macosko, 1988).

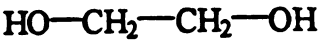

ETHYLENE GLYCOL

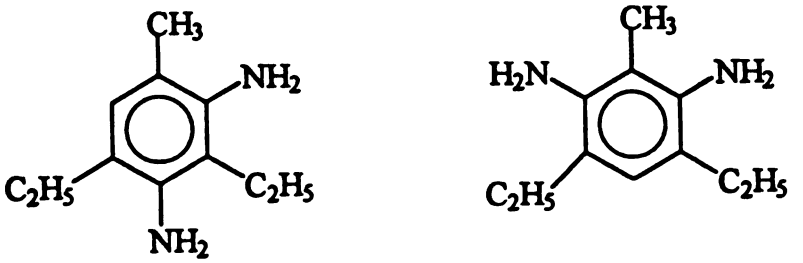

80% 20%

DIETHYLTOLUENE DIAMINE

Effective catalysts for isocyanate-hydroxyl RIM formulations are tertiary amine (Wongkamolsesh and Kresta, 1985) and tin catalysts (Camargo et al, 1985), and are used

in low concentrations (<1%) in the polyol stream. The two most commonly used tertiary amine and tin catalysts are 1,4-diazabicyclo-[1,1,1] octane (DABCO) and dibutyl tin dilaurate (DBTDL).

Nearly all RIM urethane systems build structure by phase separation rather than by cross linking (Gillis, 1982). Diisocyanate combines with the chain extender to form a hard block in the segmented copolymer which phase separates to build structure (Figure 1.3). The oligomer portion of a RIM formulation is called the soft segment because it typically has a low glass transition temperature.

There is extensive data (Saunders and Frisch, 1983) reported in the literature on final properties of segmented polyurethanes as a function of various formulation parameters. The formulation parameters which can affect phase separation of segmented polyurethanes include the chemical nature of the hard and soft segment, individual segment length and segment length distribution, intra- and interdomain hydrogen bonding, hard segment content, overall molecular weight, and molecular weight distribution, as well as the nature of the domain interface and the mixing of hard segments in the soft phase.

With hard segment content being the same, longer soft segment sequence length improves the degree of phase separation, hence increases the flexural modulus as shown in Figure 1.4 (Macosko, 1989). The reinforcing effect of the hard segment is also clearly demonstrated as the flexural modulus increases with hard segment content at a given soft segment molecular weight. Polyurethanes based on polyether polyol exhibit better low

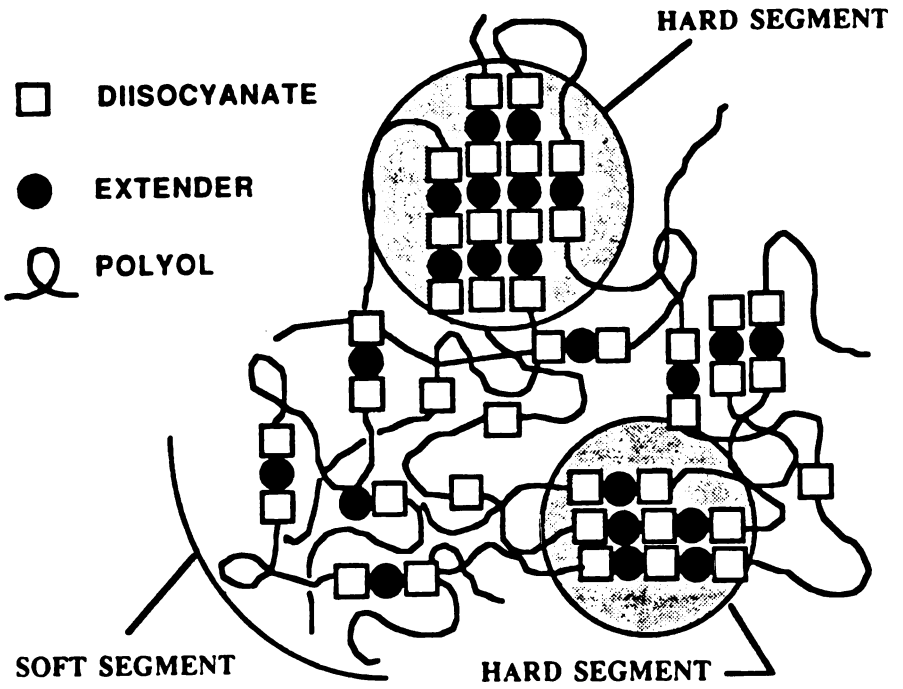

FIGURE 1.3 Schematic Representation of Phase Separation in Polyurethane Segmented Block Copolymers

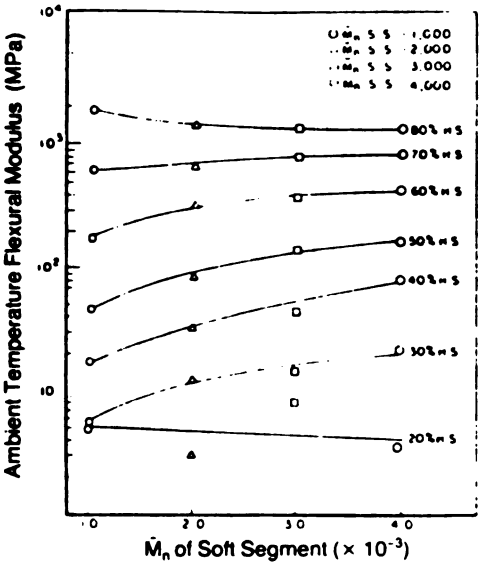

FIGURE 1.4 Flexural Modulus at 25°C vs. Soft Segment Molecular Weight and Hard Segment Content in Polyurethanes

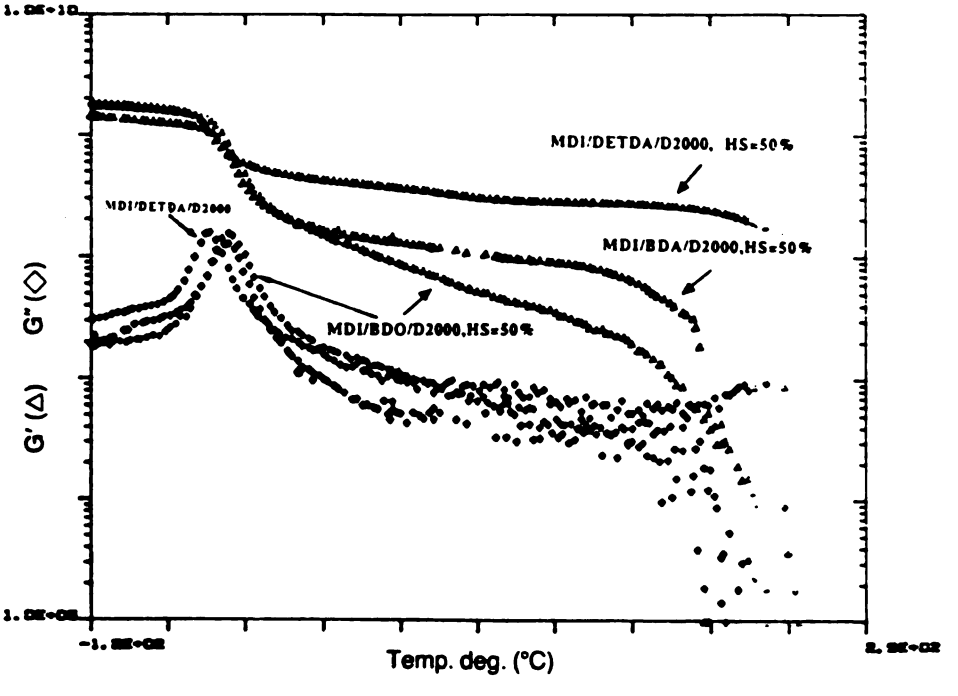

FIGURE 1.5 Dynamic Modulus vs. Temperature for Three Hard Segment Types All at 50% Hard Segment Content

temperature flexibility than the counterparts based on polyester polyol. This is attributed to less hydrogen bonding between the hard segment and the ether groups in polyether soft segment in contrast to the ester groups.

High modulus and low heat sag properties are often promoted by hard segment crystallinity and rigid bulky groups. Crystallization provides additional driving force for phase separation besides the thermodynamic incompatibility. In glycol extended polyurethanes, crystallinity is defined as an important mechanism for property development. Polymers with amorphous hard segments made of 2,4'-MDI and butanediol (BDO) shows extensive phase mixing and poor mechanical properties. Figure 1.5 (Macosko, 1989) shows the dynamic modulus vs. temperature data for typical glycol extended systems. The ethylene glycol extended system exhibits higher softening temperature and flatter rubbery plateau modulus than the BDO extended system. This is probably due to its higher hard segment transition temperature.

Figure 1.6 (Cornell et al, 1984) compares differential scanning calorimetry (DSC) curves for RIM systems containing different glycol chain extenders. The increasing hard segment melting point with decreasing glycol molecular weight is readily apparent.

Diamine chain extenders, even without the benefit of crystallinity, show improved properties over the glycol extended polyurethanes as demonstrated in Figure 1.5. Higher polarity difference between hard and soft segments and three dimensional hydrogen

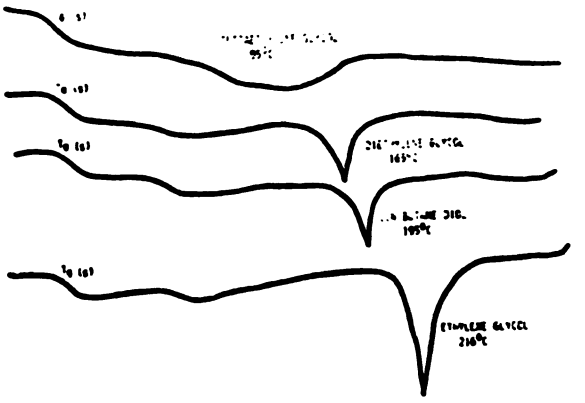

FIGURE 1.6 Differential Scanning Calorimetric Curves of Urethane Polymers Containing Various Glycols

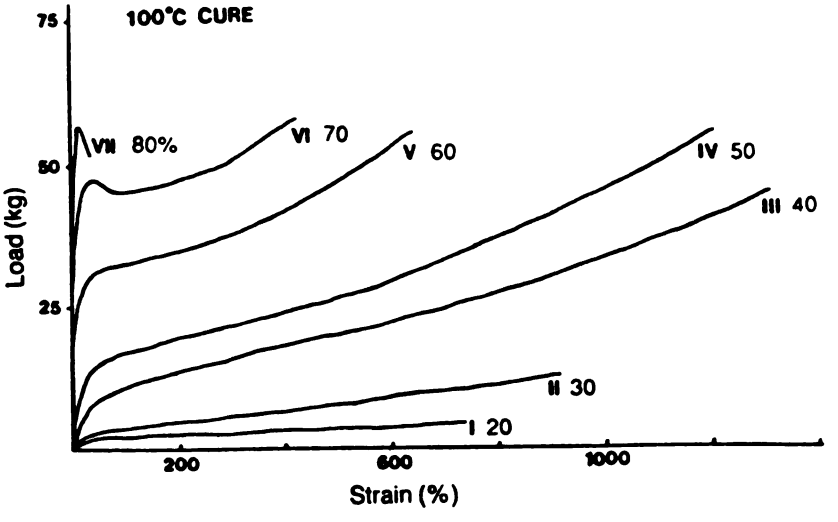

FIGURE 1.7 Load vs. Strain for Polyurethanes at Various % Hard Segment Content

bonding, made possible by the extra NH group in the urea linkage, have been proposed to account for the property improvement (Schwarz et al, 1979).

Figure 1.7 (Chang et al, 1982) shows how composition changes the stress-strain behavior of polyurethanes based on MDI/BDO/PPO-EO. With increasing hard segment content, the segmented polyurethanes exhibit a wide range of behavior, from a soft rubber at low hard segment content to a high modulus hard plastic at high hard segment content.

1.1.3 Modular Windows

Modular assemblies are widely used in the automotive industry. This concept involves supplying of modules or integrated subsystems to automobile manufacturers. A growing portion of rear quarter windows, windshields, and backlites are supplied as modules which can be directly attached to body sheet metal of an automobile. Figure 1.8 shows one such module.

The conventional gasketing technique of gluing or otherwise mechanically attaching an extruded elastomeric gasket to glass can no longer meet design and performance needs of today's automobiles with improved aerodynamics and better styling. In the modular approach, all the components required for fit and function of a window are supplied to automobile manufacturers as an integrated preassembly suitable for direct installation at the automobile production line. These components typically include glass, elastomeric gasketing material, tracks for sliding the window, and associated trims such as bezels, stud mounts, etc. The modular glass part is produced by placing the glass in a molding press

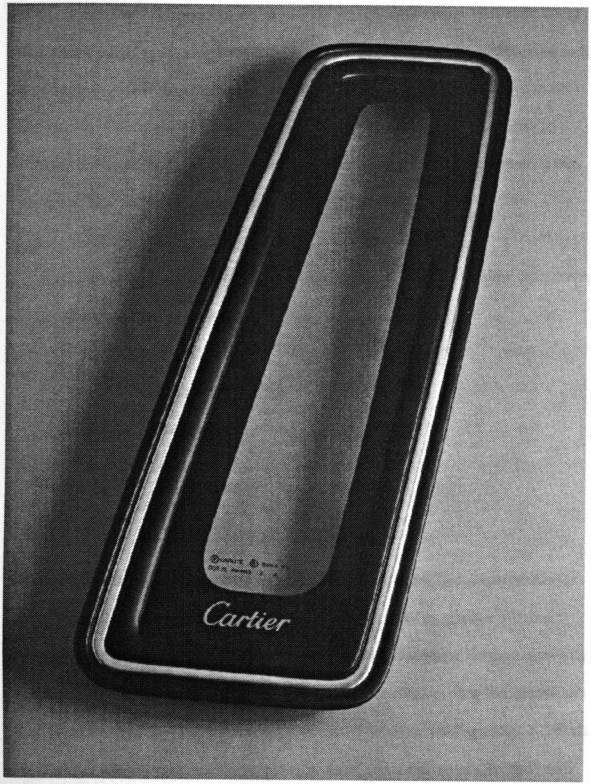

FIGURE 1.8 An Encapsulated Modular Window

and then injecting a polymeric gasketing material into the mold cavity. The mold cavity may contain clips, studs, and guides that are used to ultimately fasten the glass window to a frame of an automobile. These clips and studs get molded with the rest of the module and thus form a one-piece molded modular assembly. Modular glass is amenable to complex and curved glass shapes, variable gasket cross-sections, and incorporating trim materials. Some of the advantages in using modular glass are:

- Single source responsibility for quality and design changes
- Elimination of stack up of tolerances associated with various window components
- Reduced handling damages
- Less installation labor
- Less storage space
- Suitability for just-in-time inventory controls
- Robotic installation
- Drag and noise reduction in vehicles

The two primary modular window gasketing materials are plasticized polyvinylchloride (PVC) processed by injection molding and urethane processed by reaction injection molding (RIM) (Agrawal et al, 1991). PVC is the preferred material for fixed small side windows while RIM urethane is used for larger and more complex parts like windshields and backlites. The high melt viscosity of PVC during injection molding makes it difficult to fill larger window cavities. High molding pressure and temperature associated with PVC are known to cause excessive glass breakage and laminating material degradation in lower strength laminated windshields.

RIM urethane's low viscosity (~ 1 Poise) and low process temperature (-75°C) make it suitable for gasketing material in all types of modular windows. Urethanes for window encapsulation fall into two categories. Those based on aliphatic isocyanates are referred to as aliphatic urethanes whereas those based on aromatic isocyanates are referred to as aromatic urethanes.

Aliphatic urethane systems are inherently resistant to discoloration from solar weathering whereas aromatic urethanes are not. Due to cost and toxicity concerns, most RIM encapsulated modular windows use aromatic urethanes based on 4,4'-diphenylmethane diisocyanate (MDI) and are required to be painted to maintain weatherability. Painting of urethane surfaces can be done either in an in-mold coating (IMC) process (Agrawal, Fox and Lynam, 1991) or by painting after the molding operation. In the IMC process, a coating material is applied onto Class "A" surfaces of a mold. Upon injection of urethane into the mold, the coating bonds to the freshly formed urethane surface, detaches from the mold and becomes an integral part of the encapsulant.

Adhesion between the polymeric gasket and the glass panel is crucial for a modular window to function. Adhesion between the gasket and the glass ensures glass retention in an automobile, avoids water leakage and maintains structural integrity of the window in the long-term use. Neither PVC nor RIM urethane adhere well to the glass panel by itself. Adhesion promoters are applied to the glass perimeter prior to encapsulation for promoting adhesion of gasketing materials.

1.2 BACKGROUND ON ADHESION

There are several theories of adhesion between two dissimilar substrates. According to Kinloch (Kinloch, 1987), these theories can be categorized as follows:

(a) Mechanical Interlocking

(b) Diffusion Theory

(c) Electronic Theory

(d) Adsorption Theory

The mechanical interlocking, as the name implies, proposes that mechanical keying, or interlocking, of one substrate into the irregularities of the other substrate surface is the major source of intrinsic adhesion. The diffusion theory states that the intrinsic adhesion of polymers to themselves and to each other is due to mutual diffusion of polymer molecules across the interface. The electronic theory of adhesion suggests that electrostatic forces arising from contact of two dissimilar substrates (due to electron transfer) may contribute significantly to the intrinsic adhesion. The adsorption theory proposes that, provided sufficiently intimate molecular contact is achieved at the interface, the materials will adhere because of the interactomic and intermolecular forces which are established between the atoms and molecules in the surfaces of the substrates. Interactions that are reversible, such as Van der Waals forces and hydrogen bonding, or irreversible, such as ionic, covalent, and metallic bond formation may contribute to the overall adhesion.

The adsorption theory is the most widely applicable and accepted among all the theories. For glass/polymer systems, adsorption theory has been successfully used to explain the adhesion phenomena. Polyurethanes in general exhibit good adhesion with glass due to several factors including their polar nature, surface wetting properties and chemical reactivity with a variety of functional groups (Hepburn, 1991). It is generally accepted that the surface of glass is covered by silanol groups (Si-OH) as a result of interactions with the atmosphere (Mohai et al, 1990; Markus et al, 1981; Vaughan et al, 1974). It is quite conceivable that reaction of these silanol groups with the isocyanates present in the urethane formulation could account for the adhesion levels achieved between the glass/polyurethane systems.

Adhesion promoters such as coupling agents are commonly used in glass/polymer systems to improve adhesion and increase environmental stability of the bond. Silane based coupling agents are the most widely used adhesion promoters for glass/polymer systems. The structure of such silanes may be represented by the general structure Y $(CH_2)_nSiX_3$, where n = 0 to 3, Y is an organofunctional group usually selected for reactivity with a given matrix and X is a hydrolyzable group on silicon (Plueddemann, 1991). Several researchers have studied bonding mechanisms of silane coupling agents to glass surfaces. Garbassi et al and Vaughan et al have used surface analysis techniques such a x-ray photoelectron spectroscopy to study the bonding mechanisms (Garbassi et al, 1987; Vaughan et al, 1974). It is generally accepted that the mechanism of adhesion is through the formation of covalent bond across the interface. Koenig et al (Koenig et al, 1971) using Laser Raman spectroscopy and Chiang et al (Chiang et al, 1980) using fourier

transform infrared spectroscopy have clearly established the presence of Si-O-Si bonding across glass/silane interface. Shown below is an idealized monolayer of bonded silane coupling agent on glass surface.

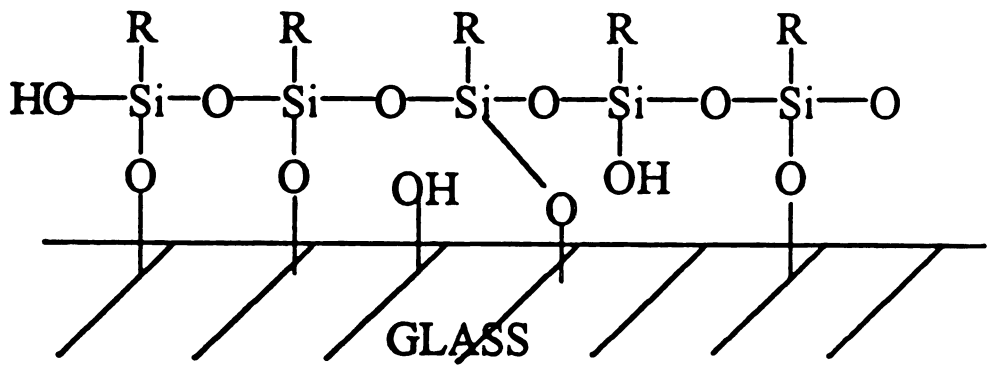

For the coupling agent/polymer matrix interface, the reaction of organofunctional group 'Y' with the matrix is believed to be a key mechanism of adhesion. It has been suggested, however, that at this interface, some form of interpenetrating network structure might well be formed instead of a simple covalent bond (Kinloch, 1987).

In glass/polyurethane systems, the most commonly used silane coupling agent is aminosilane due to the possible reaction of the amine functionality with the isocyanates present in the urethane formulation. A common aminosilane is aminopropyl triethoxysilane $H_2NCH_2CH_2CH_2Si\ (OC_2H_5)_3$.

Aminosilanes have been used in fiber sizing compositions to improve adhesion of glass fibers to urethane matrices (McWilliams et al, 1974). Drown et al (Drown et al, 1991) have studied the role of various glass fiber sizings on fiber/matrix adhesions. Aminosilane based sizings in RRIM urethanes have been studied by several researchers (Galli, 1982; Otaigbe, 1992) and been found to be very important for tensile and other mechanical properties of the resultant composites. Damani and Lee (Damani and Lee, 1990) have studied glass fiber/polyurethane interphase using single fiber fragmentation test (Broutman, 1969). They have found the fiber sizing to be an effective tool for improving chemical interaction during the interphase formation and for improving the overall adhesion of the matrix to the fibers.

CHAPTER 2

PROJECT DESCRIPTION

When urethane constituents are brought in contact with glass surfaces, its adhesion will be influenced by many factors, physical and chemical in nature. The physical interactions are caused by Van der Waals forces which can be attributed to different effects:

(a) dispersion forces arising from internal electron motions which are independent of dipole moments and

(b) polar forces arising from the orientation of permanent electric dipoles and the induction effect of permanent dipoles on polarizable molecules.

The dispersion forces are usually weaker than the polar forces but they are universal and all materials exhibit them. Another type of force that may operate is the hydrogen bond, formed as a result of the attraction between a hydrogen atom and a second, small and strongly electronegative atom such as oxygen, nitrogen, fluorine or chlorine.

Thermodynamics is a very useful way of describing and quantifying some of these physical interactions. The surface-free energy (γ) or surface tension is a fundamental parameter which can describe the interactions of liquids with other phases. In the case of a liquid drop resting on a solid surface, γ_{sv} is a force per unit length acting on the surface of a solid in equilibrium with the liquid vapor. The molecules at the surface of a liquid are subject to very different forces than molecules in the bulk liquid. For the liquid vapor interface, molecules in the bulk have the same environment in each direction. Long

distance attractive forces and short distance repulsive forces cause the molecules to maintain an intermediate spacing. Molecules on the surface have weaker interactions with the vapor phase but strong interactions with other liquid molecules. These strong forces pull the surface molecules toward the liquid phase, so they oppose spreading.

Figure 2.1 shows the vectors which represent the forces acting at the boundary between a solid (S), liquid (L), and vapor (V). The equilibrium interactions in terms of surface tensions are represented by the Young equation:

$$\gamma_{SV} - \gamma_{SL} = \gamma_{SL} \cos \theta \qquad (2.1)$$

The Young equation allows determination of information about the solid surface from knowledge of the liquid-vapor surface tension and the measured contact angle.

The chemical interactions can lead to chemical bond formation across the interface. In glass/polyurethane system, such chemical bonds may include covalent and ionic bonds.

These physical and chemical interactions along with glass surface roughness and porosity have been shown to create an interphase region in polymeric composites (Drzal, 1983; Verpoest et al, 1988) as illustrated schematically in Figure 2.2. The interphase region is defined as the region that is formed as a result of the bonding between the fiber and matrix; it has a significantly distinct morphology or chemical composition as compared to the bulk fiber or the bulk matrix. The interphase may be a diffusion zone, a nucleation zone, a chemical reaction zone, and so forth, or any combination of the above (Swain et al, 1990).

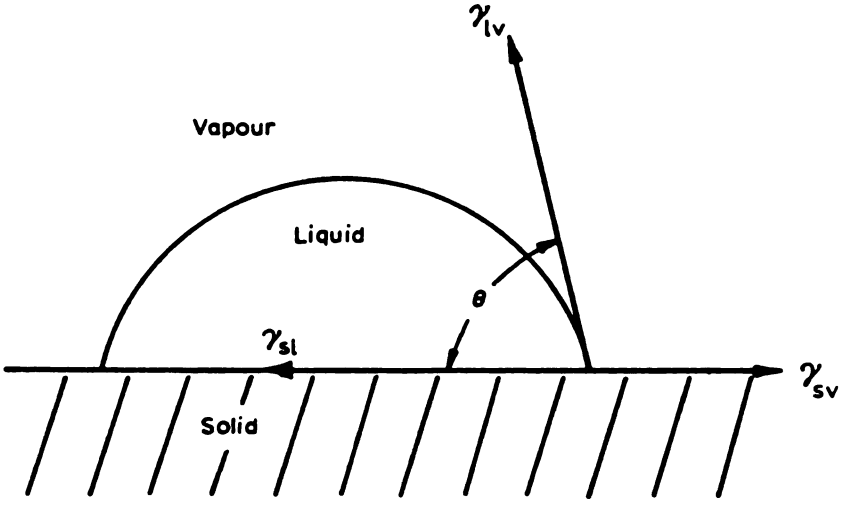

FIGURE 2.1 A Liquid Drop Resting at Equilibrium on a Solid Surface

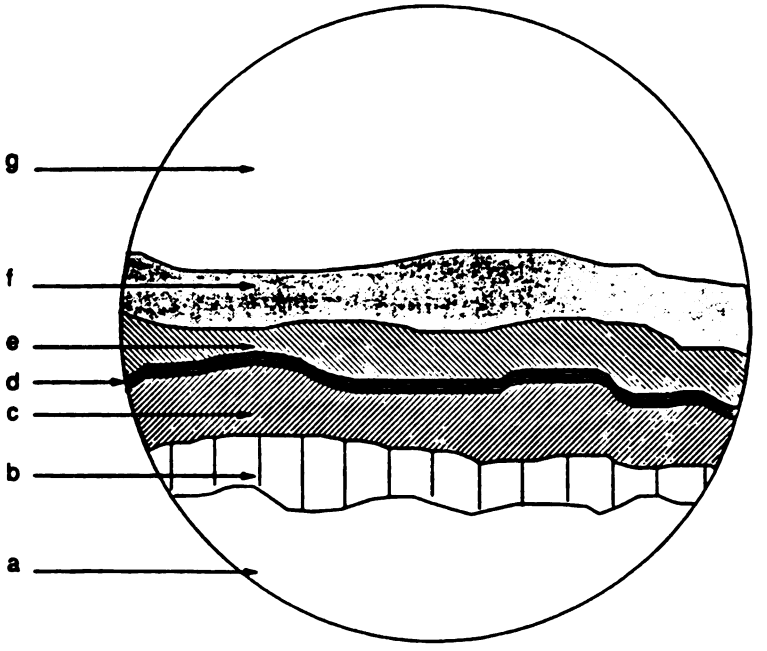

a. The bulk fiber
b. A fiber surface layer possessing a different microstructure or chemical composition compared to the bulk fiber.
c. An outer fiber layer altered by fiber surface treatments
d. A layer in which the fibers bond to the sizing
e. A sizing or coupling agent layer
f. A layer, in which the matrix microstructure or chemical composition or both gradually changes from that of the sizing to that of the bulk matrix
g. The bulk matrix

FIGURE 2.2 Schematic Representation of Interphase Region in a Polymeric Composite

The characteristics of this interphase region have been shown to depend on several factors including the composition of the matrix, surface chemistry of glass and processing variables including cure time, temperature and pressure. The thickness of this region can extend from a few to a few hundred nanometers. A multicomponent interphase has a complex microstructure or chemical composition or both and can have significant effects on the physical and thermomechanical properties of the composite.

In comparison to other polymers used in composites such as epoxies, which have single phase morphology, polyurethanes in general are phase separated systems with multiphase morphology. The hard and soft segments in polyurethanes phase separate into hard and soft domains. Figure 2.3 is a transmission electron micrograph of a polyurethane sample showing hard and soft domains (Oertel, 1993).

Polyurethanes build their structure from phase separation. The hard segment domains act as internal reinforcements in the matrix. A majority of the mechanical properties in segmented polyurethanes depend on the phase separation.

The phase separation in the bulk of the polyurethane matrix can have a significant influence on its interphase region with glass surfaces. A number of studies have shown that the surface of polyether based urethanes can exhibit an enrichment of polyether compared to the bulk (Yoon and Ratner, 1988; Hearn et al, 1988). Hearn et al have studied a cast urethane surface using secondary ion mass spectroscopy (SIMS) and x-ray photoelectron spectroscopy (XPS). They have reported that the surface of segmented

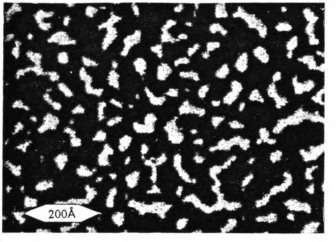

FIGURE 2.3 A Transmission Electron Micrograph of a Segmented Polyurethane

polyurethane was enriched in polyether (soft segment). The surface layer of polyether was not pure but was interdispersed (in the upper 10Å-15Å) with small quantities of hard segments. Recently, Deng and Schreiber (Deng and Schreiber, 1991) have discussed orientation phenomena at polyurethane surfaces when brought into contact with different media. Yoon and Ratner (Yoon and Ratner, 1986) have related the phase separation to its surface composition and found that where significant phase separation takes place, little or no hard segment could be found in the outermost few molecular layers of the polymers.

In addition to the phase separation, the reaction kinetics between isocyanate and polyol, and especially in a RIM urethane system, is very fast and complex. The relative reactivity of phenyl isocyanate with various active hydrogen compounds is shown in Table 2.1 (Macosko, 1989). In addition to the isocyanate-hydroxyl reaction, isoyanates can react with themselves to undergo dimerization or trimerization, or can react with urethane and urea linkages to form allophanate and biuret linkages respectively.

The isocyanates in polyurethanes can also react with the active hydrogen species present on the glass surface. The glass surfaces are usually found to be hydrated due to adsorption of water vapors. It has also been suggested (Pantano, 1981) that $NaHCO_3$ type species may be present on the surface due to adsorption of carbonaceous species from the atmosphere. The surface of soda-lime glass has also been shown to be rich in Na^+ ions relative to the bulk. Many possible reactions of urethanes with these surface active species could lead to covalent and ionic bond formations.

TABLE 2.1

Relative Reactivity of Phenyl Isocyanate with Various Active Hydrogen Compounds

		Time in s to 25% conversion
butylcarbanilate (forms allophanate)	$CH_3(CH_2)_3$-O-CO-NH-C_6H_5	3×10^5
diphenyl urea forms biuret)	C_6H_5-NH-CO-NH-C_6H_5	1800
water	H_2O	450
2-butanol	$CH_3CH\ OH\ CH_2\ CH_3$	300
1-butanol	$HO(CH_2)_3CH_3$	92
1-butanol + 0.1 mol% dibutyltin dilaurate (DBTDL)		25
1-butanol + 2 mol% DBTDL		6.5
1-butanol + 2 mol% 1,4-diazabicyclo (2,2,2) octane (DABCO)		56
1-butanol + 0.2 DABCO + 0.1 DBTDL		~10
o-toluidine	H_2N-$C_6H_4(CH_3)$	19
o-toluidine + 2 mol% DABCO		7.5
aliphatic amine	$H_2N[CH(CH_3)CH_2$ - $O]_nCH_2CH_3$	$\sim 10^{-3}$

The fast and complex reaction kinetics in polyurethane systems, the phase separation kinetics, the multiphase morphology, and the possibility of numerous physical and chemical interactions with the glass surface make the glass/polyurethane adhesion study a complicated and challenging phenomenon.

2.1 PROBLEM DEFINITION

There is extensive data reported in literature related to the adhesion of polymeric materials to glass. But the majority of the work reported is limited to homopolymers (e.g., polyolefins) or single phase morphology polymer systems (e.g., epoxies, polyesters, etc.) The small amount of work done related to polyurethane/glass adhesion (see Chapter 1) is either empirical in nature or is an extrapolation of the findings based on homopolymers or single phase materials. As explained earlier in this chapter, polyurethanes, in the majority of instances, are multiphase copolymers commonly processed through reaction injection molding. In contrast to homopolymers or single phase materials, polyurethanes undergo extremely fast and complex reaction kinetics coupled with phase separation and morphology development. All of these factors can significantly influence structure/ morphology, physical, mechanical and chemical properties of a glass/ polyurethane interphase region.

This study is an attempt to use the existing literatures on structure/property relationships in polyurethanes and the surface chemistry of glass, and couple that with the understanding of adhesion of homopolymers or single phase materials, to develop a thorough understanding of polyurethane to glass adhesion. The objective of this research

is to identify and study interfacial phenomena related to adhesion mechanisms of polyurethane to glass.

The focus of this research is around the interphase between a polyurethane matrix and a glass substrate. The characterization for structure/morphology, physical, mechanical and chemical properties of the interphase region are the subject of this work. The factors controlling the interphase region such as matrix chemistry, its properties, phase separation and glass chemistry are studied in detail in order to develop theoretical models supported with experimental results to further the understanding of adhesion mechanisms. Various adhesion theories are explored to determine the important adhesion mechanisms acting at the glass/polyurethane interphase.

The experimental and theoretical work in this thesis is organized mainly in three chapters, 3, 4, and 5. Each of these chapters is self-contained in that there is an introduction section to overview the pertinent literature, an experimental section, a results and discussion section, and finally, a conclusions section.

The glass surface chosen for this study is soda-lime float glass due to its wide use and availability in plate form. The main constituents in a soda-lime float glass are Na_2O:CaO:$6SiO_2$. There may also be small amounts of Al_2O_3, MgO, BaO, B_2O_3, and TiO_2. Typical soda-lime float glass compositions are shown in Table 2.2 (Uhlmann and Kreidl, 1983). There are two sides to a soda-lime float glass, the tin side and the air side. The air side is used in this study for adhesion testing.

TABLE 2.2

Typical Compositions of Soda-Lime Glass (Wt. %)

	1972	1977	VARIATION
SiO_2	72.19	72.15	66.2 - 74.7
Al_2O_3	1.81	2.13	1.25 - 2.5
Fe_2O_3	0.12	0.11	0.07 - 0.18
CaO	9.55	10.66	9.16 - 13.40
MgO	1.51	0.91	0.55 - 1.91
BaO	0.17	0.08	0.0 - 0.47
Na_2O	13.96	13.83	12.88 - 17.30
K_2O	0.59	0.57	0.40 - 0.85
SO_3	0.16	0.14	0.08 - 0.22

The urethane matrix developed for this study is transparent. The polyol used is a caprolactone based triol available from Union Carbide under the trade name "Tone". The diisocyanate used is toluene diisocyanate selected for its asymmetry and the chain extender used is butanediol. The chemical structures of all these constituents are shown in Figure 2.4.

The third chapter is focused on developing model urethane matrix systems, developing adhesion testing methodology, building structure-property relationships in these polyurethanes and finally correlating the findings to their adhesion behavior to glass surfaces. The model urethane matrices cover a wide range of properties from being very soft and elastomeric to very rigid and of high modulus. Different polyol molecular weights are used with different amounts of hard segments to tailor make polyurethanes with varying mechanical properties but the same chemistry. This type of experimental design allows for the study of the effects of polyol molecular weights and the hard segment contents on polyurethanes structure, property, and adhesion characteristics.

In Chapter 4, a theoretical model is developed to predict phase separation in polyurethanes. The model utilizes solubility parameters of the hard and the soft segments to determine a miscibility interaction parameter between the two phases. A phase diagram for copolymers derived from scattering studies, correlating block lengths with their weight fraction compositions, is used to calculate onset of phase separation. By comparing the onset of phase separation with the miscibility interaction parameter, the model is capable of predicting extent of phase separation in polyurethane formulations with variables such

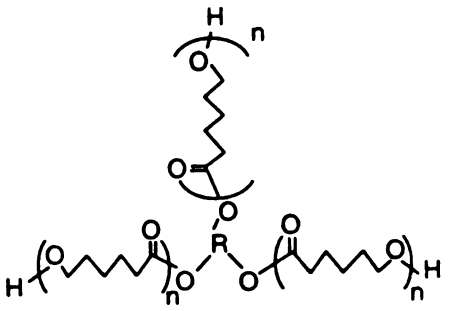

Caprolactone based polyol

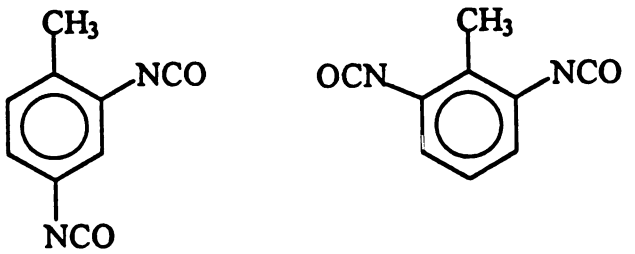

Toluene diisocyanate

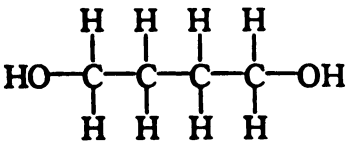

1,4 Butanediol

FIGURE 2.4 Chemical Structure of Polyurethane Constituents

as polyol molecular weights, length of chain extender and isocyanates, and the hard and soft segment contents. Experimental techniques such as near-infrared (NIR) and fourier transform infrared (FTIR) spectroscopy are used to verify the theoretical predictions. Angular dependent XPS (ADXPS) is utilized to analyze the failed glass surface from adhesion testings. Composition and thickness of the interphase region are also analyzed using ADXPS. Matrix phase separation is correlated to interphase composition and its adhesion. Based on the findings, a "beneficial" interphase region is created to improve adhesion of the poorly bonded polyurethane matrices. It is further demonstrated that by coating glass surfaces with a thin layer of butanediol (chain extender), adhesion of poorly phase separated polyurethanes can be significantly improved.

The fifth chapter is focused on investigating possible physical and chemical interactions in the interphase region. A theoretical model is developed to predict surface-free energies of the various polyurethanes. Contact angle measurements are done to experimentally determine polar and dispersive components of the surface-free energies. The surface-free energy data is used to calculate the work of adhesion and is correlated with the experimental adhesion values. The preferential segregation of butanediol to the interphase region is correlated to polar surface free energy. Silane coupling agents are used to treat the glass surface and with the use of the XPS technique, chemical interactions between urethane and glass surfaces are explored. Mechanical properties of the interphase region with excess butanediol are also evaluated to study the effects of the preferential segregation of butanediol on adhesion.

Finally, Chapter 6 presents the conclusions in a manner to coherently tie together the observations and findings of all the work done in this project. Also, Chapter 6 provides guidelines for some future work where the findings of this work can be extended to further elucidate the glass/urethane adhesion mechanisms in different urethane matrices and other glass surfaces.

CHAPTER 3

STRUCTURE - PROPERTY RELATIONSHIPS IN POLYURETHANES AND THEIR EFFECTS ON ADHESION TO GLASS

The work presented in this chapter has been accepted for publication in the Journal of Adhesion (1994).

3.1 ABSTRACT

Polyurethanes were prepared from toluene diisocyanate (TDI), 1-4-butane diol (BDO) and polycaprolactone based triols with varying molecular weights. Among each molecular weight triol based urethane, hard segment content was varied from 20% to 70%. Differential scanning calorimetry, tensile testing, and Iosipescu shear testing were done on all the various urethanes prepared. Thermal characterization data revealed the dependence of phase separation on hard segment content as well as on the triol molecular weight. Tensile data and Iosipescu shear data further confirmed the observations made from the DSC data. The data further indicated that phase separation can greatly improve modulus of cross-linked segmented urethanes. Adhesion of these urethanes to glass surface was evaluated using soda-lime float glass plate. Urethane samples were cast on the air side of the glass plates and adhesion was measured in shear mode. Adhesion data indicated that in addition to hard segment content, modulus, cross-link density, and molecular weight of the triols; phase separation seems to be a major factor in controlling adhesion. Surfaces of the failed adhesion samples were also analyzed and the failure mode was found to be cohesive with varying degree with the different urethane systems.

3.2 INTRODUCTION

Reinforced reaction injection molding (RRIM) and structural reaction injection molding (SRIM) of urethanes are widely used in the automotive industry to make body panels, fascias, bumper beams, etc. In these applications, good adhesion between the urethane matrix and the reinforcement (usually glass) is shown to be an important factor in determining overall mechanical properties of these composites (Dawson and Shortall, 1982; Kau ete al, 1989; Yang and Lee, 1987; Schwarz et al, 1979). Another important and emerging application of RIM-urethane is integral molding of gaskets onto glass panels to produce modular window assemblies (e.g., windshields) for automobiles (Reilly and Sanok, 1988; Fielder and Carsell, 1990; Agrawal et al, 1991). In these modular windows, good adhesion between urethane gasket and glass panels is essential for the structural integrity of these assemblies in the automobiles.

In the above mentioned applications of RIM-urethane polymers, urethane matrix properties vary from one extreme to the other, from being very soft and elastometric in modular window application to very rigid and of high modulus in RRIM and SRIM applications. There is extensive data reported in literature (Sanders and Frisch, 1983; Macosko, 1989) relating final properties of urethanes to various formulation parameters. These parameters control cross-linking density and phase separation in segmented polyurethanes, thus determining final matrix properties. It has been shown (Zdrahala et al, 1979; Chen et al, 1987; Chang et al, 1982; Camargo et al, 1985) that phase separation depends on individual segment length, segment length distribution, intra- and interdomain hydrogen bonding, and several other factors. Recent work by Rao and Drzal (Rao and

Drzal, 1991) has shown that for the same surface chemistry and matrix chemistry, adhesion varies directly with the matrix modulus in glassy cross-linked epoxies. This study is an attempt to extend this relationship to other systems and correlate the structure-property relationship of segmented polyurethane to its adhesion characteristics to glass substrates.

Model urethane matrix compositions have been developed that produce a transparent matrix which can be easily prepared and studied in laboratory. Thermal and mechanical characterization of the matrices have been done to establish matrix properties. Adhesion characteristics of the various matrices to soda-lime float glass plates have been evaluated and correlated to their compositions, structure, and properties.

3.3 SCOPE OF THE PRESENT WORK

In this study, we have not used any catalyst in the urethane formulations, thus increasing handling time for sample preparation. Also, the polyol used is a triol, allowing us to prepare and study a wide range of mechanical property urethanes without having to change its chemistry. Urethane formulations have ranged from the lowest possible hard segment to 100% hard segment. In this paper, the hard segment content is defined as the percent by weight of the isocyanate and the chain extender in the polymer at a fixed stoichiometry or isocyanate index. Thus, in the lowest possible hard segment formulation, there is no chain extender whereas in the 100% hard segment formulation, there is no polyol.

To study the role of polyol molecular weights, three different polyol molecular weights were used to prepare urethane formulations with the same hard segment contents.

3.4 EXPERIMENTAL

3.4.1 Materials

The polyurethanes used in this study were caprolactone-based trifunctional polyols available from Union Carbide under the trade name "Tone." Characteristics of these polyols are listed below:

Polyols	Supplier	Molecular Weight	Hydroxyl Number
Tone 0310	Union Carbide	900	187
Tone 0305	Union Carbide	540	312
Tone 0301	Union Carbide	300	560

Hard segments were made from a 80%-20% mixture of toluene 2,4-diisocyanate and toluene 2,6-diisocyanate (TDI, Aldrich Chemical Co.), and 1,4-butanediol (BDO) as chain extender (Aldrich Chemical Co.).

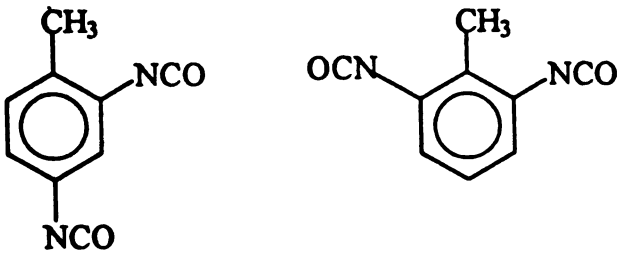

Toluene diisocyanate

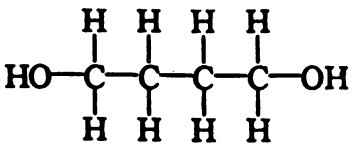

1,4 Butanediol

The various urethane formulations studied in this work are shown in Table 3.1. Their surface-free energies, based on contact angle measurements, are between 40.5 and 45.2 dynes/cm (Agrawal and Drzal, 1994). Also shown in Table 3.1 are the weight percent hard segment content and the molecular weight per cross-link (Mc). Mc is the unit weight of the polymer divided by the number of cross-link junctions in the unit weight of the polymer.

The glass substrates used for adhesion testing were annealed 2" x 5" x 1/4" soda-lime float glass plaques. Adhesion testing of urethanes were carried out on the air-side of the glass plaques.

3.4.2 Sample Preparation

For Thermal and Mechanical Characterization

A one step urethane preparation approach was used to prepare all the samples. Triol and BDO chain extender were mixed and degassed for 2-4 hours at 60°C. Silicone molds for casting tensile dogbone specimens and Iosipescu shear specimens were also subjected to degassing at the same time. The stoichiometric amount of TDI was then added to the triol-chain extender mixture and homogenized with a magnetic stirrer for about a minute. The resultant mixture was then quickly cast into the degassed silicone molds. Silicone molds were then heated for 24 hours at 90°C in a convection oven. After curing, samples were taken out of the molds and were sanded and polished to achieve uniform thickness.

TABLE 3.1

Urethane Formulations at Isocyanate Index of 1.0

Sample Designation	Polyol Type			BDO (Mole%)	TDI (Mole%)	Hard Segment (wt %)	Molecular Weight per Cross-Link (Mc)
	Tone 0301	Tone 0305	Tone 0310				
10A	-	-	X	0	60	22	1160
10B	-	-	X	22	56	37	1424
10C	-	-	X	31	54	47	1692
10D	-	-	X	34	53	60	2222
10E	-	-	X	41	52	67	2752
5B	-	X	-	7	58	37	854
5C	-	X	-	20	56	47	1013
5D	-	X	-	31	54	59	1324
5E	-	X	-	36	53	67	1646
1C	X	-	-	0	60	47	563
1D	X	-	-	18	57	59	739
1E	X	-	-	26	55	67	912
HS	-	-	-	50	50	100	-

For Adhesion Testing

The air side of 2" x 5" x 1/4" annealed soda-lime float glass plaques was cleaned with methyl-ethyl-ketone solvent and dried. Silicone molds with a 1/4" x 1/4" x 1/4" cavity were placed on the air side of the glass plaques and were secured to the glass plaques using clamps. The degassed and homogenized mixture of the polyol, the chain extender, and the isocyanate was then poured into the 1/4" x 1/4" x 1/4" cavities formed by the glass plaques and silicone molds. The glass plaque-silicone mold assemblies were then cured for 24 hours at 90°C in a convection oven. Upon cooling, silicone molds were separated from the glass plaques and the samples were stored for adhesion testing. Figure 3.1 shows the drawing of an adhesion sample with two urethane blocks cast on a soda-lime glass plate.

3.4.3 Tests and Characterization

Differential Scanning Catorimetry (DSC)

DSC scans on all the cured urethane samples were done on a Shimadzu TA50 thermal analysis system. Sample weights used for the scans were approximately 20-25 mg. The DSC cell, with the sample inside the cell, was cooled down to -80°C by liquid nitrogen and scans were done at 10°C/min to up to 280°C. For the second DSC scan on the same sample, the DSC cell was allowed to cool down to ambient temperature and then liquid nitrogen was used to further cool it down to -80°C.

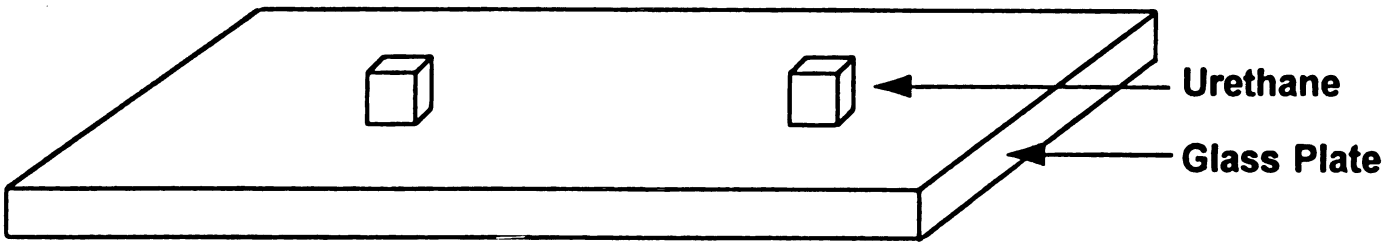

FIGURE 3.1 Glass - Urethane Adhesion Sample

Dynamic Mechanical Analysis (DMA)

Rectangular bars (30 mm x 4 mm x 1.25 mm) of various urethane samples were used for dynamic mechanical analysis on a Seiko Instrument's DMS-90 system. Values of E' and tanδ at various temperatures were obtained in a clamped three-point bending oscillation mode of deformation at 1 Hz fixed frequency. The temperature was varied from -70°C to 280°C at 10°C/min.

Iosipescu Shear Testing

All urethane samples for the Iosipescu testing were sanded and polished to a uniform thickness of 2.5 mm. Strain gage rosettes (from Micro Measurements Inc.) were attached to the front of each specimen. Testing was done on a servohydraulic material testing machine MTS 900 using a modified Wyoming fixture (Ho et al, 1993) at .05"/minute crosshead speed. Strain gage on each sample was connected to a wheatstone bridge with a half-bridge configuration. The wheatstone bridge was connected to a signal-conditioning amplifier, and the amplified analog signal was converted to digital signal through a circuit completion box which was connected to a microcomputer controlled data acquisition system. At least three samples were tested for each urethane formulation. For softer urethane formulations such as 10A and 10B, reinforcing tabs were glued to the sample ends to facilitate testing.

Tensile Testing

Dogbone-shaped urethane samples were tested on a tabletop material testing machine, Instron 4201, using pneumatically actuated grips. Grips were separated at 2"/minute and

the sample stress-strain curve to its failure was recorded on a chart recorder. At least four samples were tested for each urethane formulation.

Adhesion Testing

Adhesion of urethane matrix to glass surface was evaluated using soda-lime float glass plates as the substrate. Plate glass was chosen rather than fibers as the glass-matrix interface/interphase in plate glass could further be analyzed with relative ease using visual, microscopic, spectroscopic, and chemical means.

The lap-shear configuration for adhesion testing with glass plates could not be used successfully due to the brittleness of the glass plates. In the lap-shear configuration trials, glass plates broke during sample loading or during sample testing due to the slight misalignment or bending. To overcome this, ASTM test method D4501 for measuring shear strength of adhesive bonds between rigid substrates by the block-shear method was modified for this study. Figure 3.2 shows the front and the rear view of the test fixture with an adhesion sample clamped in place.

Instron 4201, tabletop material testing machine, was utilized for the adhesion testing. The test fixture was mounted on the Instron. An adhesion sample was loaded in the test fixture carefully such that the cast urethane block of the sample would engage with the shearing bar of the test fixture. Upon the sample loading, the jaws of the Instron machine were moved apart at 0.2"/minute. In this fashion, the cast urethane block was shear loaded in a plane parallel to the glass plaque. The maximum load required for the

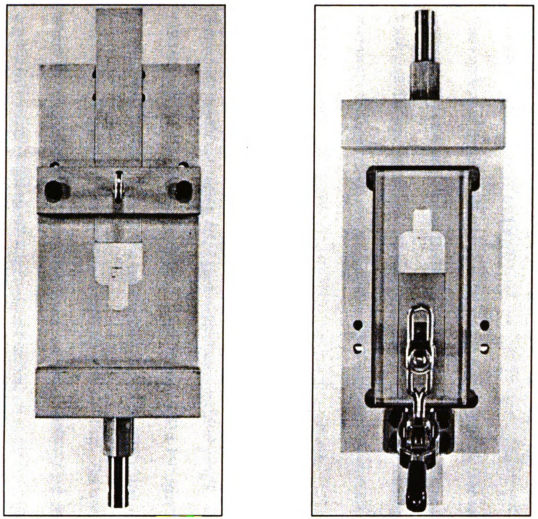

FIGURE 3.2 Glass-Urethane Adhesion Testing Fixture
a) Front View of Fixture with Specimen Clamped in Place
b) Rear View of Fixture with Specimen Clamped in Place

detachment of the urethane block from the glass surface was recorded. At least five samples were tested for each urethane formulation. After failure, glass and urethane samples were saved for failure mode analysis.

Scanning Electron Microscopy (SEM)

Glass surfaces of the failed adhesion samples were examined by SEM. The surfaces were gold coated by a Denton Vacuum DESK II coater. A total thickness of approximately 100Å gold film was deposited on the sample surfaces. An ISI-SS130 scanning electron microscope was used to examine the samples. A 50X magnification was utilized in the SEM examination.

X-Ray Photoelectron Spectroscopy (XPS)

Subsequent to adhesion testing, failed glass surfaces were analyzed using Perkin-Elmer PHI5400 x-ray photoelectron spectrometer. Approximately 1/4" x 1/4" square area was sectioned from the failed glass surface and was placed inside the XPS chamber. The XPS spectra were obtained at a base pressure of approximately 10^{-9} Torr. The standard Mg Kx source was used for all samples analysis and was operated at 300W (15 kV, 20 mA). A continuously variable angle sample stage was used and was set to 45° (photoelectron take-off angle). The portion of the sample analyzed by the spectrometer is set through an initial lens system and was set for a 2.0 mm diameter circle. Data was collected in the fixed analyzer transmission mode utilizing a position sensitive detector and a 180° hemispherical analyzer. Pass energies were set at 89.45 eV for the survey scans (0-1000 eV) and at

35.75 eV for the narrow scans of the elemental regions. Data collection and manipulation was performed with an Apollo 3500 workstation running PHI ESCA software.

3.5 RESULTS AND DISCUSSION

Figure 3.3 shows a simplified two-dimensional schematic representation of possible molecular arrangements in some of the urethane formulations studied in this work. Figure 3.3A shows urethane formulation 10A which has no chain extender. From the schematic, it is clear that sample 10A is a cross-linked single-phase urethane system. Figures 3.3B, C, and D represent urethane formulations 10E, 5E, and 1E respectively, all with the same hard segment content (~67%). among these three samples, sample 10E has the highest amount of the chain extender. This can lead to longer hard segment chain lengths resulting in better phase separation (Macosko, 1989; Zdrahala et al, 1979). In Figure 3.3D, the soft segment chain length is almost equal to the chain extender and thus very little phase separation is expected.

3.5.1 Thermal Characterization

Phase separation phenomena in segmented urethanes can be related to their thermal transition behavior. DSC analysis was used to study thermal transitions in all the synthesized urethane samples. DSC thermograms for Tone 0310 are shown in Figure 3.4. There can be several thermal transitions in a segmented urethane related to soft segment, hard segment, hydrogen bonding between domains, crystallization, phase melting, etc. (Byrne et al, 1992; Chen et al, 1992; Hepburn, 1992). In Figure 3.4, soft segment transition, which is below 0°C, is difficult to detect consistently and reliably, and thus is

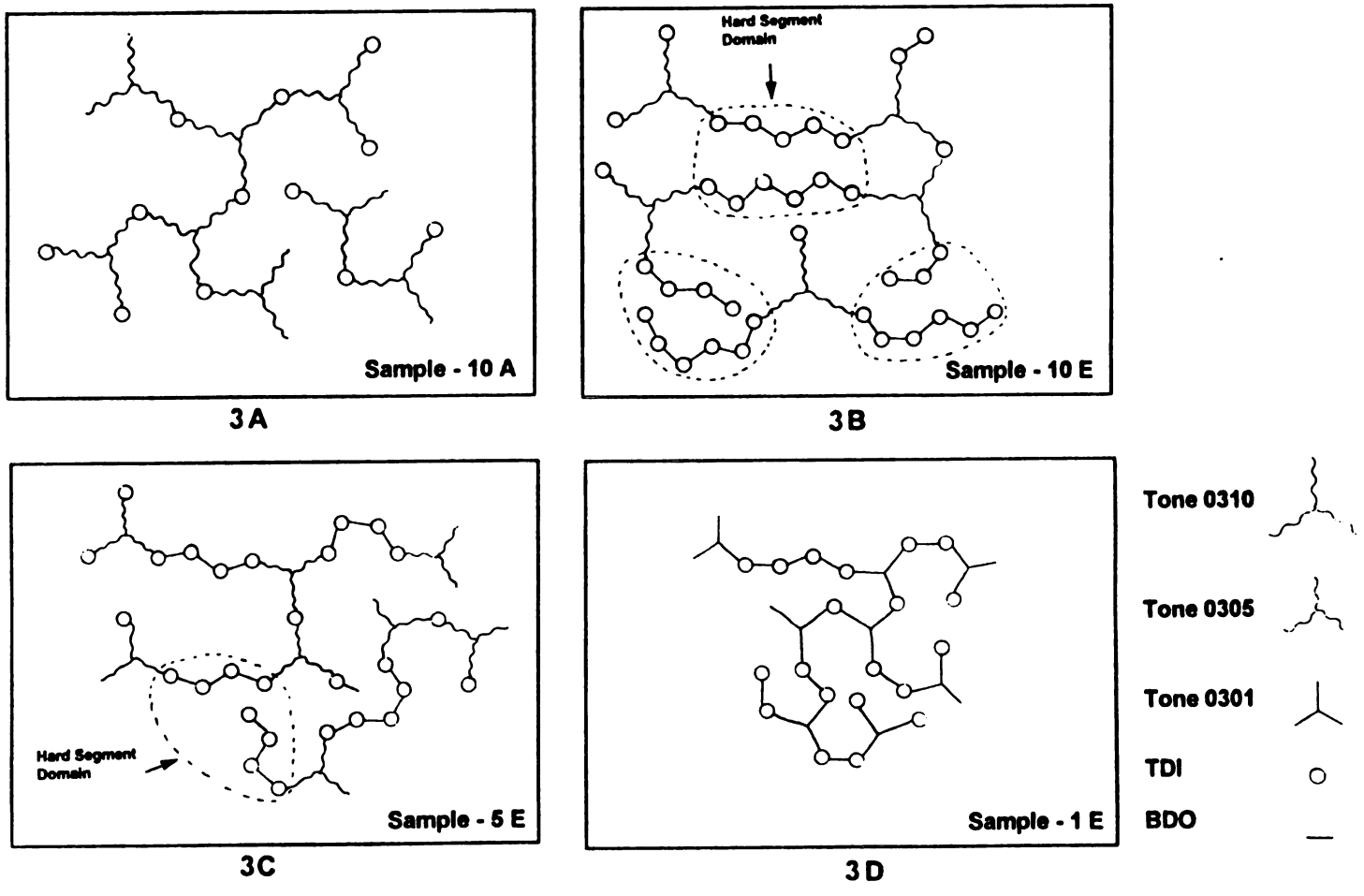

FIGURE 3.3 Model of Molecular Arrangements in Urethanes

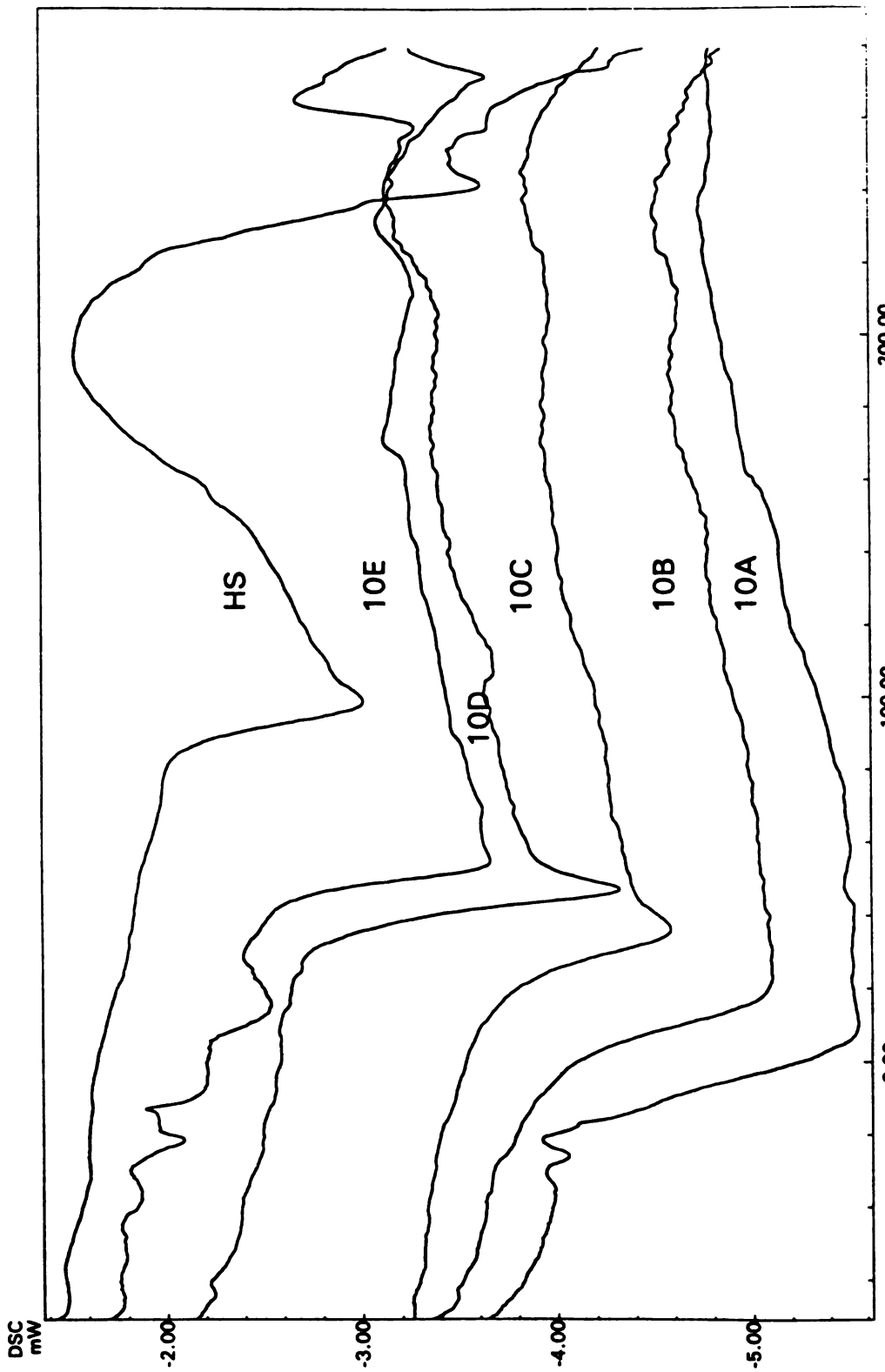

FIGURE 3.4 DSC Thermograms of Tone 0310 Based Polyurethanes with Varying Hard Segment Content (1st Run)

not reported here. The thermal transition above 0°C which is the most prominent in these scans can be related to the hard segment. This hard segment thermal transition data is shown in Table 3.2 for all the samples based on Tone 0310 (the highest molecular weight trial) based polyurethanes. The glass transition temperature for all the Tone polyols is approximately -60°C, whereas for the formulation with 100% hard segment (Sample HS, Table 3.1) is 98.4°C. From Figure 3.4 it is clear that in Tone 0310 system, as the hard segment content increases, the transition temperature increases. With higher hard segment content, hard segment chain length increases and longer chain lengths improve phase separation (Macosko, 1989; Zdrahala, 1979). Thus, the increase of thermal transition temperature with hard segment suggests that degree of phase separation improves with hard segment content. Figure 3.5 shows second DSC thermograms on the same samples after annealing and quenching. The thermal transition data from the second DSC run are, in general, higher than the corresponding thermal transition temperature from the first DSC run. This suggests that sample annealing-quenching improves phase separation in segmented polyurethanes (Hepburn, 1992). The first and second DSC run thermograms of Tone 0305 and Tone 0301 polyol-based urethanes are shown in Figures 3.6, 3.7, 3.8, and 3.9 respectively; and the thermal transition temperature data is shown in Table 3.2. In the first and second DSC runs of Tone 0305 system, the thermal transition temperature increases with increasing hard segment content. But sample annealing-quenching does not seem to have much effect on the transition temperatures as evident by comparing the corresponding first and second DSC transition temperatures. In Tone 0301 based polyurethanes, transition temperature decreases with increasing hard segment content in the first DSC run and remains the same or increases somewhat in the second DSC run.

TABLE 3.2

Effects of Hard Segment and Polyol Molecular Weight
on Thermal Transitions in Cross-Linked Segmented Polyurethanes

Sample	1st Run Transition Temperature (°C)	2nd Run Transition Temperature (°C)
10A	6.1	5.3
10B	19.2	26.5
10C	35.5	36.3
10D	46.1	56.7
10E	54.3	68.2
5B	44.4	49.4
5C	59.4	59.9
5D	64.0	64.8
5E	73.0	72.2
1C	100.6	102.2
1D	98.7	101.3
1E	86.7	106.9
HS	98.4	109.8

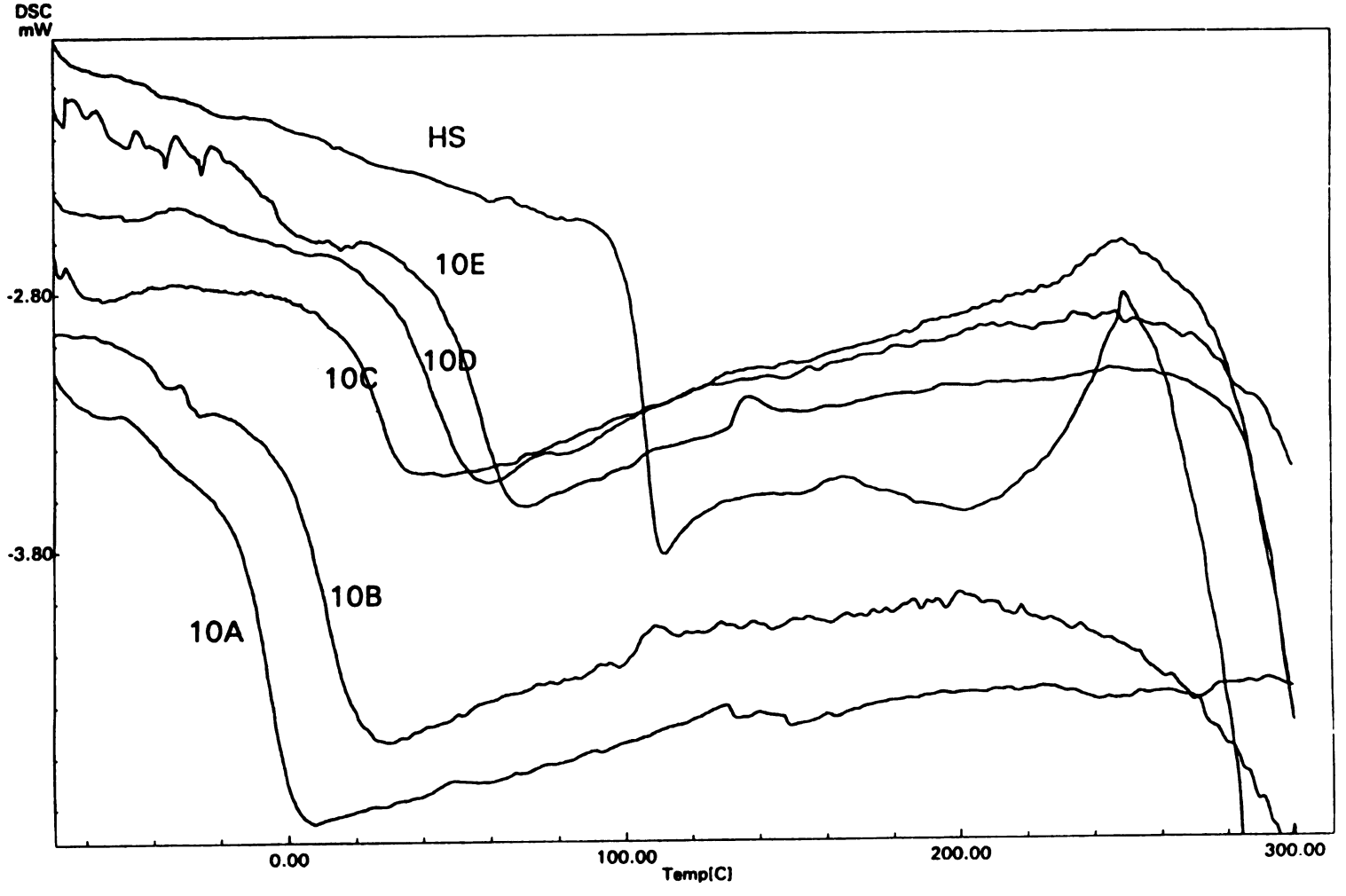

FIGURE 3.5 DSC Thermograms of Tone 0310 Based Polyurethanes with Varying Hard Segment Content (2nd Run)

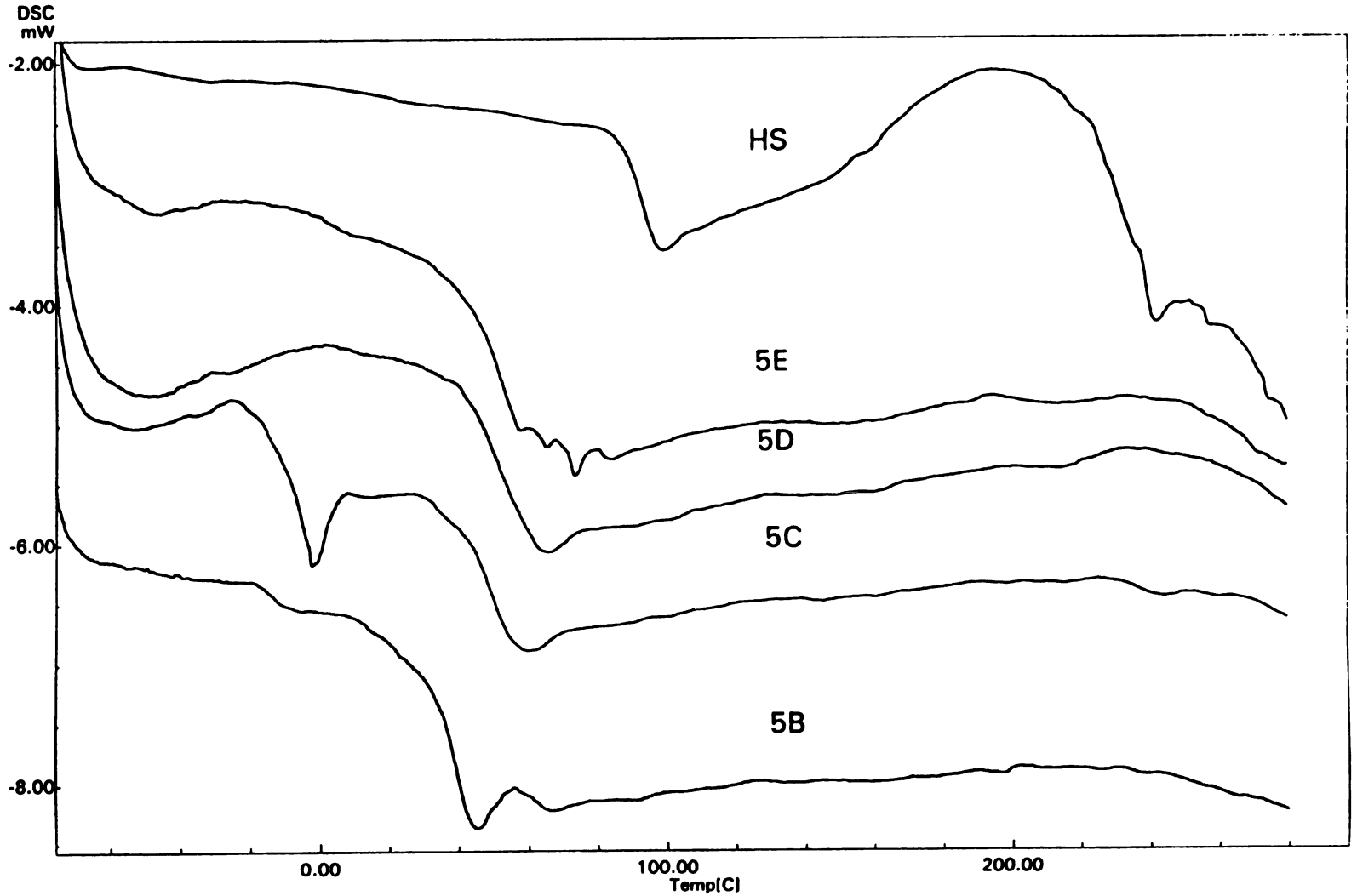

FIGURE 3.6 DSC Thermograms of Tone 0305 Based Polyurethanes with Varying Hard Segment Content (1st Run)

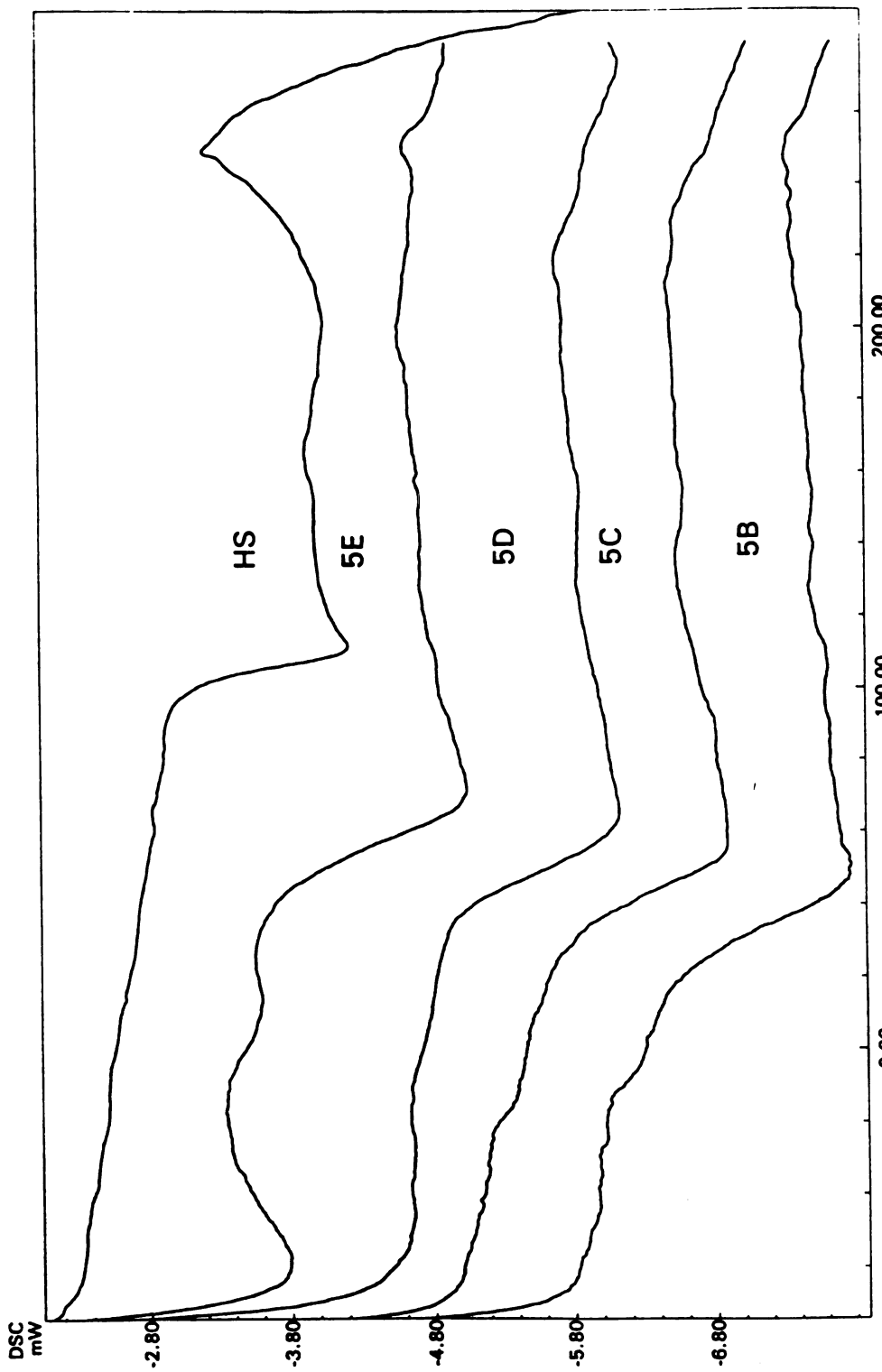

FIGURE 3.7 DSC Thermograms of Tone 0305 Based Polyurethanes with Varying Hard Segment Content (2nd Run)

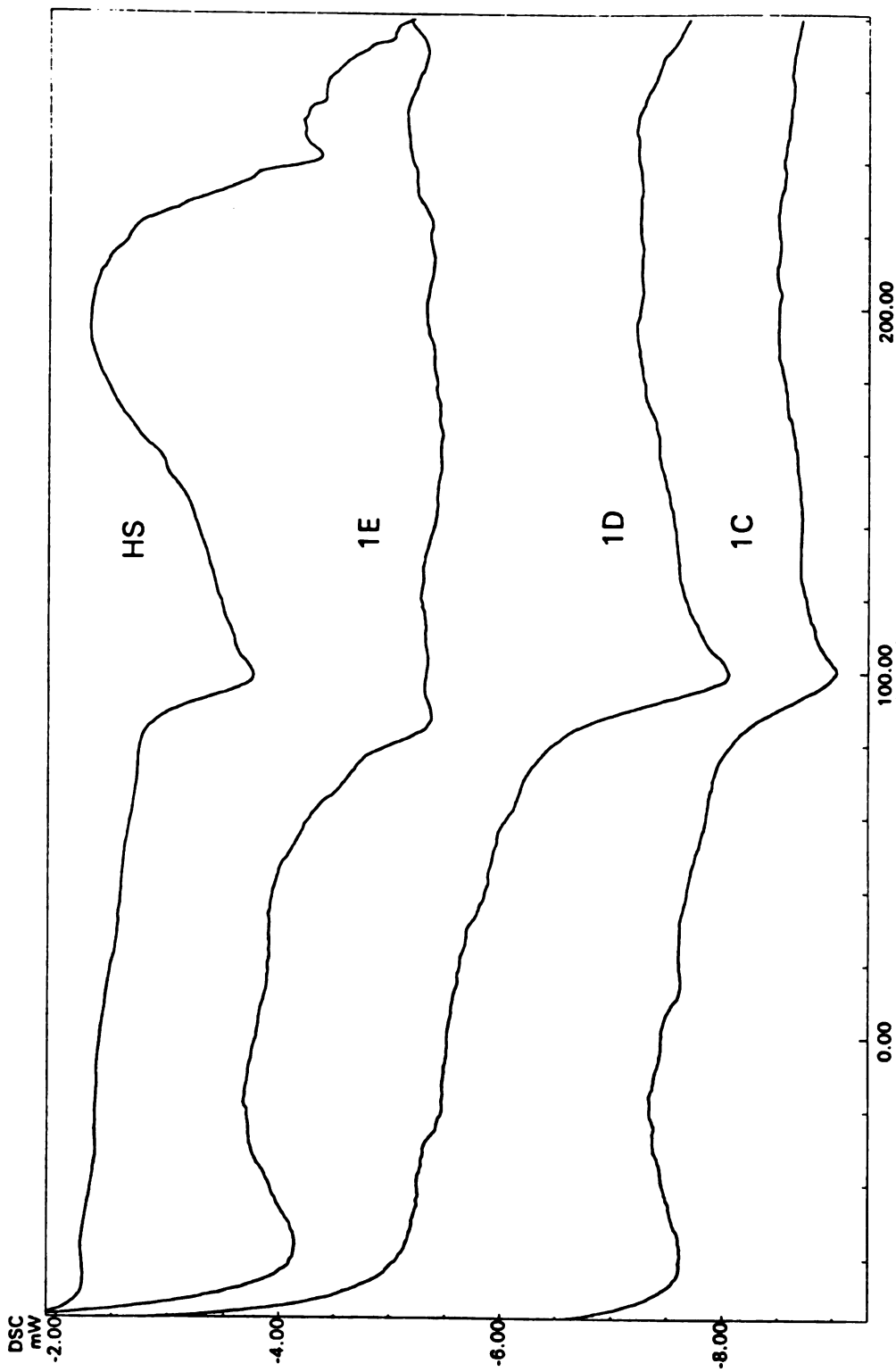

FIGURE 3.8 DSC Thermograms of Tone 0301 Based Polyurethanes with Varying Hard Segment Content (1st Run)

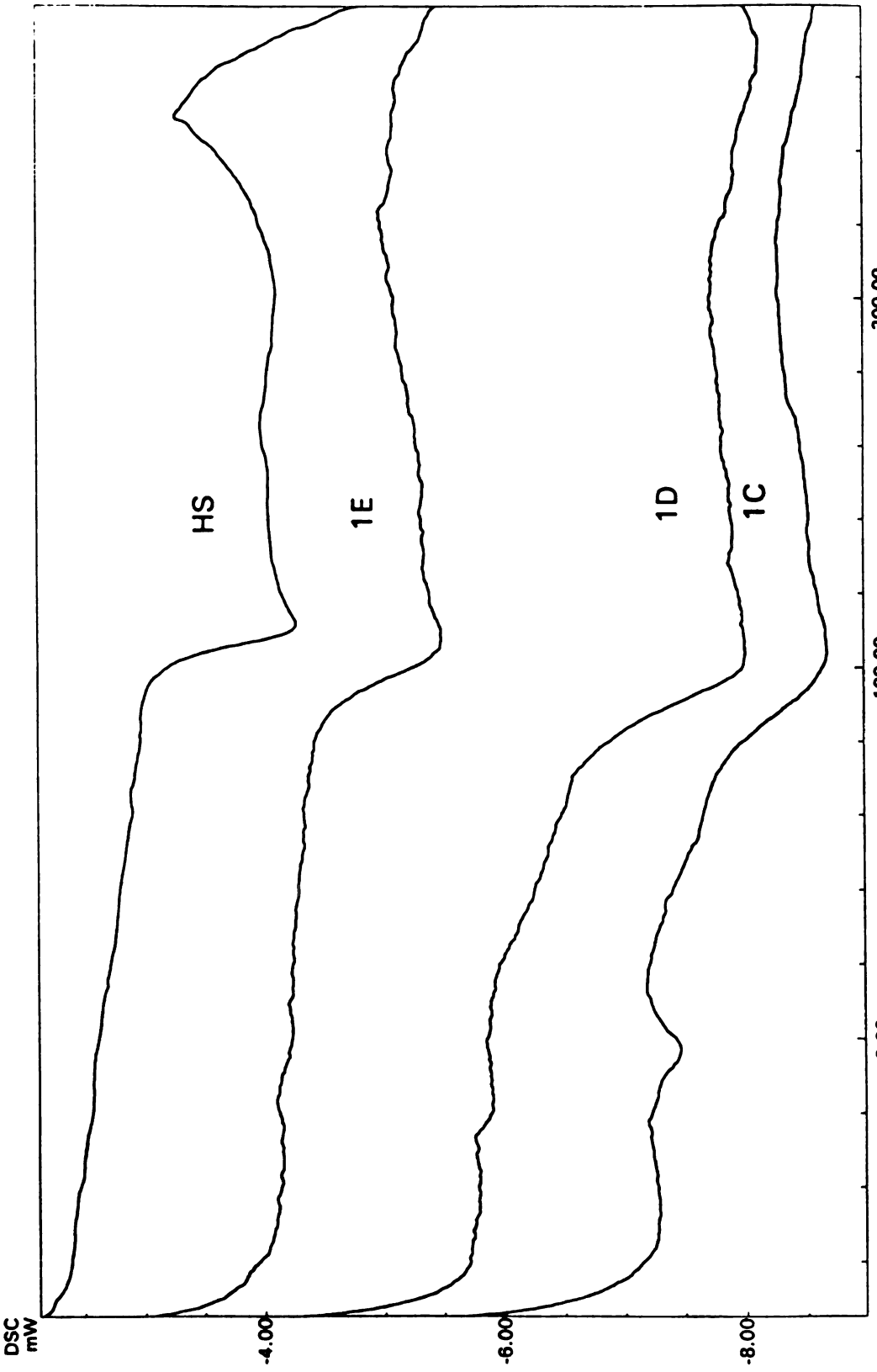

FIGURE 3.9 DSC Thermograms of Tone 0301 Based Polyurethanes with Varying Hard Segment Content (2nd Run)

We think the lower transition temperature of 1E sample in the first DSC run could be the result of extremely short gel time. This may explain why the transition temperature of 1E increases to 106.9°C in the second DSC run from 86.7°C in the first DSC run.

The DSC transition temperature of Tone 0310, 0305, and 0301 based polyurethanes from the first run are graphed in Figure 3.10 and from the second run are graphed in Figure 3.11. From both of these graphs it is clear that the rate of increase of transition temperature with the hard segment content is the highest for Tone 0310 followed by Tone 0305 and Tone 0301. This suggests that degree of phase separation increases with hard segment content at a greater rate for higher polyol molecular weight polyurethanes.

These observations are also supported by the dynamic mechanical analysis. Figure 3.12 shows log (E') vs. temperature for samples 10E and 1E which have the same hard segment content. In the figure, we see that the modulus plateau in the rubbery region for the sample 10E is flatter than that for the sample 1E even though the cross-link density in 10E is lower than 1E. This suggests that the degree of phase separation in 10E is greater than in 1E (Camargo et al, 1985).

3.5.2 Mechanical Characterization

All the urethane samples were tested in the tensile mode at 2"/minute cross-head separation speed. Load versus displacement response of Tone 0310 based polyurethanes is shown in Figure 3.13 and is found to be highly nonlinear. Samples 10A and 10B showed typical nonlinear and high elongation characteristics of soft rubbery material. This

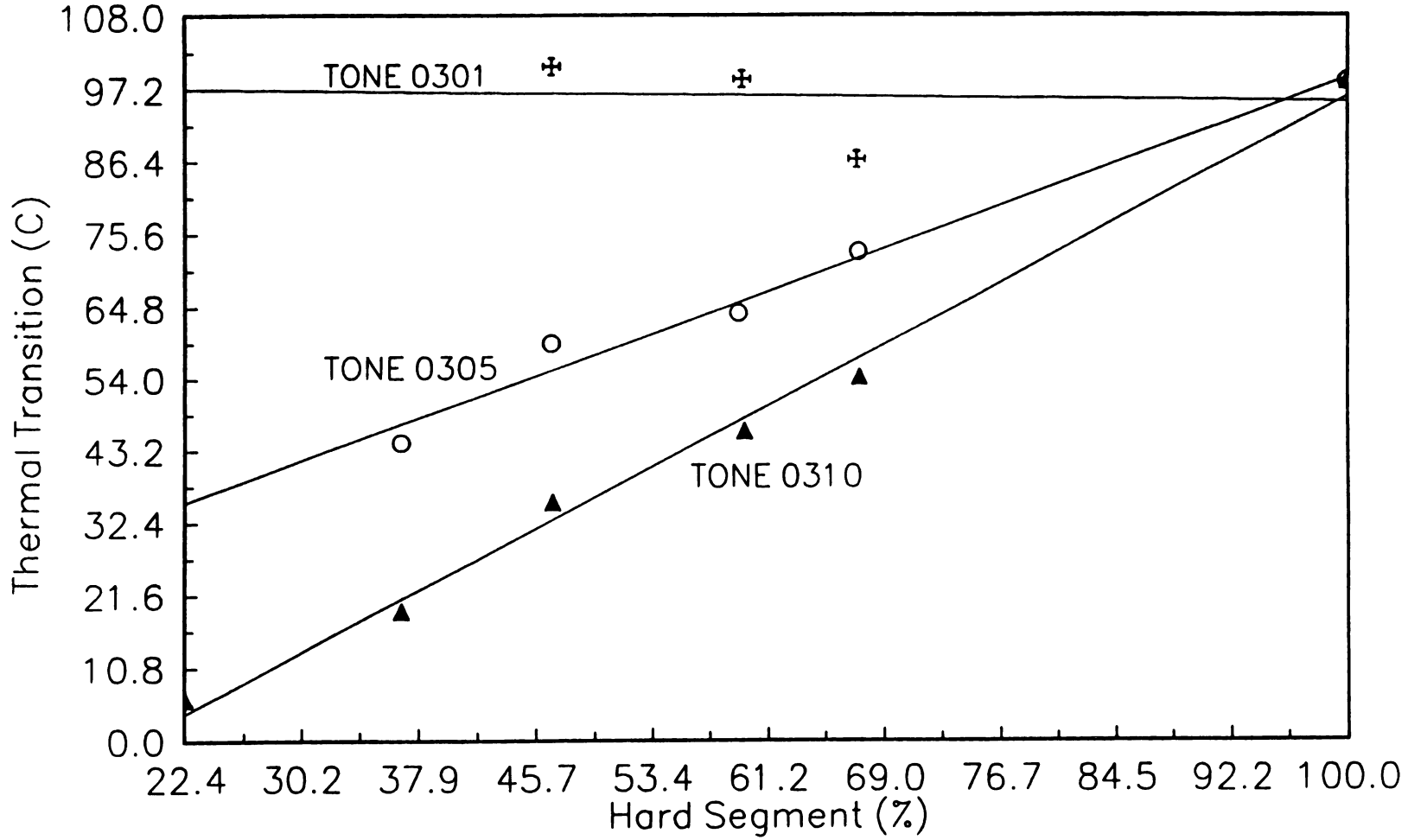

FIGURE 3.10 Thermal Transition Temperature Versus Hard Segment Content in Different Molecular Weight Triol Based Urethane Systems (1st DSC Run)

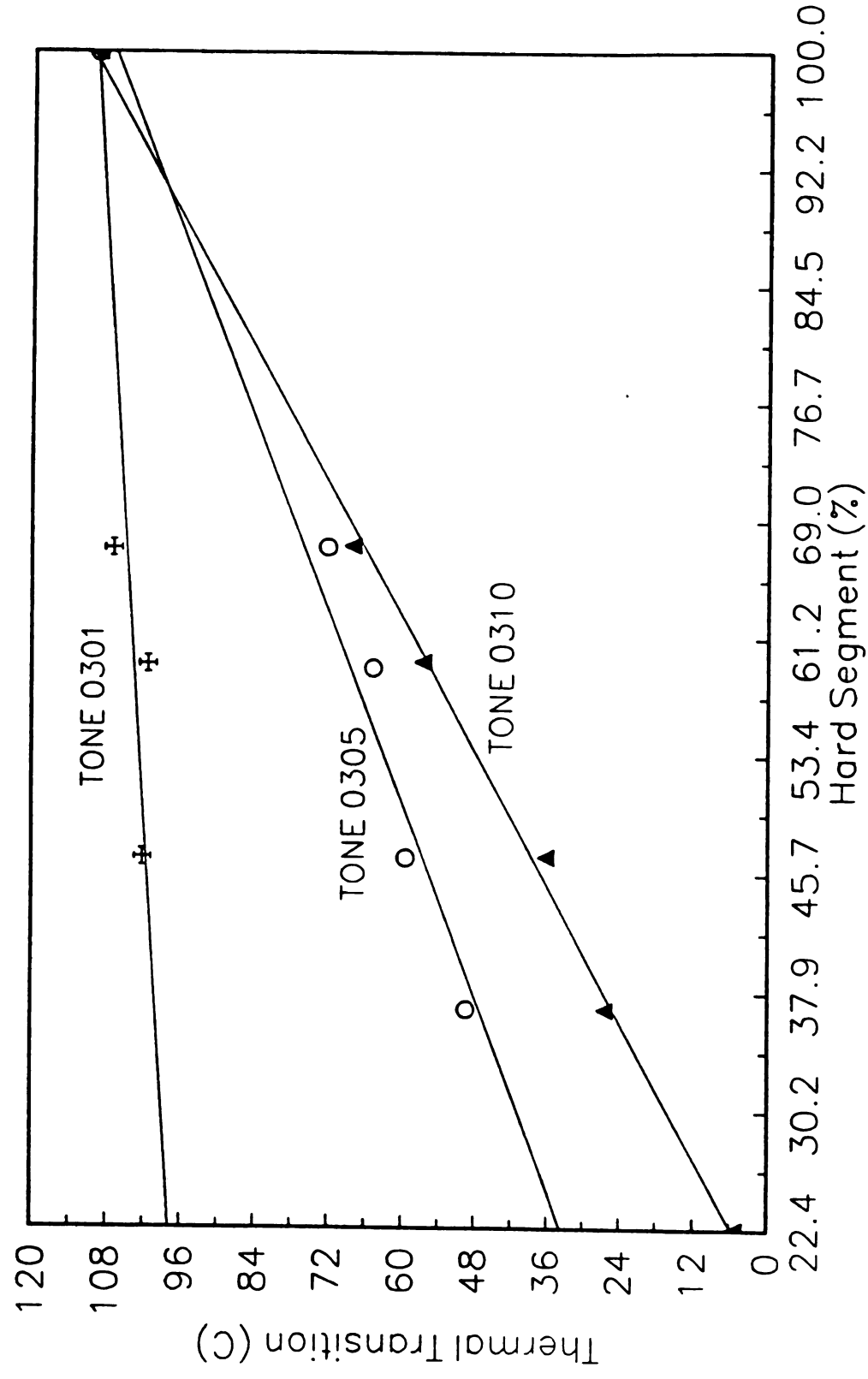

FIGURE 3.11 Thermal Transition Temperature Versus Hard Segment Content in Different Molecular Weight Triol Based Urethane Systems (2nd DSC Run)

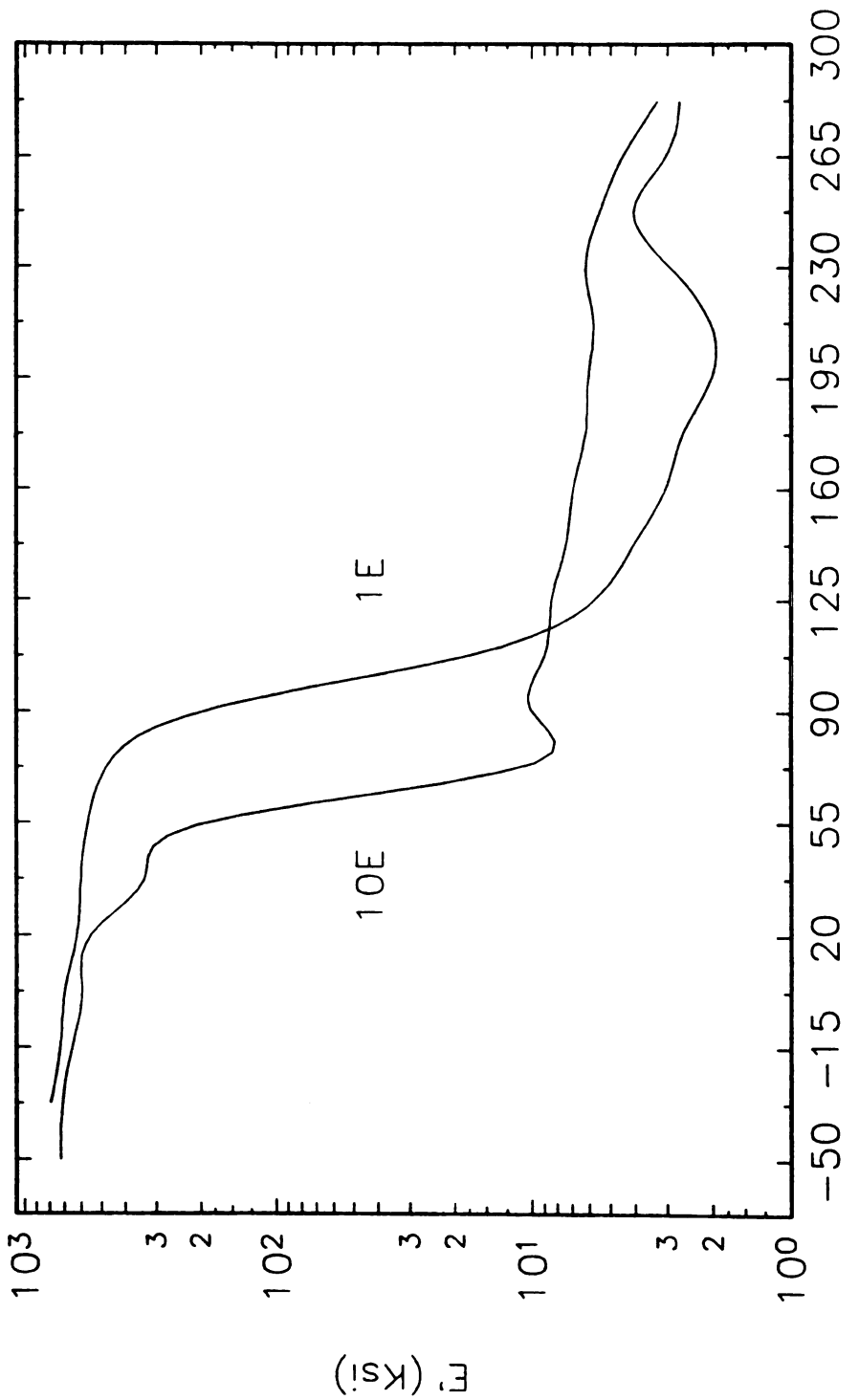

FIGURE 3.12 DMA Scan of Tone 0310 and Tone 0301 Polyols Based urethanes with Constant Hard Segment Content

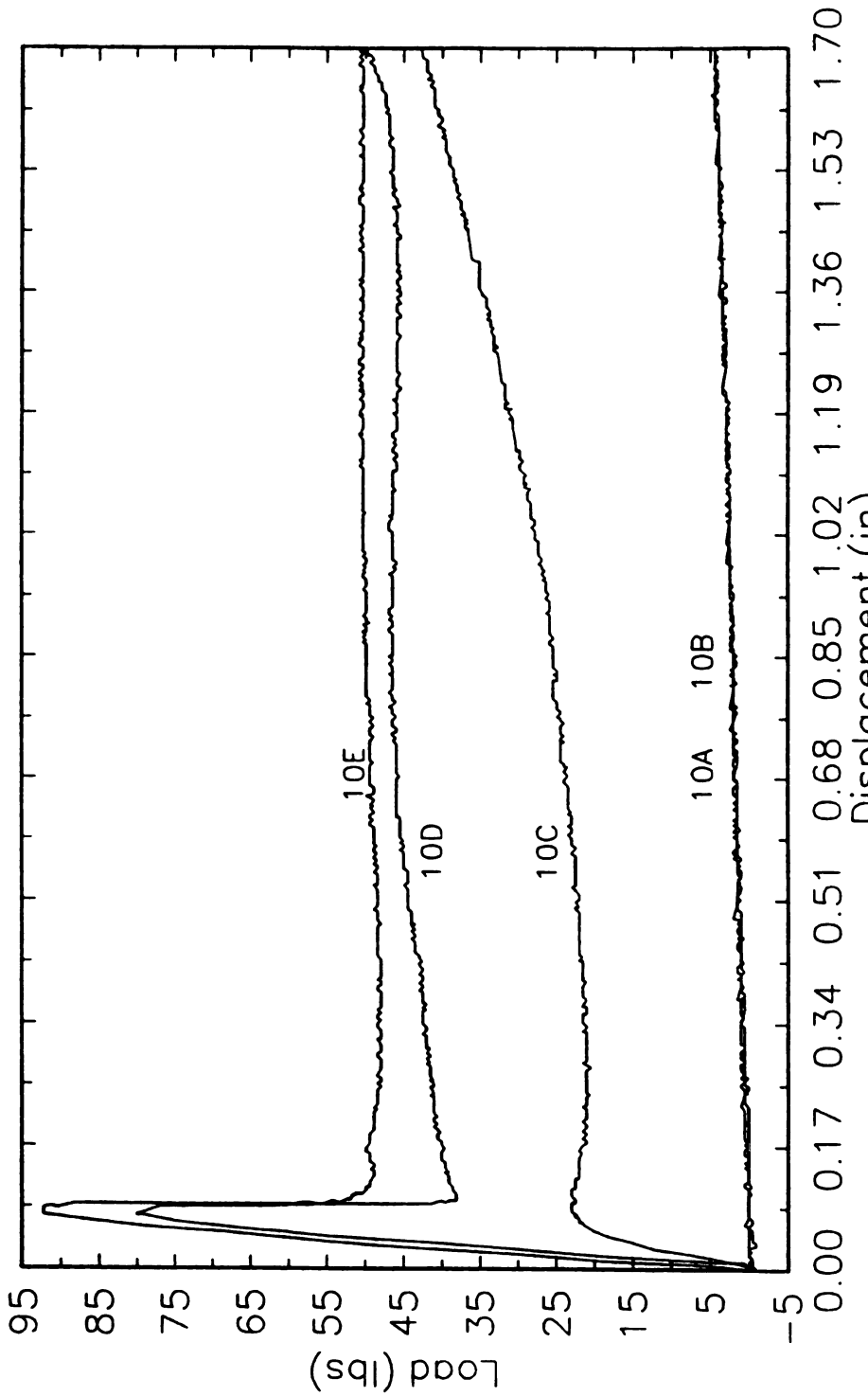

FIGURE 3.13 Load/Displacement Response of Tone 0310 Based Polyurethanes at Different Hard Segment Content

could be due to strain induced crystallization in these samples (Macosko, 1989; Hepburn, 1992) even though samples remained translucent at high strain. Higher hard segment content samples 10C, 10D, 10E and all other samples based on Tone 0305 and Tone 0301 polyols showed yield behavior. Strain at yield for these samples are shown in Table 3.3.

Figure 3.14 shows a semilogarithmic plot of 2% secant tensile modulus versus hard segment content of all the urethane samples. The dependence of modulus on hard segment is nonlinear for Tone 0310 based urethanes whereas is almost linear on this semilogarithmic plot for Tone 0301 and Tone 0305 based urethanes. The abrupt change in the slope of Tone 0310 system between sample 10B and 10C suggests that modulus buildup is taking place due to phase separation (Macosko, 1989; Camargo et al, 1985). This further supports the observation made earlier with DSC data that higher polyol molecular weight increases the degree of phase separation. Tensile strength data for all the urethanes tested is shown in Table 3.3 and is graphed in Figure 3.15. It is clear that for a given hard segment content, lower molecular weight polyol system has a higher tensile strength. This could be due to the higher cross-linking density associated with lower molecular weight triols.

Because the adhesive or matrix shear properties have been shown to be a key predictor and scaling parameter, Iosipescu shear testing of all the samples was conducted. Stress-strain data was recorded only up to 8% strain due to the strain gage limitation. Only the shear modulus was determined. Shear strength of most of the samples could not be determined as the samples could not be strained to failure due to Iosipescu testing fixture's

TABLE 3.3

Mechanical Properties of Various Polyurethane Systems

Samples	Shear Modulus (PSi) 2% Secant	Tensile Modulus (PSi) 2% Secant	Strain at Yield (%)	Tensile Strength (PSi)	Hardness (Shore D)
10A	-	950	-	910	33
10B	-	1,400	-	8,700	50
10C	67,036	103,000	8.0	6,600	75
10D	150,653	215,000	8.2	10,600	80
10E	178,971	250,000	8.7	12,300	85
5B	128,506	116,000	8.0	8,000	80
5C	149,699	277,000	8.0	11,600	84
5D	165,404	287,000	8.5	12,600	85
5E	171,787	306,000	9.0	13,600	85
1C	176,060	152,000	11.0	15,500	87
1D	184,962	310,000	11.0	16,500	88
1E	188,733	349,000	9.5	15,300	88

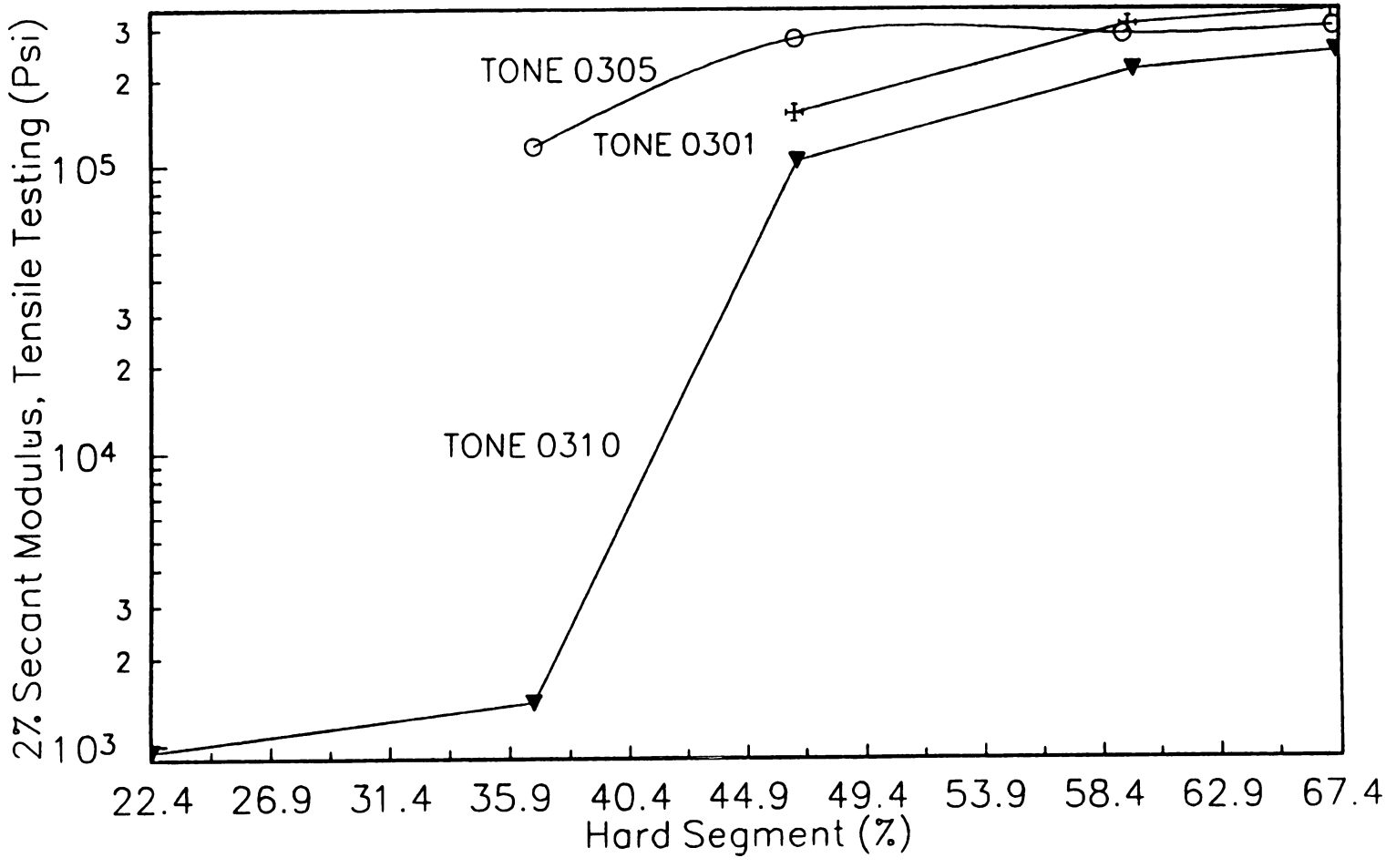

FIGURE 3.14 2% Secant Tensile Modulus Versus Hard Segment Content in Various Urethane Systems

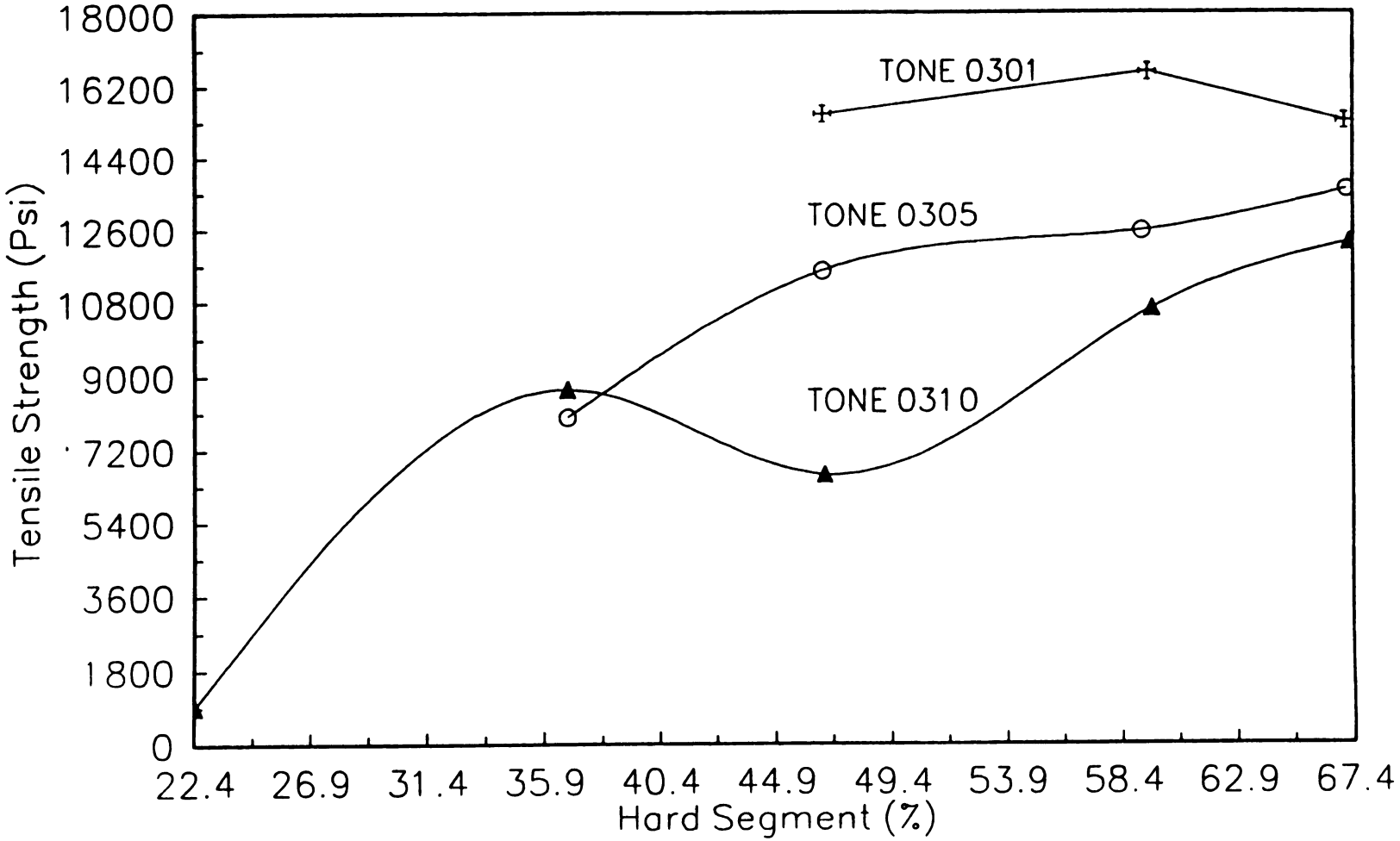

FIGURE 3.15 Tensile Strength Versus Hard segment Content in Various Urethane Systems

limitation. The samples that did fracture showed a failure pattern characteristic of pure planar shear loading (Figure 3.16).

Reproducible data for soft low modulus samples 10A and 10B could not be obtained and are not reported here. Stress-strain response for all the other samples are shown in Figure 3.17. A 2% secant modulus was calculated and shown in Table 3.3. Good agreement was found between Iosipescu testing and tensile testing. Figure 3.18 shows shear modulus versus hard segment contents for all the different types of urethanes. From the graph we see that for the same hard segment content, lower molecular weight polyol based urethanes have higher modulus. This is due to the higher cross-linking density for the same hard segment content in lower molecular weight triol-based systems. Figure 3.19 shows the effect of molecular weight per cross-link (M_c) on shear modulus. As M_c increases, cross-link density decreases (see Figure 3.3) and shear modulus increases. For the same M_c, lower molecular weight polyol systems exhibit higher modulus due to higher hard segment content. Also, in Figure 3.18, the slope of Tone 0310 based urethane system is higher than that of Tone 0305 and Tone 0301 systems which is consistent with tensile testing and suggests that higher molecular weight polyol undergoes phase separation more readily.

3.5.3 Adhesion to Glass

Adhesion samples were tested in the shear fixture and the peak load values recorded are shown in Table 3.4. Samples with Tone 0310 and Tone 0305 showed very good reproducibility whereas Tone 0301 based samples had a larger amount of variation and

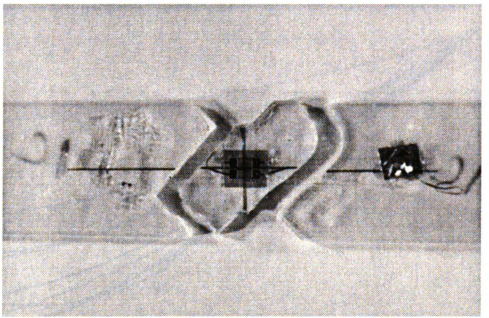

FIGURE 3.16 Fractured Urethane Sample After Iosipescu Shear Testing

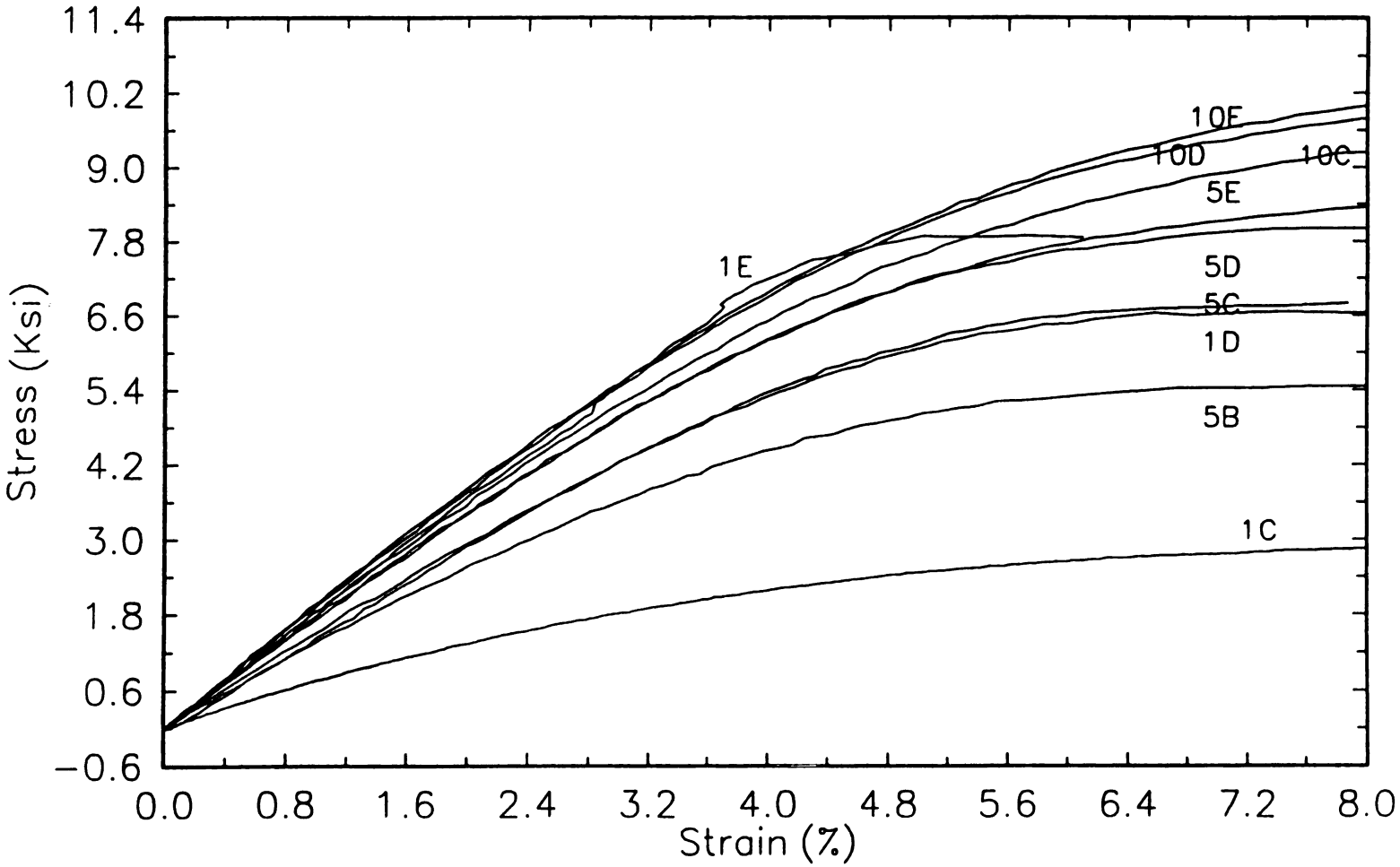

FIGURE 3.17 Stress/Strain Response of Different Urethanes in Iosipescu Shear Testing

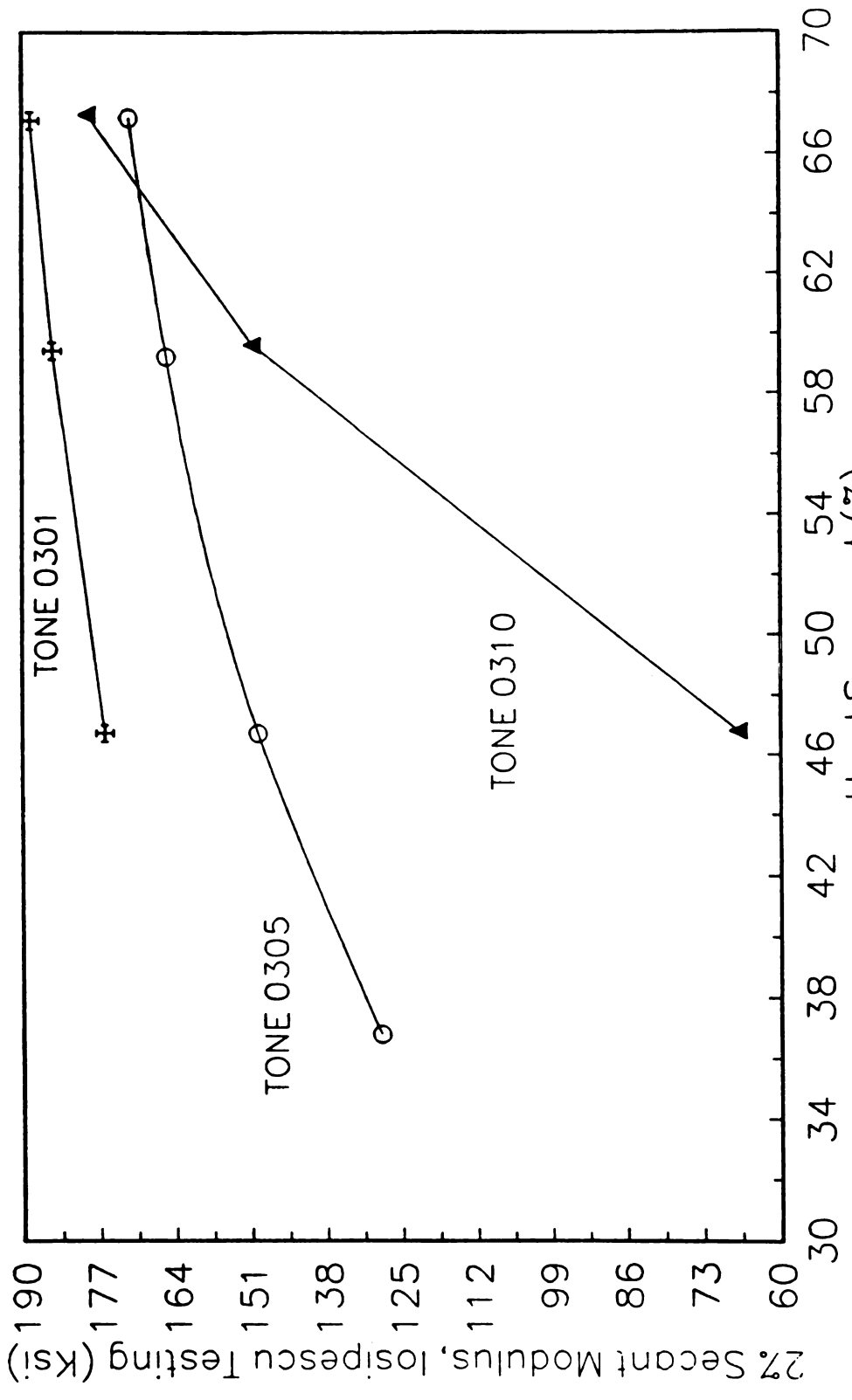

FIGURE 3.18 2% Secant Shear Modulus Versus Hard Segment Content in Various Urethane Systems

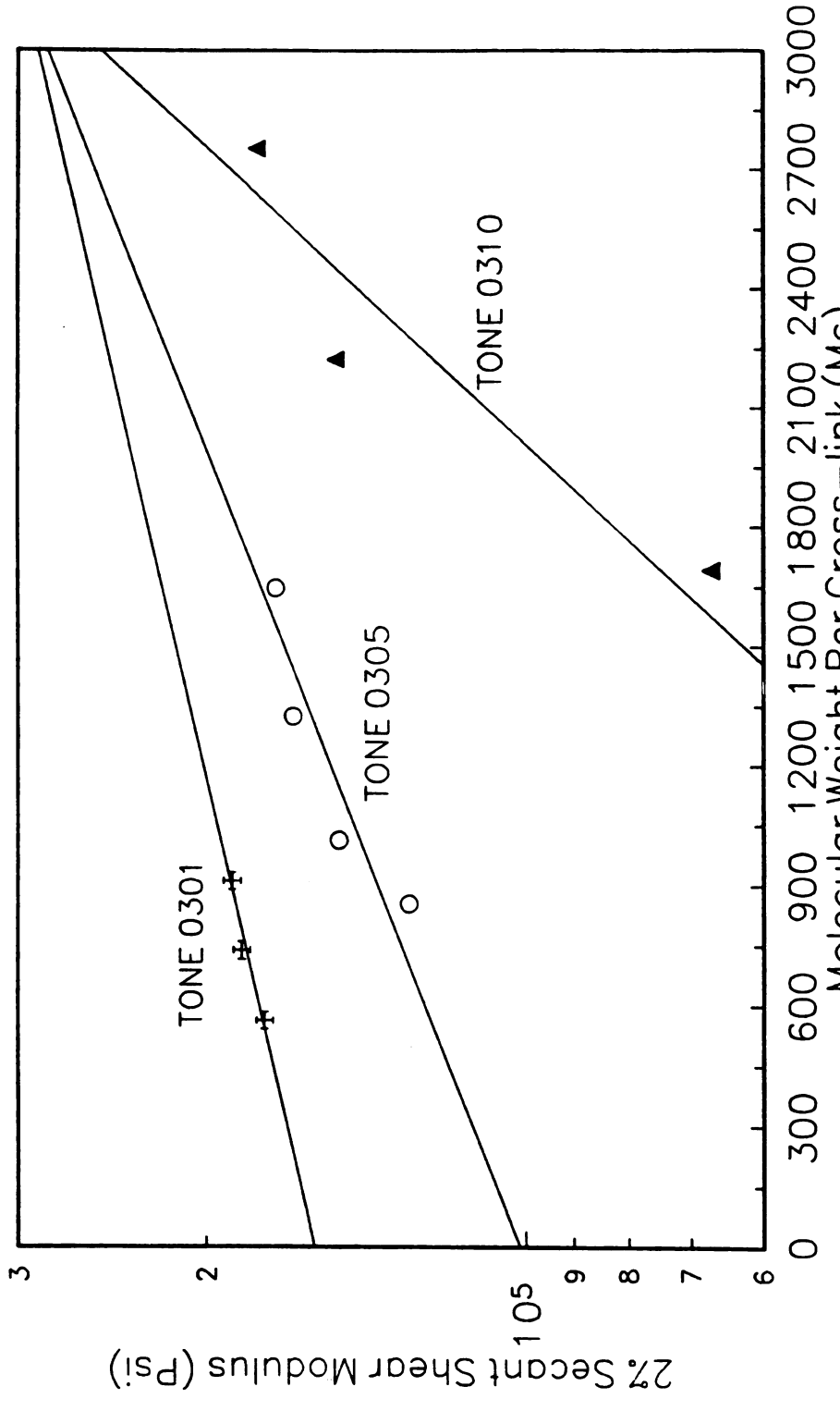

FIGURE 3.19 2% Secant Shear Modulus Versus Molecular Weight per Cross-Link (M_c) in Various Urethane Systems

TABLE 3.4

Adhesion of Various Polyurethanes to Glass Surface

Sample	Shear Adhesion (PSi)
10A	706 ± 4
10B	1590 ± 30
10C	2690 ± 60
10D	4640 ± 80
10E	5370 ± 300
5B	4160 ± 110
5C	4280 ± 90
5D	5240 ± 220
5E	5080 ± 360
1C	825 ± 340
1D	2120 ± 530
1E	3020 ± 1360

especially with sample 1E. Thus, a large number of 1E samples were tested to get reliable mean and standard deviation.

Figure 3.20 shows adhesion values to glass versus hard segment content for all the three types of urethane systems. Within each family of urethane systems, adhesion values increase with increasing hard segment content. For the same hard segment content (for example, 10C, 5C and 1C or 10D, 5D, and 1D) Tone 0305 based urethane shows better adhesion than Tone 0310, and Tone 0310 based urethane shows better adhesion than Tone 0301 based urethane.

Rao et al (Rao and Drzal, 1991, 1992) have shown that adhesion of graphite fibers to epoxy resin is dependent on the shear modulus of the matrix. A plot is made between the shear modulus of the various urethanes and their respective adhesion values to glass and is shown in Figure 3.21. From this figure we see that adhesion does increase with modulus in all the urethane systems and different urethane systems show different depencies. Higher modulus urethanes based on Tone 0301 show poor adhesion to glass. From the least square fit lines, we see that same level of adhesion could be obtained from lower modulus sample based on Tone 0310 polyol. Tone 0310 polyol has the highest molecular weight among all the polyols studied and based on thermal and mechanical characterization of these urethanes, we have seen that higher molecular weight polyol enhances phase separation. This suggests that along with modulus and hard segment content, phase separation in a segmented urethane system can have significant effect on its adhesion to glass.

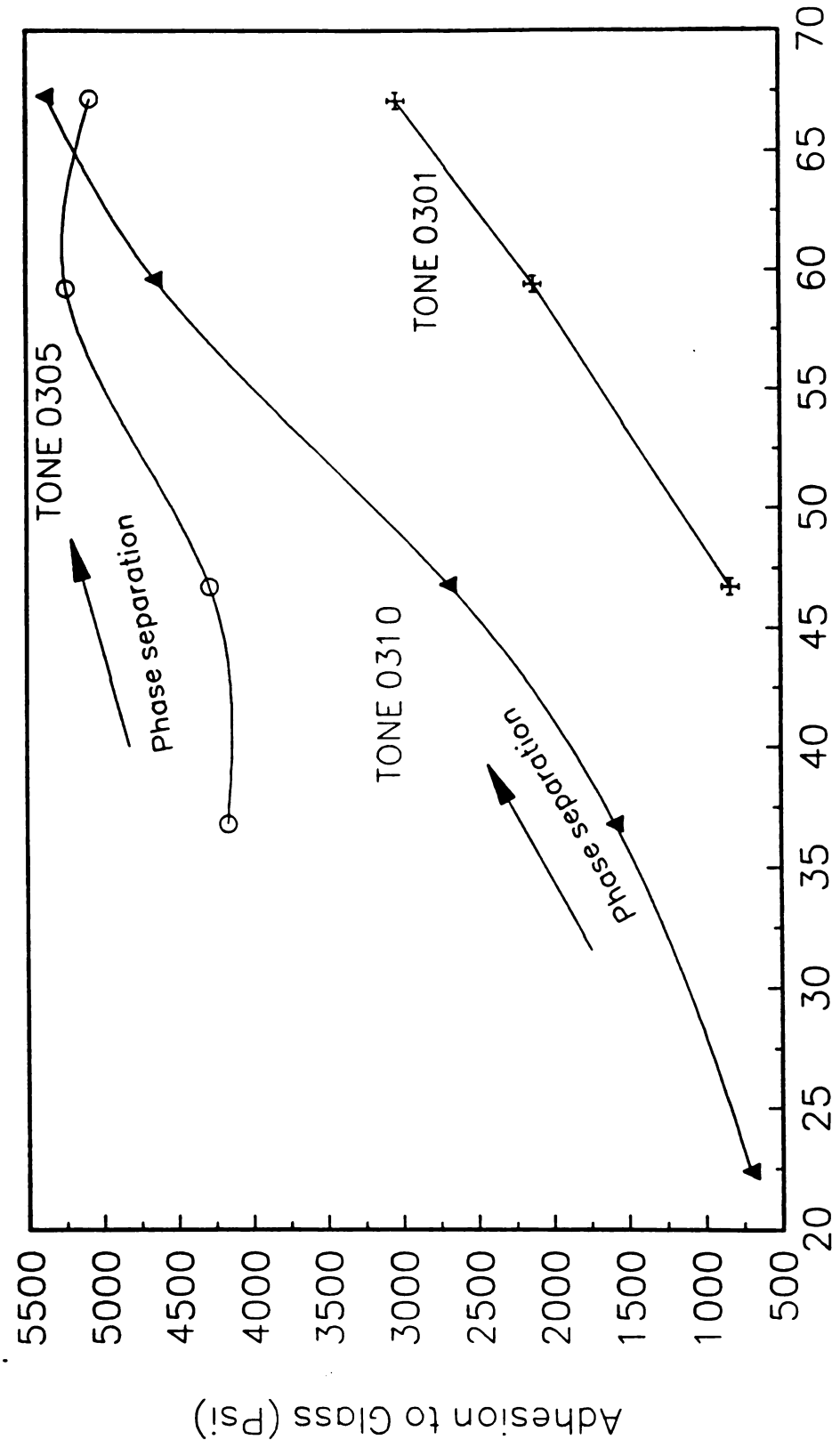

FIGURE 3.20 Adhesion to Glass Versus Hard Segment Content in Various Urethane Systems

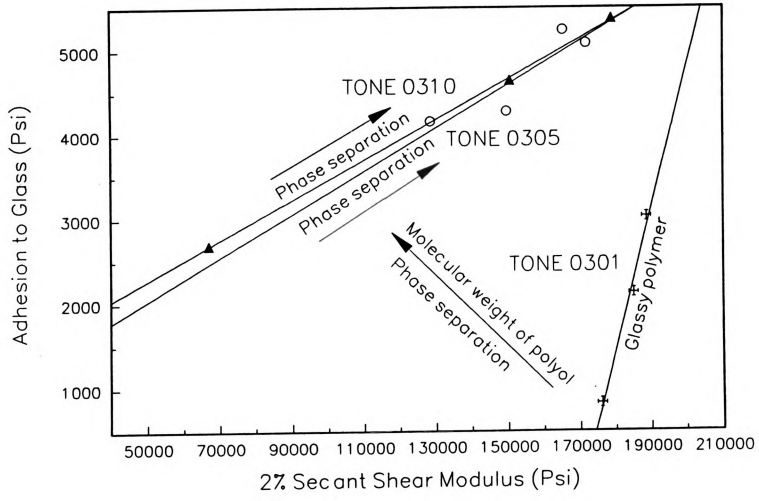

FIGURE 3.21 Adhesion to Glass Versus Shear Modulus of Various Urethane Systems

After adhesion testing, glass surfaces of the samples were observed for failure mode. Some of the samples had chunks of urethane left on the glass surface while other samples showed brittle failure and did not leave any visibly noticeable urethane. SEM micrographs of Tone 0310 based urethane samples are shown in Figure 3.22. As seen under optical microscope, SEM confirms the adhesive failure mode in samples 10A, 10B, and 10C and cohesive failure mode in samples 10D and 10E. The circular patterns in micrographs of 10D and 10E could be due to the microvoids present in the sample. To further analyze failure modes, x-ray photoelectron spectroscopy was used for all the samples. A control sample of glass was also run to obtain baseline data. Availability of nitrogen on the surface was then used as the indicator of urethane presence. Surface atomic concentration ratio of nitrogen per 100 carbon atoms was calculated from the narrow scans of the elemental regions for all the samples and are shown in Table 3.5. The control sample has atomic ratio of 0.84. All the urethane samples showed higher N/100C ratio than the control glass. This suggests that all the samples had some degree of cohesive failure in urethanes. Table 3.5 also shows theoretically calculated values of N/100C for all the urethane samples. These values are higher than the experimental values obtained from the glass surfaces. Hearn, et al (Hearn et al, 1988) have reported that air cured urethane surfaces in segmented polyurethanes tend to be richer in soft segments. This observation would help explain why surface concentration of nitrogen at the interface could be less than the bulk nitrogen concentration.

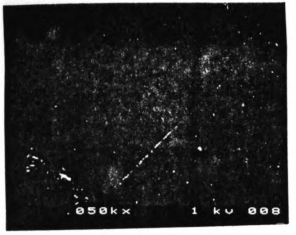

Sample - 10 A

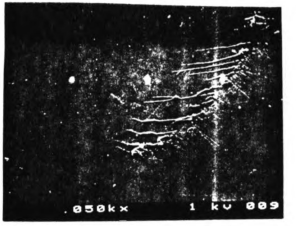

Sample - 10 B

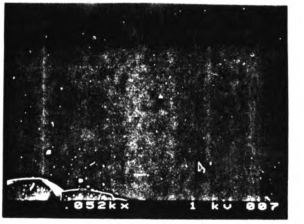

Sample - 10 C

Sample - 10 D

Sample - 10 E

FIGURE 3.22 SEM Micrographs of Glass Surfaces After Adhesion Testing of Tone 0310 Based Polyurethanes

TABLE 3.5

Atomic Concentration Ratio on Failed Glass Surface
from X-Ray Photoelectron Spectroscopy

Samples	N/100C	Theoretical Value
10A	2.8	6.8
10B	3.5	9.0
10C	5.9	10.4
10D	6.2	12.2
10E	9.0	13.3
5B	3.7	10.1
5C	6.2	11.4
5D	8.6	12.9
5E	7.8	13.9
1C	4.2	13.0
1D	5.7	14.1
1E	8.2	14.7
Glass	0.8	

3.6 CONCLUSIONS

Three different urethane systems were prepared from caprolactone-based triols with different molecular weights and the same chain extender and the same diisocyanate. Within each urethane system, hard segment content was varied by adding different amounts of the chain extender and the isocyanate. This type of experimental design allowed us to study effects of hard segment and triol molecular weight on thermal, mechanical, and adhesion characteristics of cross-linked segmented polyurethanes. DSC results showed that the transition temperature related to hard segment increased with increasing amount of hard segment content. This could be due to the increased hard segment chain length at higher hard segment content, promoting phase separation in urethanes. Thus, in a urethane system, phase separation phenomena is favored by increasing hard segment content. Also, the rate of increase of thermal transition temperature in different molecular weight triol-based urethanes indicated that phase separation phenomena was also favored by the higher triol molecular weight.

Both tensile and Iosipescu testing of the urethane samples showed nonlinear stress-strain behavior. The tensile and shear modulus data indicated that even though with increasing hard segment content within a urethane system, cross-linking density decreases, its modulus increases. This could be due to several factors including increased amount of aromatic isocyanate content, increased hydrogen bonding, increased phase separation, and many other factors. The modulus of the same hard segment content urethanes was found to be higher for lower molecular weight triols. Thus, cross-linking density seems to be the determining factor for modulus in the constant hard segment content urethanes. In the

case of higher molecular weight triol-based urethanes, the rate of increase of modulus with hard segment content is higher than that for the lower molecular weight triol-based polyurethanes. This indicates that phase separation is favored by larger polyol molecules.

Adhesion to glass for these cross-linked polyurethanes seems to be a coupled phenomena controlled by several factors, including hard segment content, modulus, molecular weight of triols, cross-linking density, and phase separation. In urethanes based on same molecular weight triols, higher modulus and higher hard segment content proved to improve adhesion to glass. In urethanes made with different molecular weight polyols, same level of adhesion was obtained with higher molecular weight polyol-based urethanes having lower modulus and lower hard segment content as compared to urethanes made with lower molecular weight polyols having higher modulus and higher hard segment content. This suggests that among many other factors, phase separation in cross-linked segmented urethanes can be a key factor in controlling adhesion to glass surfaces.

CHAPTER 4

PHASE SEPARATION IN POLYURETHANES AND ITS EFFECTS ON ADHESION TO GLASS

The work presented in this chapter has been submitted for publication in the Journal of Adhesion Science and Technology (1994).

4.1 ABSTRACT

Polyurethanes were prepared from different molecular weight polycaprolactone based polyols with varying amount of hard segment content made from toluene diisocyanate and butanediol. A theoretical model based on hard and soft segment miscibility was used to predict phase separation in these polyurethanes. Wide angle x-ray diffraction, near-infrared spectroscopy, and fourier transform infrared spectroscopy were used to experimentally determine phase separation in these polyurethanes. Good agreement was found between the experimental results and the theoretical predictions. The glass surfaces of the previously tested glass/urethane adhesion samples were analyzed using angular dependent x-ray photoelectron spectroscopy (ADXPS). ADXPS data revealed that an interphase region of approximately 20-100Å thickness was present between the urethane matrix and the glass substrate in each sample. The data also showed that the composition of the interphase region was influenced not only by the matrix composition but also by the phase separation in the matrix. The curve fitted C-1s spectra of the interphase region showed the presence of C-O type linkages which could be due to the presence of C-OH from the polyols and/or the butanediols and C-O-Si type bonds. These observations were

supported by the adhesion results of the various urethanes to glass substrates coated with a 2% solution of butanediol in acetone.

4.2 INTRODUCTION

Polyurethanes and especially segmented polyurethanes are widely used as elastomers and as engineering plastics. Polyurethanes are available as thermoplastics as well as thermosets. Thermoplastic polyurethanes are typically processed by injection molding and thermoset (cross-linked) polyurethanes are typically processed by reaction injection molding. In both types of urethanes, chopped glass fibers are commonly used as fillers to improve urethanes mechanical properties. Good adhesion between the glass reinforcement and the urethane matrix is desired to achieve the maximum benefits of the reinforcement. In other structural applications, good adhesion between urethane and glass surfaces may also be desired. Such applications include laminated windshields and modular windows. In modular windows for automobiles, for example, a glass panel is insert molded and encapsulated by a urethane gasket (Reilly and Sanok, 1988; Fielder and Carswell, 1990; Agrawal et al, 1991). Good adhesion between the glass panel and the urethane gasket is necessary to prevent water leaks and also to maintain the structural integrity of these glass modules.

In our previous study (Agrawal and Drzal, 1994), we investigated the relationship between the urethane structure and properties to its adhesion to glass surfaces. We found that, along with modulus and cross-link density, phase separation in the urethane also is a factor in adhesion to glass surfaces. The surface composition of the failed glass surfaces

after adhesion testing, as determined by the x-ray photoelectron spectroscopy (XPS), was quite different than the stoichiometric compositions of the urethane matrices indicating that an interphase had formed.

Several reports have been published in recent years discussing phase separation in polyurethanes. Numerous experimental techniques including fourier transform infrared spectroscopy (Yoon and Ratner, 1988; Camargo et al, 1982), near-infrared spectroscopy (Miller et al, Part I and II, 1990), differential scanning calorimetry (Yoon and Ratner, 1988; Camberlin and Pascault, 1983; Byrne et al, 1992; Chem et al, 1992), dynamic mechanical analysis (Camargo et al, 1985; Estes and Cooper, 1970), transmission electron microscopy (Schneider et al, 1975; Chang, 1984), x-ray photoelectron spectroscopy (Yoon and Ratner, 1988; Hearn et al, 1and 2, 1988; Vargo et al, 1991), and many others have been used by researchers to analyze phase separation in polyurethanes. The hard and soft segments have generally been found to phase separate into discrete phases with a domain size of 10-20 nm (Hearn et al, 1, 1988). Interfacial studies have shown that the surface of polyether based urethanes are enriched with the polyether when compared to the bulk (Yoon and Ratner, 1988; Hearn et al, 1, 1988). Recently, Deng and Schreiber (Deng and Schreiber, 1991) have discussed orientation phenomena at polyurethane surfaces in contact with different media. Yoon and Ratner (Yoon and Ratner, 1986) have related the urethane phase separation to its surface composition and found that where significant phase separation takes place, little or no hard segment could be found in the outermost few molecular layers of the polymers.

This study is an extension of our previous work and is directed at elucidating the relationship between polyurethane structure and adhesion to the glass surface. In this study, we have tried to correlate phase separation in polyurethanes to their adhesion behavior to glass surfaces. Theoretical and experimental techniques have been used to explore phase separation in model urethane compounds. A theoretical model based on phase miscibility has been used to predict phase separation and is coupled with by near-infrared and fourier transform infrared spectroscopy to experimentally determine the phase separation. Adhesion experiments have been performed to provide evidence regarding the role of phase separation in polyurethanes and its role in promoting adhesion to glass surfaces. X-ray photoelectron spectroscopy has been utilized to study the failed glass surfaces after adhesion testing to quantify the interphase structure and thereby understand the role of phase separation in urethanes and its role in adhesion.

4.3 EXPERIMENTAL

4.3.1 Materials

The polyurethanes used in this study were based on caprolactone polyols available from Union Carbide under the trade name "Tone." Hard segments were made from a 80%-20% mixture of toluene 2,4-diisocyanate and toluene 2,6-diisocyanate (TDI, Aldrich Chemical Co.) and 1,4-butanediol (BDO, Aldrich Chemical Co.) as the chain extender. The various urethane formulations studied in this work are shown in Table 4.1.

For adhesion testing, annealed soda-lime float glass plaques were used. ¼" x ¼" x ¼" blocks of urethanes were cast on the air side of the glass plaques. The details of urethane

TABLE 4.1

Urethane Formulations at Isocyanate Index of 1.0

Sample Designation	Polyol Type			BDO (Mole%)	TDI (Mole%)	Hard Segment (wt %)	Molecular Weight per Cross-Link (Mc)
	Tone 0301	Tone 0305	Tone 0310				
10A	-	-	X	0	60	22	1160
10B	-	-	X	22	56	37	1424
10C	-	-	X	31	54	47	1692
10D	-	-	X	34	53	60	2222
10E	-	-	X	41	52	67	2752
5B	-	X	-	7	58	37	854
5C	-	X	-	20	56	47	1013
5D	-	X	-	31	54	59	1324
5E	-	X	-	36	53	67	1646
1C	X	-	-	0	60	47	563
1D	X	-	-	18	57	59	739
1E	X	-	-	26	55	67	912
HS	-	-	-	50	50	100	-

mixing and adhesion sample preparation can be found in our previous publication (Agrawal and Drzal, 1994).

4.3.2 Wide Angle X-ray Diffraction (WAXD)

Wide angle x-ray diffraction patterns of the various urethane samples were recorded on a Rigaku RU200B diffractometer using a graphite monochromated CuKα radiation operated at 50kV and 100mA. The urethane sample size was 6mm x 6mm x 2mm and the reflected intensity was recorded as a function of 2θ angle at a rate of 0.25°/minute.

4.3.3 Near-Infrared Spectroscopy (NIR)

A 'Lambda-9' spectrophotometer made by Perkin-Elmer was used in transmission mode for near-infrared analysis of the urethane samples. Urethanes were cast directly onto the air-side of soda-lime glass plaques (similar to the plaques used for adhesion testing) and were cured for 24 hours @ 90°C. The cast urethane film thickness on glass was approximately ⅛". Although the total spectral range was 1100-2500 nm, only the region 1600-2100 nm was used for phase separation analysis. A slit width of 2 nm was used along with a 240 nm/minute scanning speed.

4.3.4 Fourier Transform Infrared Spectroscopy (FTIR)

The urethanes of this study were cross-linked urethanes. Thus, the conventional sample preparation methods of solution casting thin urethane films or salt plate methods could not be used. Also, liquid nitrogen grinding of urethanes for diffuse reflectance was not used due to the possible disruption of the urethane structure. To overcome this, urethane was

directly cured onto a silicone wafer. In this method, a small amount of urethane mixture was taken from the mixing vial and was quickly smeared on a silicon wafer using a cotton swab. The silicon wafer was then subjected to the same curing cycle as the glass-urethane adhesion samples (24 hours @ 90°C).

Fourier transform infrared spectra were acquired on a Bio-rad FTS-40 spectrometer in transmission mode. A silicon wafer was used in the background scan. All samples were scanned at room temperature using 4 cm^{-1} resolution and sixty-four scans were averaged for each sample.

4.3.5 X-Ray Photoelectron Spectroscopy (XPS)

Subsequent to adhesion testing, failed glass surfaces were analyzed using a Perkin-Elmer PHI5400 x-ray photoelectron spectrometer. An approximate ¼" x ¼" square area was sectioned from the failed glass surface and was placed inside the XPS chamber. The angular dependent XPS spectra were obtained at a base pressure of approximately 10^{-9} Torr. The standard Mg Kα source was used for all sample analysis and was operated at 300W (15 kV, 20 mA). A continuously variable angle sample stage was used and was programmed for 15°, 45°, and 90° angles (photoelectron take-off angle). A 2.0 mm diameter circle of the sample was analyzed by the spectrometer. Data was collected in the fixed analyzer transmission mode utilizing a position sensitive detector and a 180° hemispherical analyzer. Pass energies were set at 89.45 eV for the survey scans (0-1000 eV) and at 35.75 eV for the narrow scans of the elemental regions. Data collection and manipulation was performed with an Apollo 3500 workstation running PHI ESCA

software. The curve fitting was carried out using a modified Gauss-Newton nonlinear least squares optimization procedure that is part of the instrumental software. The C-1s binding energy of the graphitic peak was set to 285.0 eV for calibration purposes.

4.4 THEORETICAL CONSIDERATION OF PHASE SEPARATION

The hard and soft segments in polyurethane molecules can phase separate into hard and soft domains in the bulk. One of the important driving forces for this phase separation is the difference in solubility between the hard and the soft blocks (Macosko, 1989). Several researchers (Macosko, 1989; Camberlin and Pascault, 1984; Rayn et al, 1988) have used the Flory-Huggins interaction parameter χ to successfully estimate soft and hard segment miscibility in segmented polyurethanes.

$$\chi_{HS} = \chi_{(\Delta S)} + \frac{V_R}{RT}(\delta_H - \delta_S)^2 \tag{4.1}$$

Here χ_{HS} is interaction parameter between hard and soft segments, δ_H and δ_S are solubility parameters of hard and soft segments and V_R is a reference volume. $\chi_{(\Delta S)}$ is an entropy term and can be neglected for polymer systems so that equation (4.1) becomes

$$\chi_{HS} = \frac{V_R}{RT}(\delta_H - \delta_S)^2 \tag{4.2}$$

At T = 298K with RT in calories and the reference volume V_R taken as 100 cm^3/mol (Camberlin and Pascault, 1984), the equation (4.2) reduces to

$$\chi_{HS} = \frac{1}{6}(\delta_H - \delta_S)^2 \tag{4.3}$$

The soft segment in the urethanes of this study is based on the polycaprolactone polyol and its solubility parameter is $\delta_s = 9.1$ $(cal/cm^3)^{1/2}$ (Brandrup and Immergut, 1989). The hard segment is based on toluene-diisocyanate and butanediol and its structure is shown below:

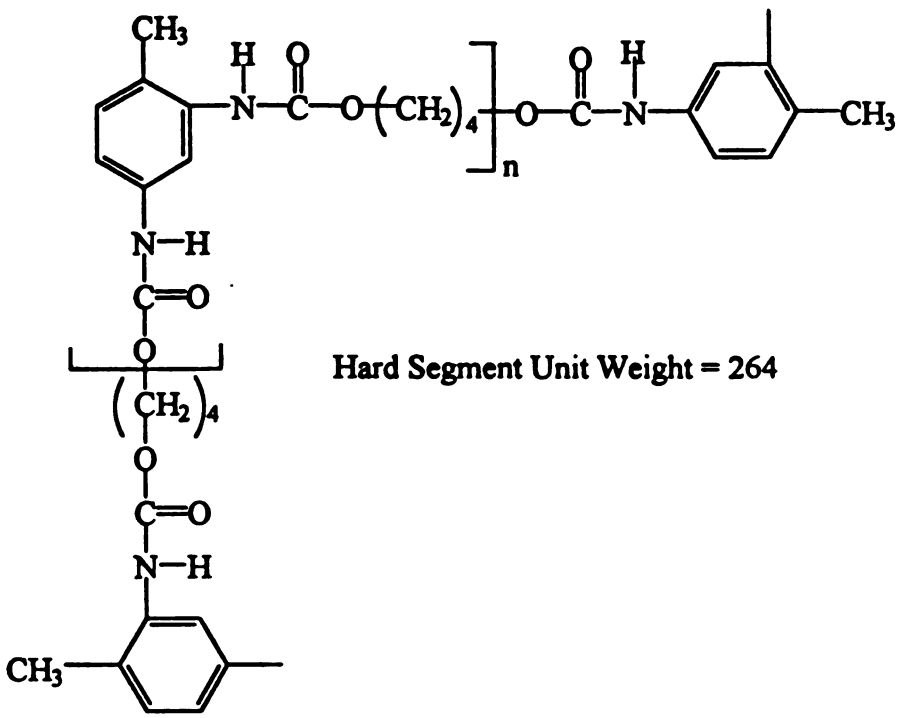

Hard Segment Unit Weight = 264

Since the solubility parameter of this hard segment could not be found in the literature δ_H was estimated from the group contribution method (Van Krevelen, 1990) using cohesive energy data reported by various authors; and Small's approach. Very good agreement was found between the δ_H values obtained by the different approaches. An average of the various calculated δ_H value was taken and was found to be 12.44 $(cal/cm^3)^{1/2}$. The details of δ_H calculations are listed in Appendix A.

Thus, the hard and soft segment miscibility can be characterized by

$$\chi_{HS} = \frac{1}{6}(12.44-9.1)^2 = 1.86\ cal/cm^3 \tag{4.4}$$

The onset of phase separation, for a mixture of two polymers, A and B, can be predicted using the Flory-Huggins relationship (Macosko, 1989) to estimate the critical interaction parameter.

$$\chi_C = \frac{1}{2}\left[\frac{1}{\sqrt{N_A}} + \frac{1}{\sqrt{N_B}}\right]^2 \tag{4.5}$$

where N_A and N_B are the numbers of repeat units in polymers A and B.

In segmented polyurethanes, the above equation is not applicable, as polyurethanes are not blends of two polymers but are block copolymers. Benoit and Hadziioannou (Benoit and Hadziioannou, 1988) have developed phase diagrams as a function of repeat sequence in a multiblock copolymers having various architectures. The phase diagrams provide $\chi_C(N_H + N_s)$ for various hard segment contents where χ_C is the critical interaction parameter for the onset of phase separation. N_H and N_s are numbers of monomer units in hard and soft chain segments. These monomer units are not taken in the classical sense of polymer chemistry. They are subunits having the same volume.

The molar volume of caprolactone is ~ 105 cm^3/mol (calculated by group contribution method, Van Krevelen, 1990) and its molecular weight is 114. These values were

assigned to a repeat unit and used to calculate the values of N_s and N_H. Listed in Table 4.2 are the N_s values for the various polyols and in Table 4.3 are the N_H values for the different hard segment lengths. The average lengths of hard blocks are calculated for stoichiometric formulations of the various urethanes and are shown in Table 4.4.

Table 4.5 shows the calculated $\chi_C$values based on the phase diagram developed by Benoit and Hadziioannou (Benoit and Hadziioannou, 1988). Phase separation will occur when $\chi_{HS}>\chi_C$ (χ_{HS} = 1.86). The phase separation predictions for the various urethane formulations are also shown in Table 4.5. The relative degree of phase separation can also be judged by the difference between the χ_{HS} and χ_C values.

4.5 RESULTS AND DISCUSSION

4.5.1 Bulk Morphology

WAXD curves for the various urethane samples were obtained. Due to the small sample size, the scans were noisy but adequate for qualitative assessment of hard segment crystallinity. The curves showed no sharp crystalline reflection and were characteristic of amorphous systems. This indicated the absence of three dimensional order in the hard segment domains of these samples. This finding is as expected due to the molecular asymmetry in TDI and also with the observations reported by other researchers (Legge et al, 1987).

Infrared spectroscopy was used to evaluate phase separation in the samples. Hydrogen bonding has been considered as an essential part in the stabilization of hard-segment

TABLE 4.2

'N_s' Values for Various Polyols

Soft Segment	Molecular Weight	N_s
Tone 0301	300	~ 3
Tone 0305	540	~ 5
Tone 0310	900	~ 8

TABLE 4.3

'N_H' Values for Different Hard Segment Lengths

Hard Segment	Calculated Molar Volume cm^3/Mol (Ref. 26)	N_H
O	132.4	~1
O-O	347.6	~3
O-O-O	562.8	~5
O-O-O-O	778.0	~7

Designation: Toluene diisocyanate - 'O'
Butanediol - '-'

TABLE 4.4

'$N_H + N_s$' Values for Various Urethane Formulations

Urethane Formulations	Appoximate Hard Segment Length Percentages				Avg. N_H	N_s from Table 2	$N_H + N_s$
	O	O-O	O-O-O	O-O-O-O			
10A	100				1	8	9
10B	33	66			2.3	8	~10
10C		66	33		3.6	8	~12
10D		28	72		4.4	8	~12
10E				100	7	8	~15
5B	86	14			1.3	5	~6
5C	46	54			2.1	5	~7
5D		68	32		3.6	5	~9
5E			86	14	5.3	5	~10
1C	100				1	3	4
1D	55	45			1.9	3	~5
1E		100			3	3	6

Designation: Toluene diisocyanate - 'O'
Butanediol - '-'

TABLE 4.5

Calculation of Critical Interaciton Parameter χ_c

Urethane Formulations	Wt. % Hard Segment	χ_c	Phase Separation ($\chi_{HS} > \chi_C$)
10A	22	5.6	No
10B	37	1.4	Yes
10C	47	0.97	Yes
10D	60	0.89	Yes
10E	67	0.76	Yes
5B	37	2.33	No
5C	47	1.66	Yes
5D	59	1.19	Yes
5E	67	1.14	Yes
1C	47	2.9	No
1D	59	2.14	No
1E	67	1.9	No

structure, and has been taken into account in different hard segment models (Bonart et al, 1974; Blackwell and Gardner, 1979). The extent of interurethane hydrogen bonding can be estimated by infrared spectroscopy. In urethanes, a large fraction of the N-H groups of the urethane linkage $\overset{(-N-C-O-)}{\underset{H\ O}{|\ \ ||}}$ is hydrogen bonded.

A recent review article (Miller, 1991) discusses use of near-infrared spectroscopy (NIR) in polymer analysis. Also, Miller et al (Millert et al, I and II, 1990) have shown the usefulness of NIR in phase separation studies in polyurethanes. Since soda-lime float glass is transparent in NIR region and sample preparation was very easy NIR was selected for phase separation evaluation in this study. Figures 4.1, 4.2, and 4.3 show the NIR transmission spectra (in the region 1600-2100 nm) of the various urethane samples. This region of NIR spectra is dominated by carbonyl stretching bands (1915 nm), C-H stretching first overtone region (1600-1800 nm) and N-H combination band (around 2045 nm). Peak assignments are taken from the published literature (Miller et al, I and II, 1990; Miller, 1991). The absorption peaks in general are very broad and the carbonyl peak at 1915 nm is very weak. Thus, the N-H peak alone was used to study hydrogen bonding.

Each sample shown in Figure (4.1, 4.2, and 4.3) has a NIR spectrum similar to the 100% hard segment (HS) composition which is independent of the polyol type and quantity. The N-H band in the HS sample appears at 2065 nm, which has a high degree of hydrogen bonding. In Figure 4.1, for urethanes based on the high molecular weight polyol Tone 0310, the N-H band for sample 10A appears at 2045 nm which can be assigned to

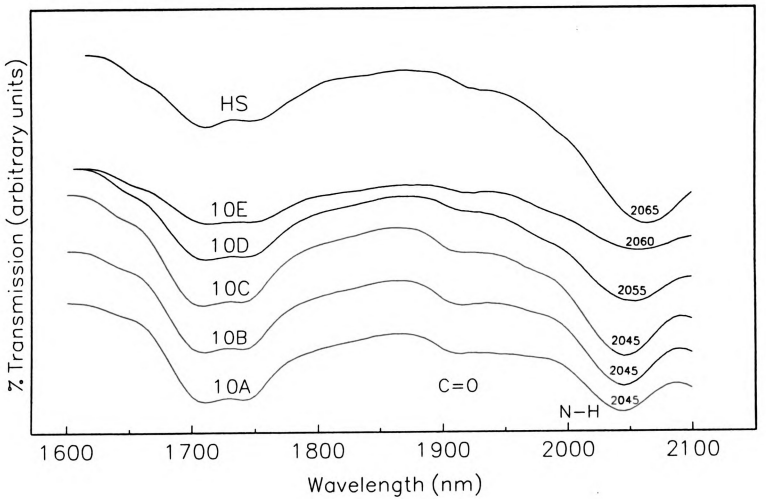

FIGURE 4.1 NIR Spectra of Tone 0310 Based Polyurethanes with Varying Hard Segment Content

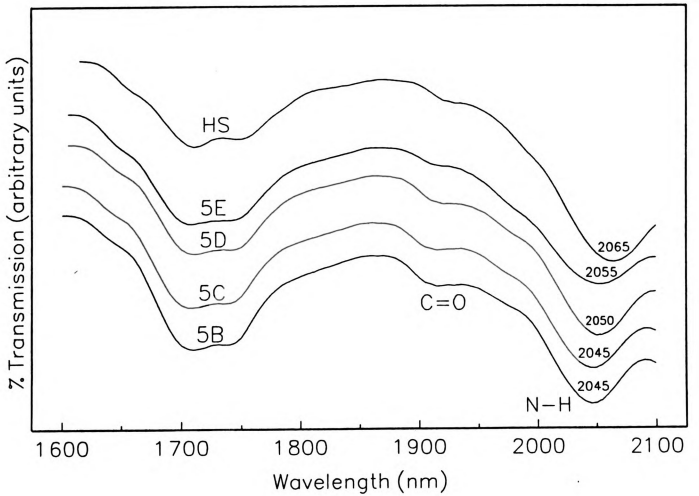

FIGURE 4.2 NIR Spectra of Tone 0305 Based Polyurethanes with Varying Hard Segment Content

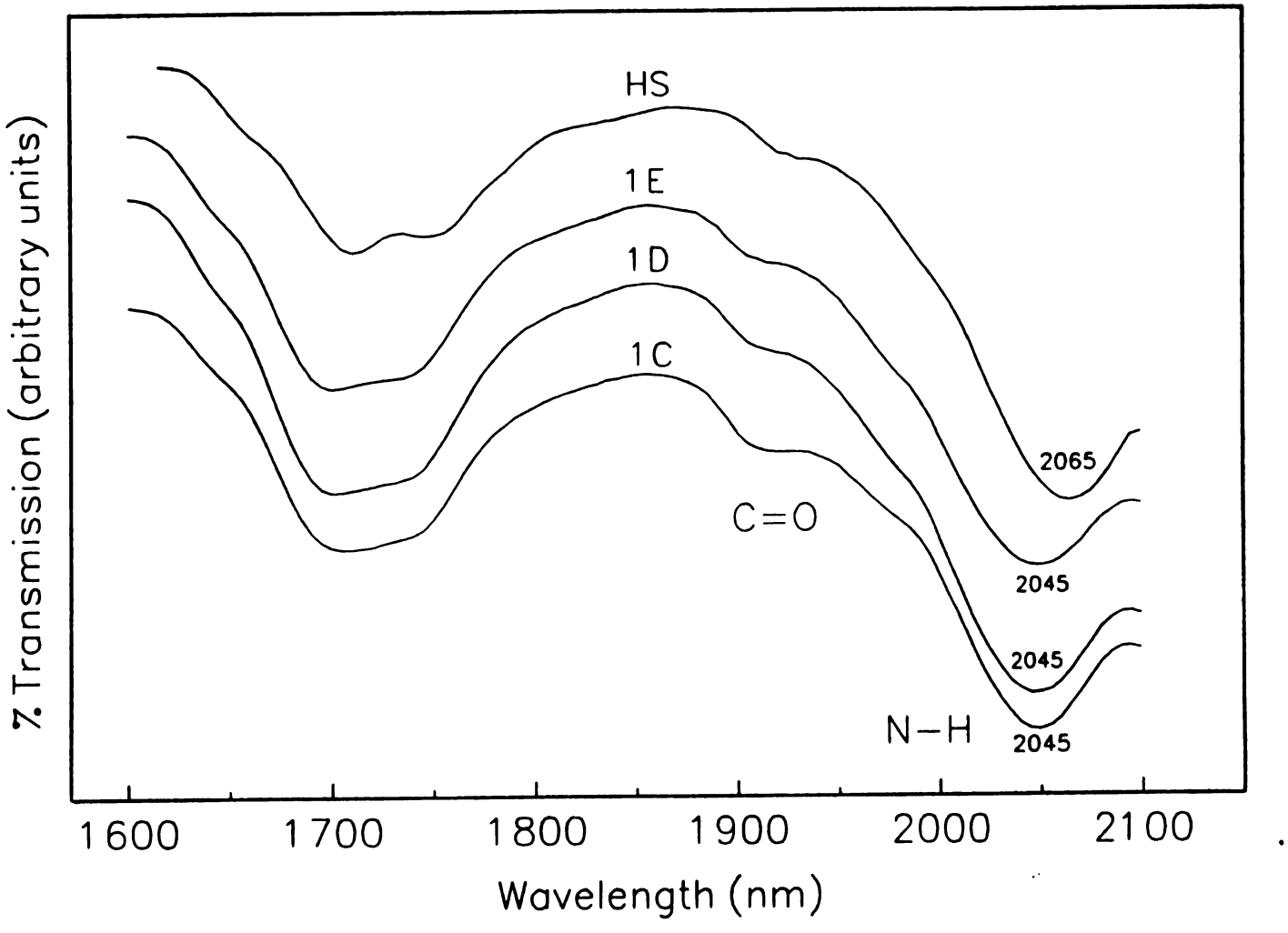

FIGURE 4.3 NIR Spectra of Tone 0301 Based Polyurethanes with Varying Hard Segment Content

unbonded N-H (Miller et al, II, 1990). We see that for the higher hard segment content samples 10B, 10C, 10D, and 10E, the N-H bands incrementally shift toward the HS sample band at 2065 nm with largest shift in the sample 10E. Small spectral shifts can be due to several things including crystallinity and hydrogen bonding as discussed by Garton (Garton, 1992). Since the hard segments in these polyurethane samples are amorphous, these spectral shifts could be due to the increased hydrogen bonding with increased hard segment content in these samples. This suggests that phase separation in the urethanes based on Tone 0310 increases with increasing hard segment content and samples 10D and 10E have some degree of phase separation. Similar trends but to a lesser degree can also be seen in urethanes based on the medium molecular weight polyol Tone 0305 (Figure 4.2). On the other hand, in the urethanes based on the lowest molecular weight polyol Tone 0301 (Figure 4.3), the N-H band occurs around 2045 nm for all the samples with different hard segment content (1C, 1D, and 1E) and no spectral shift is observed. This suggests that the urethane samples based on Tone 0301 are not phase separated.

FTIR spectroscopy was used to verify the observations from the NIR spectroscopy. Figure 4.4 is an FTIR spectra of the cured urethane sample 10B. The isocyanate asymmetric vibration band usually occurs between 2260-2280 cm^{-1}. In Figure 4.4, there is no free isocyanate peak present. Thus, it can be concluded that the urethane reactions in sample 10B must have been completed. The peak at ~3335 cm^{-1} is assigned to hydrogen bonded amide hydrogen and the region around 1700 cm^{-1} is assigned to a carbonyl band (Yoon and Ratner, 1988; Camargo et al, 1982). These regions are analyzed here in detail for the various urethane formulations.

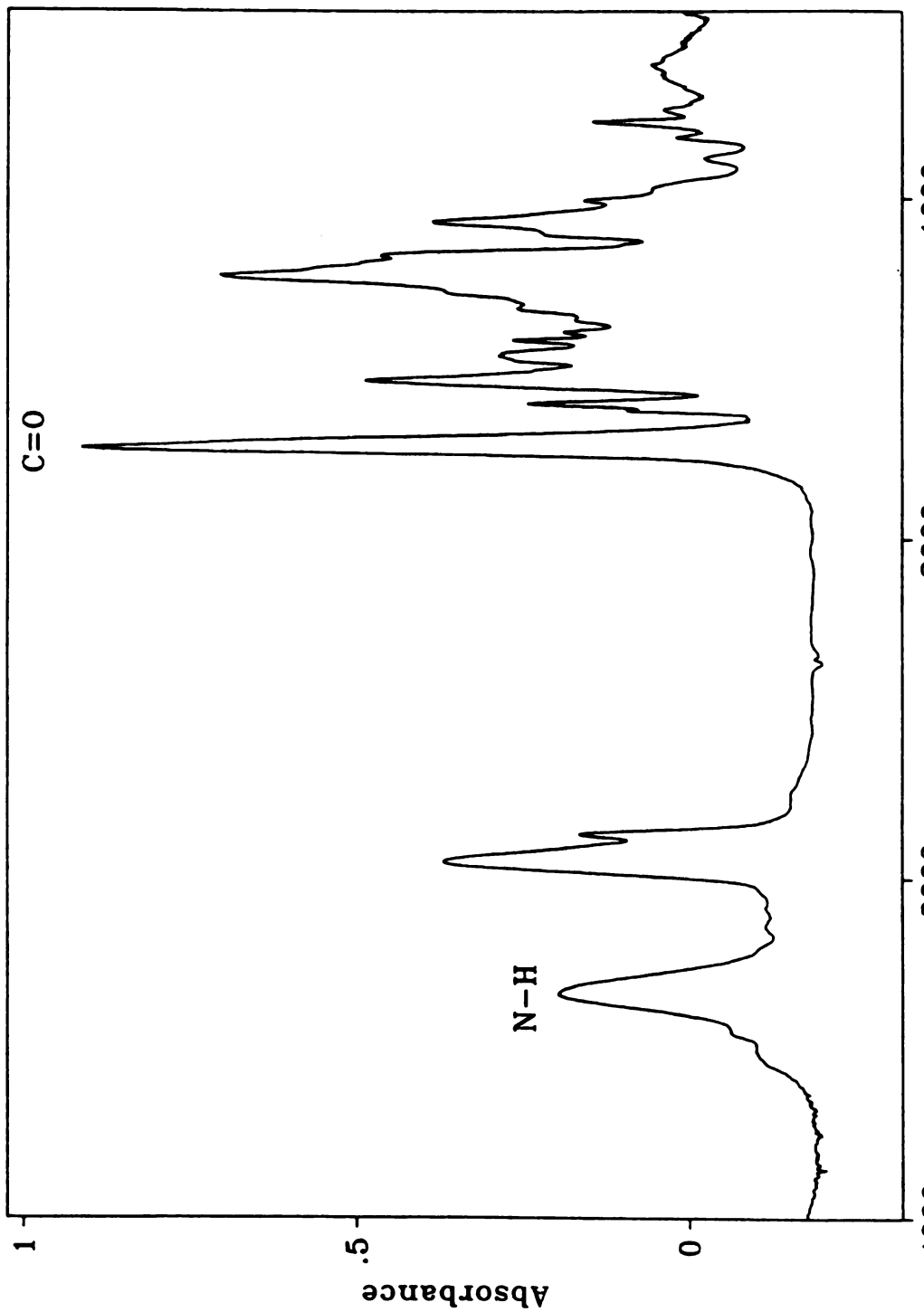

FIGURE 4.4 FTIR Spectrum of Sample 10B

Figure 4.5 shows the N-H band for Tone 0310 based urethane samples 10A, 10B, 10D, and 10E in the increasing order of the hard segment content. The peak locations are 3343 cm^{-1} for sample 10A, 3337 cm^{-1} for sample 10B, 3323 cm^{-1} for sample 10D, and 3323 cm^{-1} for sample 10E. This spectral shift is in agreement with the NIR data and suggests that the degree of phase separation increases with increasing hard segment content.

Figure 4.6 shows the carbonyl region of the FTIR spectra for the samples 10A through 10E. The band at 1736 cm^{-1} is associated with C=O stretching absorption in a non-hydrogen bonded state while the lower wave number peak at 1712 cm^{-1} represents the absorption of C=O hydrogen bonded with the N-H groups. The 1736 cm^{-1} peak is a result of the nonbonded carbonyl peaks of the urethane linkages in the samples and the ester linkages in the polyol portion of the samples. Thus we do not expect the 1736 cm^{-1} band to ever disappear but the 1712 cm^{-1} peak should increase in intensity with respect to the 1736 cm^{-1} peak as phase separation increases. It is clear from the graph that the 1712 cm^{-1} peak intensity increases with increasing hard segment content. This supports the earlier made observation from the N-H peak regarding phase separation. Thus, the order of phase separation in the samples studied is 10E>10D>10C>10B>10A.

4.5.2 Interphase Composition

The phase separation discussed applies to the bulk polyurethane samples. The bulk phase separation affects mechanical properties such as modulus, but in our previous study (Agrawal and Drzal, I, 1994) we found that modulus alone could not explain the adhesion

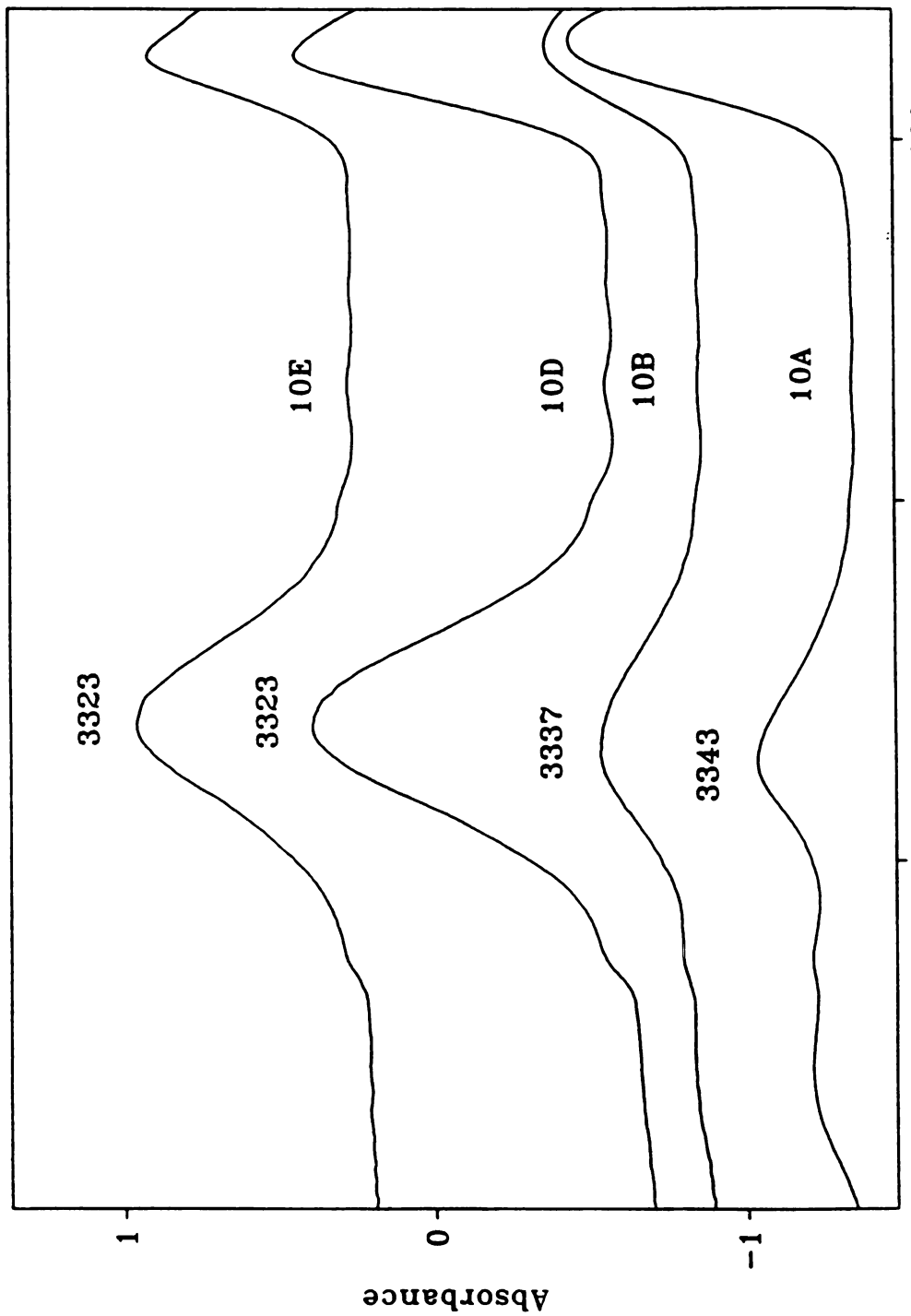

FIGURE 4.5 FTIR Spectra of N-H Band in Tone 0310 Based Polyurethanes with Varying Hard Segment Content

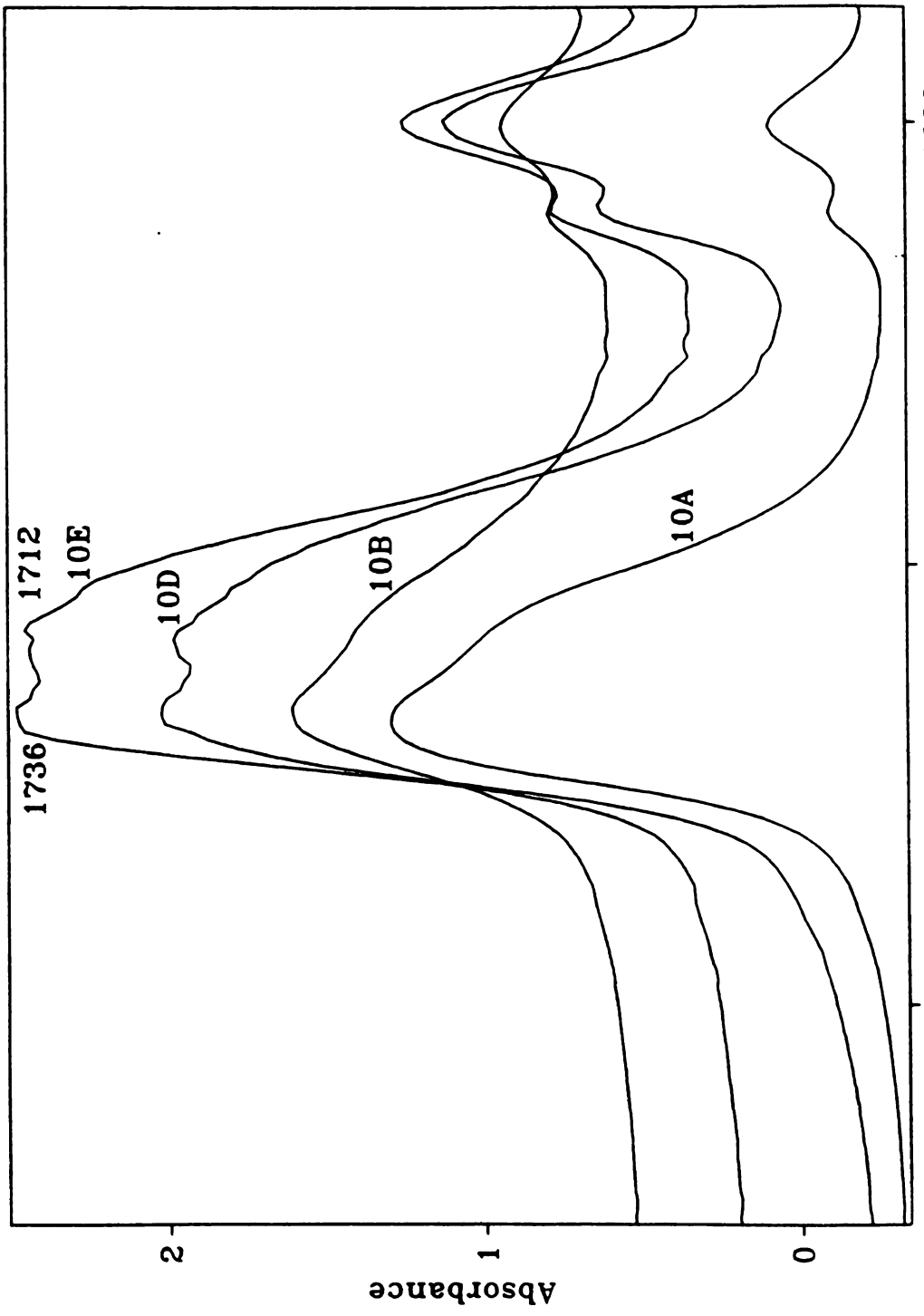

FIGURE 4.6 FTIR Spectra of Free (1736 cm^{-1}) and Hydrogen Bonded (1712 cm^{-1}) Carbonyl Bands in Tone 0310 Based Polyurethanes with Varying Hard Segment Content

results of these urethane samples to glass surfaces. Several researchers have reported that compositional gradients exist within the surface region of urethanes (Yoon and Ratner, 1988; Hearn et al, 1, 1988). Hearn et al (Hearn et al, 2, 1988) have also linked phase separation in urethanes to its surface composition. They found that when significant phase separation took place, little or no hard segment was found on the outermost surface. To explore the effects of phase separation on adhesion, some selected failed glass surfaces of the adhesive joints tested in our previous study (Agrawal and Drzal, 1994) were analyzed using angular dependent XPS. Samples 10D, 5D, and 1D, all of which have the same hard segment content and 10B, which has very low hard segment content and very low modulus were included in the XPS study.

Figure 4.7a shows a low resolution (pass energy 89.45 eV) survey spectrum of a bare soda-lime glass with major peak assignments. The presence of sodium and calcium is indicative of the glass being a soda-lime glass. Figure 4.7b is a survey spectrum of a failed glass sample 1D after adhesion testing. The distinct presence of the nitrogen peak indicates presence of residual urethane on the failed glass surface.

High resolution (pass energy 35.75 eV) angular dependent XPS scans of samples 10D, 5D, 1D, and 10B were obtained at three different photoelectron take-off angles 15°, 45°, and 90° to vary the sampling depth. The 15° angle scans provided the composition in the uppermost atomic layer (~20Å) whereas the sampling depth in the 90° angle scans could be ~100Å and the 45° angle scans, somewhere in between. Figure 4.8 shows the curve fitted C-1s spectra of the four samples studied at 90° angle. These spectra have been

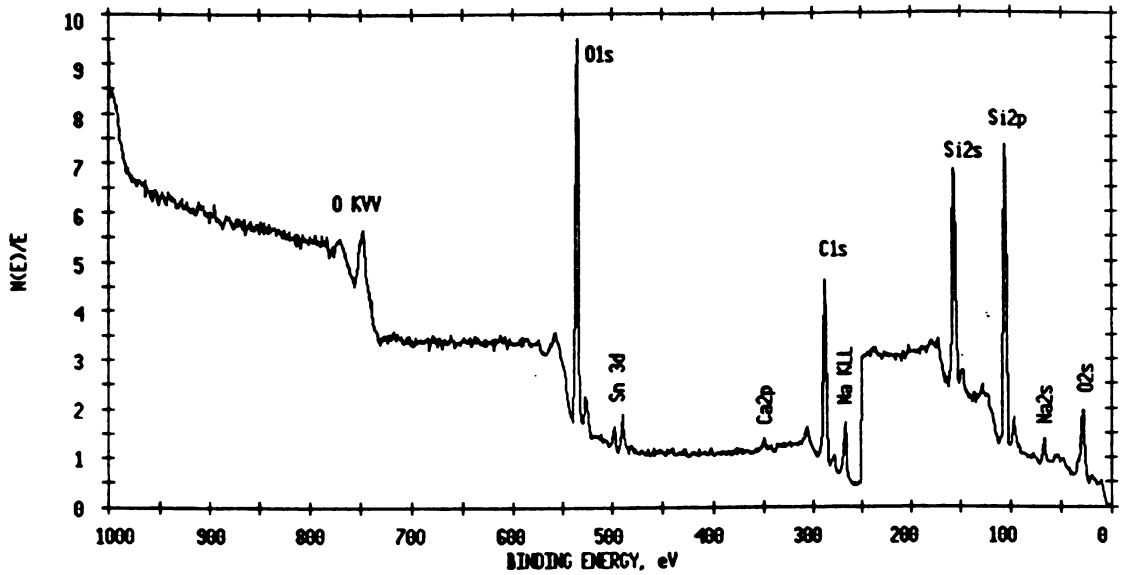

a

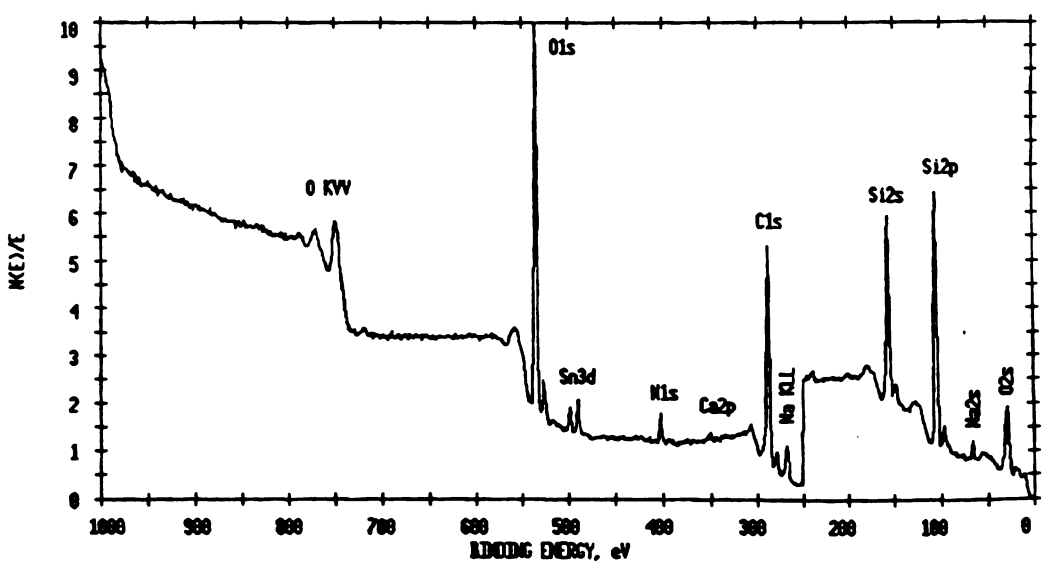

b

FIGURE 4.7 XPS Survey Scans (a) Bare Soda-Lime Glass, (b) Failed Glass Sample 10B

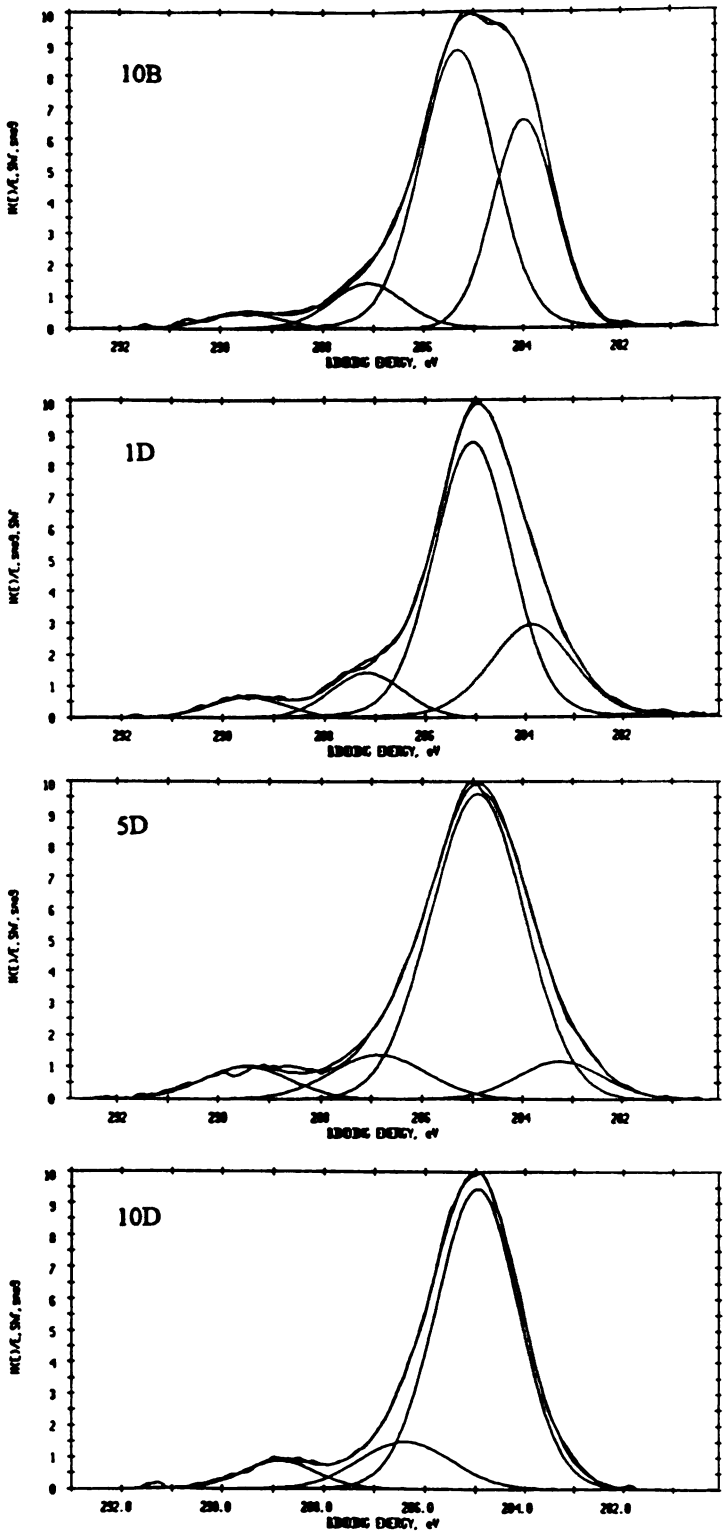

FIGURE 4.8 Curve Fit C 1s Spectra of Failed Glass Samples at 90° Photoelectron Take-Off Angle

charge corrected with the C-C peak referenced to 285.0 eV. A cursory look at the spectra reveals that there are several binding states of carbon present on the samples, both at higher and at lower binding energies of C-C bonds (285.0 eV). The lower binding energy peak can be associated to carbon attached to positively charged sodium (Na^{+}) and calcium (Ca^{++}) ions present in the soda-lime glass substrate. The higher binding energy component (~286.5 eV) can be due to the energy shift caused by C-O single bond environment. This may include C-O-C ether type linkage, unreacted free hydroxyls C-OH from polyols and chain extenders and C-O-Si type linkages with the glass surface. Since the polyols used in these urethanes are polyester type, the presence of the ether linkage is unlikely. The even higher binding energy component at ~289.5 eV can be due to the urethane linkage (Hearn et al, 2, 1988; Vargo et al, 1991) present on the samples. The C-1s peak binding energies and the relative peak areas for the samples are shown in Table 4.6. As seen from the table, the lower binding energy component (~283.5 eV) is much smaller for the sample 10D than the other samples and is very high for the sample 10B. This might be due to the thickness variation of the residual film on the glass surfaces, with the film being thickest in the sample 10D and thinnest in the sample 10B. The Na^{+} and the Ca^{++} ions might have migrated into the residual film and are within the sampling depths of the XPS in 10B, 1D, and 5D while not so in the case of the sample 10D due to the greater residual film thickness.

The atomic percent concentrations of O, N, C, and Si obtained from the high resolution XPS spectra at different photoelectron take-off angles are shown in Table 4.7. It is clear from the data that as the sampling depth increases, the Si concentration increases with

TABLE 4.6

C 1s Peak Binding Energies and Relative Peak Areas
of Carbon Chemical States on Various Failed Glass Samples

Sample	Peak I		Peak II		Peak III		Peak IV	
	B.E. (eV)	Area (%)	B.E. (eV)	Area (%)	B.E. (eV)	Area (%)	B.E. (eV)	Area (%)
10D	283.71	3.24	284.96	76.94	286.38	13.33	288.86	6.50
5D	283.23	8.26	284.89	74.17	286.85	10.52	289.45	7.05
1D	283.86	23.92	285.06	62.67	287.15	9.15	289.49	4.27
10B	283.98	33.38	285.32	54.62	287.09	8.99	289.51	3.00

TABLE 4.7

O 1s, N 1s, C 1s, and Si 2p Atomic Percent Concentrations at Different Photoelectron Take-Off Angles

Samples	15°				45°				90°				Stoichiometric			
	O	N	C	Si	O	N	C	Si	O	N	C	Si	O	N	C	Si
10D	28.40	2.21	58.76	10.63	39.24	2.24	43.32	15.20	47.91	1.51	30.04	20.54	21.03	8.62	70.34	-
5D	30.12	1.79	54.50	13.58	40.65	3.03	39.67	16.65	52.62	1.69	24.56	21.13	20.77	9.05	70.17	-
1D	37.57	0.50	46.17	15.76	47.23	1.46	31.78	19.53	50.91	1.57	25.43	22.09	20.53	9.8	69.67	-
10B	47.97	0.82	35.76	15.45	54.57	0.81	23.13	21.49	45.84	1.94	29.34	22.89	21.03	8.62	70.33	-

being highest at the 90° angle and is close to that of the bare glass. The Si atomic concentration can also be used to compare the relative thicknesses of the residual films on the glass surfaces. The Si concentration in 10D is the lowest followed by 5D and 1D in the 15° angle scans. The Si concentration in 1D and 10B are almost the same. The same trend can also be seen in the 45° and the 90° XPS scans. This suggests that the residual film is thicker in the sample 10D, followed by the samples 5D and 1D. The residual films in the samples 1D and 10B are almost of the same thickness. The C-1s concentrations in the various samples also indicate the same residual film thickness trend.

In Table 4.7, the stoichiometric atomic concentrations of the various urethane samples are also listed in the far right column. On comparing the XPS derived atomic concentrations with the stoichiometric values, we see that the carbon and nitrogen atomic concentrations are much less than that of the bulk matrix.

Based on the atomic compositions of the residual films in all the samples and their variation with the sampling depths, we can state that the residual films on the glass substrates have a general thickness range 10-100Å and have both inorganic and organic constituents. These residual films are an interphase region which has a composition intermediate to that of the glass substrate and the urethane matrices.

The urethane matrix composition directly affects the proposed interphase region between the matrix and the glass substrate. The XPS data also suggests that the phase separation in the matrix also affects the composition and thickness of the interphase region. The high

C-1s atomic concentration and the greater thickness of the interphase region in the sample 10D could be the result of phase separation phenomena, causing the preferential segregation of the polyol and/or the low molecular weight chain extender butanediol to the surface. Whereas in the poorly phase separated sample 1D, preferential segregation of the polyol and/or the chain extender didn't take place to any appreciable extent resulting in a thinner interphase region not so rich in the C-O type linkages.

The curve fit C-1s spectra also reveals that the amount of the high energy component (~289.5 eV) carbon is in good agreement with the N-1s atomic concentration. This suggests that the 286.5 eV component in the interphase region is likely due to the presence of the butanediol rather than the polyols since the polyol should contribute to the ~289.5 eV peak.

4.5.3 Adhesion Results

An adhesion experiment was designed to check the validity of the above made observations. The air side of clean soda-lime glass plaques were coated with a thin layer of a 2% (by weight) solution of 1,4 butanediol in acetone in order to facilitate phase separation in the interphase. Upon drying of the film, various urethane blocks were cast onto the glass surface (detailed procedure can be found in Ref. Agrawal and Drzal, 1994). Upon curing, the samples were allowed to age for a week prior to the adhesion testing. The adhesion of the urethanes to the glass substrate was evaluated using a block-shear method (Agrawal and Drzal, I, 1994) and the results are shown in Table 4.8. Also

TABLE 4.8

Adhesion of Various Polyurethanes to Glass Surfaces (Psi)

Samples	2% Secant Shear Modulus (Psi) Iosipescu Testing (Ref. 4)	Adhesion to Bare Glass Substrate (Psi) (Ref. 4)	Adhesion to Glass Substrate Coated with a 2% BDO Solution (Psi)
10D	150,653	4640 ± 80	4550 ± 80
5D	165,404	5240 ± 220	4560 ± 270
1D	184,962	2120 ± 530	4980 ± 850
1C	176,060	825 ± 340	4120 ± 130
10B	1,400*	1590 ± 30	1510 ± 50

*Tensile Modulus, sample was too soft for Iosipescu testing

shown in Table 4.8 are the adhesion data for the urethanes without any coating on the glass substrates.

The data reveal that the adhesion values of the urethane samples 10D, 5D, and 10B are not significantly affected by the 2% BDO coating on the glass surface. On the other hand, the adhesion values of the samples 1D and 1C have significantly improved over the previously reported values obtained on bare glass. This experiment indicates that by coating the glass substrate with the 2% BDO solution, we have modified the interphase region in the samples 1D and 1C to be similar to the interphase regions in the other urethane samples. Interphase modification of the samples 10D and 5D with the BDO coating showed little effect on the adhesion in these samples because the adhesion values obtained with or without the 2% BDO coating are all close to the cohesive strength of the glass substrate. The adhesion data for the sample 10B remain unchanged because it is an elastomeric material with very low modulus as compared to the other urethane samples (Table 4.8). This suggests that both the interphase region and the matrix are contributing factors in adhesion of urethanes to bare glass and either one may be a limiting factor.

4.6 CONCLUSIONS

A theoretical approach based on miscibility of hard and soft segments was used to predict phase separation in the various urethane formulations consisting of caprolactone polyols of different molecular weights and hard segments made from toluene diisocyanate and 1,4 butanediol. The Flory-Huggins interaction parameter (χ) between the hard and the soft segment was calculated from their solubility parameters and compared with the onset of

phase separation (χ_c) estimated from a phase diagram for the various stoichiometric hard and soft block chain lengths. The comparison of the estimated χ_c values to the Flory-Huggins χ values suggested that higher molecular weight polyols promote phase separation and in a phase separating urethane system, phase separation increases with increasing amount of hard segment content.

Wide angle x-ray diffraction of the urethane samples confirmed the expected amorphous nature of the hard segments. Both near-infrared and fourier transform infrared spectroscopy were used to experimentally evaluate the phase separation in these samples. In both the infrared techniques, hydrogen bonding analysis was used as the basis for determining the phase separation. The spectral shift in NIR N-H band wavelength due to possible hydrogen bonding indicated phase separation in higher molecular weight polyols (Tone 0310 and 0305) with hard segment content above 40% and was also supported by the spectral shift of both the N-H band and the carbonyl band in FTIR spectroscopy. Both the FTIR and NIR data were in good agreement with the theoretically predicted phase separation results.

Angle resolved x-ray photoelectron spectroscopic analysis was conducted on selected failed glass samples after adhesion testing. The XPS derived atomic concentrations indicated the presence of a urethane type polymeric layer with constituents of glass such as silicon present in it. The various sampling depths analyzed by the angle resolved XPS indicated gradients of atomic concentration present in all the samples. The Polymeric layer thickness was thinnest in the low molecular weight and thickest in the high molecular

weight samples. The C-1s and N-1s atomic concentrations in all the residual films were found to be lower than their respective stoichiometric values. It was proposed that the residual films were an interphase region with compositions intermediate to that of the respective matrices. Based on the variations in compositions and thicknesses of these interphase regions in the various urethane samples studied, it was also concluded that matrix composition and phase separation in the matrix affected the interphase region significantly. The curve fitted spectra of the C-1s region indicated that these interphase regions might be rich in C-O type linkages which could be from C-O-Si and/or C-OH type species.

To support the above mentioned hypotheses and create a "beneficial" interphase, adhesion of the various urethanes to glass substrates coated with a 2% solution of butanediol was measured. The data indicated that modification of the interphase region of a poorly phase separated urethane sample dramatically improved the adhesion. On the other hand, in the well phase separated samples the interphase modification had little effect on the overall adhesion values which were close to the cohesive strength of the glass substrate. This suggests that phase separation in urethane plays a large role in adhesion to glass substrates by affecting the composition, thickness, and properties of the interphase region.

The introduction of phase separated material at the glass-urethane interphase in elastomeric systems had little effect on the adhesion. This indicated that along with optimum interphase properties, the modulus of the urethane matrix itself can be a limiting factor in adhesion to the glass substrates.

CHAPTER 5

INVESTIGATION OF POSSIBLE PHYSICO-CHEMICAL INTERACTIONS AT THE INTERPHASE

The work presented in this chapter will be submitted for publication in the Journal of Adhesion (1995).

5.1 ABSTRACT

Surface free energies of polyurethanes made from toluene diisocyanate and 1,4 butanediol based hard segments and caprolactone polyol based soft segments were theoretically calculated using additive functions such as molar parachors and cohesive energy densities. Good agreement was found between the theoretically calculated values and the experimentally determined values based on contact angle measurements. The phase separated polyurethanes were found to have higher polar surface free energy component (γ^P). This was linked to the preferential segregation of butanediol to the polyurethane surfaces due to phase separation. The adhesion values of these polyurethanes to soda-lime glass were correlated with their respective γ^P values and a linear relationship was found. It was also shown that the adhesion values of the low γ^P polyurethanes improved substantially when the glass surfaces were coated with a thin layer of butanediol prior to the bonding. The modulus of the interphase region rich in butanediol was evaluated and was determined not to be a significant factor in controlling adhesion of the butanediol coated glass substrates. The chemical interactions at the polyurethane/glass interphase were investigated by pretreating the glass surfaces with methyltrimethoxysilane and

trimethyl chlorosilane prior to adhesion testing. The adhesion data showed no significant difference between the uncoated and the silane treated glass substrates. Based on this experimental evidence, the possibility of any covalent or ionic bonding at the polyurethane/glass interphase was assumed negligible. It was determined that the mechanism of adhesion between the polyurethanes and the glass surface could be through the formation of an interphase region in which hydrogen bonding between the butanediol rich interphase region and the hydroxylated glass surface plays a key role.

5.2 INTRODUCTION

Glass/polyurethane adhesion has become increasingly important in the automotive and other industries in a variety of applications including laminated windshields, reaction injection molded modular windows for automobiles, long and short glass fiber reinforced thermoplastic and thermoset composites, etc. Also the use of polyurethane coatings on the inside glass surface of windshields is being investigated to impart antilacerative property to the windshield to protect occupants in the event of a collision. In all of these applications, good adhesion between the glass and the polyurethane is imperative.

Adhesion between two dissimilar surfaces such as glass and polyurethane is regarded as a complex phenomenon influenced by many factors including physical and chemical interactions. The reversible physical interactions are caused by Van der Waals forces which may also include hydrogen bonding. The irreversible chemical interactions may include ionic and covalent bond formation across the interface between the two materials. Several researchers have studied polyurethane surfaces to determine the surface

compositions and surface properties. Vargo et al (Vargo et al, 1991) have found that the polyurethane surface is enriched in the low molecular weight polyether component. Sengupta et al (Sengupta et al, 1991) have determined the polar and the dispersive components of the surface-free energies of polyurethanes and have tried to relate these to the surface soft segment contents.

The glass surface is also very complex reflecting its composition and history of environmental exposure. Fowkes et al (Fowkes et al, 1990) have used the acid-base interaction approach to study adhesion of glass to various polymers. The chemical composition of the surface of glass has also been studied by several authors using x-ray photoelectron spectroscopy and other surface sensitive techniques (Pantano, 1981; Vaughan and Peek, 1974; Lassas et al, 1993; Markus and Priel, 1981; Mohai et al, 1990). The research indicates that glass surfaces, exposed to ambient atmosphere, are enriched in sodium ions relative to the bulk. The glass surfaces are usually found to be hydrated due to the adsorption of water vapors. It has also been suggested that $NaHCO_3$ type species may be present on the surface due to the adsorption of carbon monoxide and dioxide species from the atmosphere. All of these studies have addressed either the surface composition of the urethanes or the glass surfaces but have done little to correlate the actual chemical and physical nature of the interface to adhesion of these polyurethanes to the glass surfaces.

In our previous studies on glass/polyurethane adhesion (Agrawal and Drzal, I and II, 1994) we found that polyurethane to glass adhesion is greatly influenced by the modulus

of the polymer in the interphase. We also found that along with modulus, phase separation in polyurethane also influences its adhesion to glass. An interphase region was found between the polyurethane matrix and the glass substrate of our previous studies which had a composition intermediate to that of the matrix and the glass surface. The composition and the thickness of this interphase region was found to be related to the phase separation in the matrix.

In the present study, we have investigated the physico-chemical interactions at the polyurethane/ glass interface. Surface free energies of the various urethane formulations were evaluated using theoretical and experimental techniques, and the dependence of the surface free energies on the surface composition and/or the phase separation has also been studied. The thermodynamic work of adhesion to the glass surface has been evaluated for the various phase-mixed and phase-separated polyurethanes and compared with the experimental adhesion data reported earlier (Agrawal and Drzal, I, 1994). The role of chemical interactions at the polyurethane/glass interface has been explored by coating the glass surfaces with an alkyl silane to make the surface chemically "inert" prior to the adhesion testing.

5.3 EXPERIMENTAL

5.3.1 Materials

The polyurethanes used in this study were based on caprolactone polyols available from Union Carbide under the trade name "Tone." Hard segments were made from a 80%-20% mixture of toluene 2,4-diisocyanate and toluene 2,6-diisocyanate (TDI, Aldrich Chemical

Co.) and 1,4-butanediol (BDO, Aldrich Chemical Co.) as the chain extender. The various urethane formulations studied in this work and previous are shown in Table 5.1.

For adhesion testing, annealed soda-lime float glass plaques were used. ¼" x ¼" x ¼" blocks of urethanes were cast on the air side of the glass plaques. The details of urethane mixing and adhesion sample preparation can be found in our previous study (Agrawal and Drzal, I, 1994).

5.3.2 Surface Energy Measurements

The various urethane formulations were cast on clean 75 x 50 mm glass slides. The samples were then heated for 24 hours at 90°C in a convection oven. The final polyurethane coating thickness on the glass slides was about 1-2 mm. The glass slides were handled carefully throughout the sample preparation to avoid any surface contamination of the polyurethane surfaces.

The surface free energy of the samples thus prepared were obtained from the experimental determination of contact angles for sessile drops using a Rame-Hart Model 100 goniometer. All experiments were conducted at room temperature (~23°C). The data were obtained for wetting by a series of fluids with varying surface tensions which are shown in Table 5.2. The liquids used covered wide range of properties from being non-polar such as ∝-bromo-naphthalene to a highly polar liquid such as water. By doing so, a comprehensive wettability profile was developed for each urethane formulation. Liquids

TABLE 5.1

Urethane Formulations at Isocyanate Index of 1.0

Sample Designation	Polyol Type			BDO (Mole%)	TDI (Mole%)	Hard Segment (wt %)	Molecular Weight per Cross-Link (Mc)
	Tone 0301	Tone 0305	Tone 0310				
10A	-	-	X	0	60	22	1160
10B	-	-	X	22	56	37	1424
10C	-	-	X	31	54	47	1692
10D	-	-	X	34	53	60	2222
10E	-	-	X	41	52	67	2752
5B	-	X	-	7	58	37	854
5C	-	X	-	20	56	47	1013
5D	-	X	-	31	54	59	1324
5E	-	X	-	36	53	67	1646
1C	X	-	-	0	60	47	563
1D	X	-	-	18	57	59	739
1E	X	-	-	26	55	67	912
HS	-	-	-	50	50	100	-

TABLE 5.2

Surface Free Energies of Liquids Used for Contact Angle Measurements
(Van Krevelen, 1990; Table 8.5)

Liquid	Surface Free Energy (dynes/cm)		
	γ^D	γ^P	γ
Water	21.8	51.0	72.8
Glycerol	37.0	26.4	63.4
Formamide	39.5	18.7	58.2
Methylene Iodide	48.5	2.3	50.8
α-bromonapthalene	44.6	0.0	44.6

with very low surface tensions such as n-alkanes were not used in this study due to the difficulty and errors associated with measuring small (<10°) contact angles.

5.3.3 Surface Tension Measurements

The surface tensions of the various caprolactone-based polyols could not be found in the literature and thus were measured using a Cahn DCA-322 dynamic contact angle analyzer. A freshly flamed glass slide was used for the measurement. The slides advancing and receding speed was set at 22μ/minute. The surface tension of water was determined using this technique and was found to be accurate (72.8 dynes/cm) and reproducible.

5.3.4 Dynamic Mechanical Analysis

Rectangular bars (30 mm x 4 mm x 1.5 mm) of urethane samples were used for dynamic mechanical analysis on a Polymer Laboratories MK III DMTA system. Elastic storage modulus (E') at various temperatures were obtained in a single cantilever bending oscillation mode of deformation at 1 Hz fixed frequency. The temperature was varied from 10°C to 50°C at 5°C/min.

5.3.5 Glass Pretreatment

A 2.0 weight percent solution of methyltrimethoxysilane, available from Dow Corning under the trade name Z6070, was prepared in reagent grade methanol. Approximately 10 weight percent (of the amount of Z6070) deionized water was added to the solution and the solution was aged for a week prior to use. Another 2.0 weight percent solution of trimethyl chlorosilane, available from Aldrich Chemical Co., was prepared in reagent grade

tetrahydrofuran. Cotton swabs were used to apply an even coating of these solutions to the air side of the soda-lime glass plaques. The coated glass plaques were allowed to dry for 30 minutes and then were used to prepare urethane adhesion samples.

5.3.6 X-Ray Photoelectron Spectroscopy (XPS)

Subsequent to adhesion testing, failed glass surfaces were analyzed using a Perkin-Elmer PHI5400 x-ray photoelectron spectrometer. Approximately ¼" x ¼" square area was sectioned from the failed glass surface and was placed inside the XPS chamber. The angular dependent XPS spectra were obtained at a base pressure of approximately 10^{-9} Torr. The standard Mg Kx source was used for all samples analysis and was operated at 300W (15 kV, 20 mA). A continuously variable angle sample stage was used and was programmed for 15°, 45°, and 90° angles (photoelectron take-off angle). The portion of the sample analyzed by the spectrometer is set through an initial lens system and was set for a 2.0 mm diameter circle. Data was collected in the fixed analyzer transmission mode utilizing a position sensitive detector and a 180° hemispherical analyzer. Pass energies were set at 89.45 eV for the survey scans (0-1000 eV) and at 35.75 eV for the narrow scans of the elemental regions. Data collection and manipulation was performed with an Apollo 3500 workstation running PHI ESCA software. The curve fitting was carried out using a modified Gauss-Newton nonlinear least squares optimization procedure that is part of the instrumental software. The C-1s binding energy of the graphitic peak was set to 285.0 eV for calibration purposes.

5.4 THEORETICAL CONSIDERATION OF SURFACE FREE ENERGY

The surface free energy of the polyurethanes of this study can be estimated theoretically. The polyurethanes are composed of soft and hard segments. By knowing the free energies of these segments, the overall surface free energies of the polyurethanes can be evaluated by using an approach described by Eberhardt (Eberhardt, 1966).

The hard segment in the urethanes is based on toluene diisocyanate and butanediol and its structure is shown below:

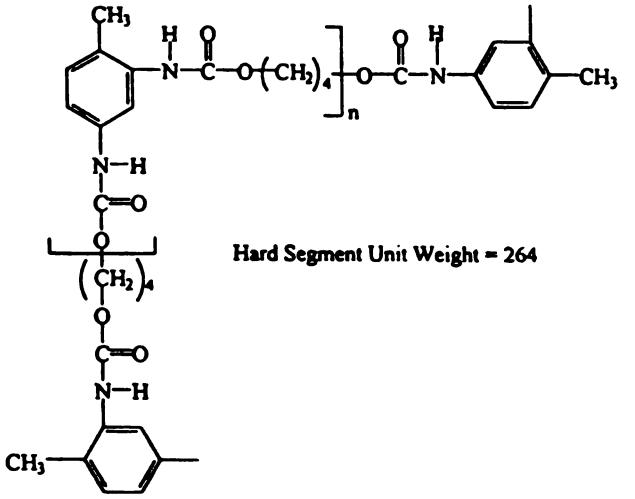

Hard Segment Unit Weight = 264

The surface free energy γ_H of this hard segment can be estimated by an additive function, the molar parachors P_S as proposed by Sugden (Sugden, 1924) and discussed by Van Krevelen (Van Krevelen, 1990). The relationship between the surface free energy and the molar parachors is as follows:

$$\gamma_H = \left(\frac{\Sigma P_S}{\Sigma V} \right)^4 \tag{5.1}$$

where V is the molar volume contribution of the groups in the glassy (amorphous) state of the polymer. The molar volume contributions can be evaluated from the Van der Waals volume (Vw) as follows:

$$V = 1.6\, V_w \tag{5.2}$$

The V_w and P_s values for the hard segment groups are taken from the reference Van Krevelen, 1990 (Tables 4.2 and 8.1). The calculated ΣV and ΣP_s values are 210.22 cm^3/mol and 556.7 $(cm^3/mol)(erg/cm^2)^{1/4}$ respectively. The details of these calculations are shown in Appendix B. Thus,

$$\gamma_H = \left(\frac{556.7}{210.22}\right)^4 = 49.2 \ \textit{dynes/cm} \tag{5.3}$$

The surface tension of the hard segment can also be estimated using an empirical relationship (Van Krevelen, 1990)..

$$\gamma_H \approx 0.75\ e_{coh}^{2/3} \tag{5.4}$$

where γ_H is expressed in dynes/cm and the cohesive energy density e_{coh} in MJ/m^3. The cohesive energy density of the hard segment can also be estimated using group contribution approach and is calculated to be 519.2 MJ/m^3 (Appendix B). Thus,

$$\gamma_H \approx 0.75\ (519.2)^{2/3} = 48.5 \text{ dynes/cm.} \tag{5.5}$$

Both the γ_H values estimated from the parachors and the cohesive energy density contributions are very close to each other and both values were used here to determine the overall polyurethane surface free energies.

The free energy of the soft segment γ_s is difficult to estimate from the group contributions of the molar parachors or the cohesive energy density as the exact structure of the repeating unit is not known. Thus, the γ_s values were experimentally determined using dynamic contact angle measurements. The advancing and receding surface tensions were determined for the various polyols and little difference was found between the values for

the different polyols. A hysteresis of ~9 dynes/cm was observed between the advancing and the receding surface tensions. The advancing surface tension value is used here as it signifies the first contact between the glass slides and the polyols. The average γ_s value was found to be 38.1 dynes/cm with a standard deviation of 0.4 dynes/cm.

The surface free energy of the soft segment can also be estimated indirectly by evaluating cohesive energy density from its solubility parameter. The solubility parameter of the polyols is $\delta_s = 18.6\ (J/cm^3)^{1/2}$ (Brandrup and Immergut, 1989).

$$\gamma_S \approx 0.75\ (e_{coh})^{2/3} \tag{5.6}$$

$$\gamma_S \approx 0.75\ (\delta_S^2)^{2/3} \tag{5.7}$$

$$\gamma_S \approx 0.75\ (18.6)^{4/3} = 37.0 \text{ dynes/cm} \tag{5.8}$$

This value is close to the experimentally determined value of 38.1. The $\gamma_s = 38.1$ is used here for the overall calculation of the surface free energy of the polyurethanes.

According to Eberhardt's approach, the surface free energy of polyurethanes can be expressed as:

$$\gamma_U = N_S\gamma_S + N_H\gamma_H \tag{5.9}$$

where γ_U is the surface free energy of the polyurethanes and the N_s and N_H are the mole fractions of the soft and the hard segments on the surface of the polyurethanes. Assuming that the surface composition is same as the bulk composition, the N_s and the N_H values can be calculated from the various urethane's stoichiometric formulations and are listed in Table 5.3. Based on the N_s, N_H, γ_H and γ_s values, the γ_U for the various polyurethanes

TABLE 5.3

Calculated Surface Free Energies of the Polyurethanes

Samples	Mole Fraction		Surface Free Energy (dynes/cm)	
	N_S Soft Segment	N_H Hard Segment	γ_U (Molar Parachor)	γ_U (Cohesive Energy Density)
10A	0.401	0.599	44.7	44.3
10B	0.222	0.778	46.7	46.2
10C	0.154	0.846	47.5	46.9
10D	0.132	0.868	47.7	47.1
10E	0.069	0.931	48.4	47.7
1C	0.398	0.602	44.8	44.3
1D	0.260	0.740	46.3	45.8
1E	0.194	0.806	47	46.4
HS	0.0	1.0	49.2	48.5

were calculated and are shown in Table 5.3. The calculated γ_U values based on molar parachors and cohesive energy density are very close. It should be noted that as the hard segment content increases in the polyurethanes, the γ_U values also increase and is the highest for 100% hard segment content sample HS.

5.5 RESULTS AND DISCUSSION

5.5.1 Physical Interactions

The surface free energies of the various model polyurethanes were determined from the contact angle measurements of several liquids with different surface tensions and chemical functionalities. Zisman (Zisman, 1964) plots of Cosθ versus γ were developed for all the urethane samples. Figures 5.1a and 5.1b show the sample Zisman plots for polyurethane sample 1c with 46.7 wt. % hard segment and sample HS with 100 wt. % hard segment. The extrapolated critical surface tension γ_C at Cosθ = 1 for all the samples are shown in Table 5.4. The γ_C signifies the empirical value of the maximum surface tension of liquids able to spread on the given surface. The γ_C data reveal that the critical surface tension of the various polyurethanes studied are close to each other, considering the experimental errors involved in the measurements. Also, no clear trend in the data with increasing hard segment content can be observed, as can be inferred from the theoretically calculated surface free energies.

Along with the critical surface free energy, polar and dispersive components of the surface free energies of these polyurethanes were also evaluated from the contact angle measurements. According to Schultz et al (Schultz et al, 1977), the surface free energy

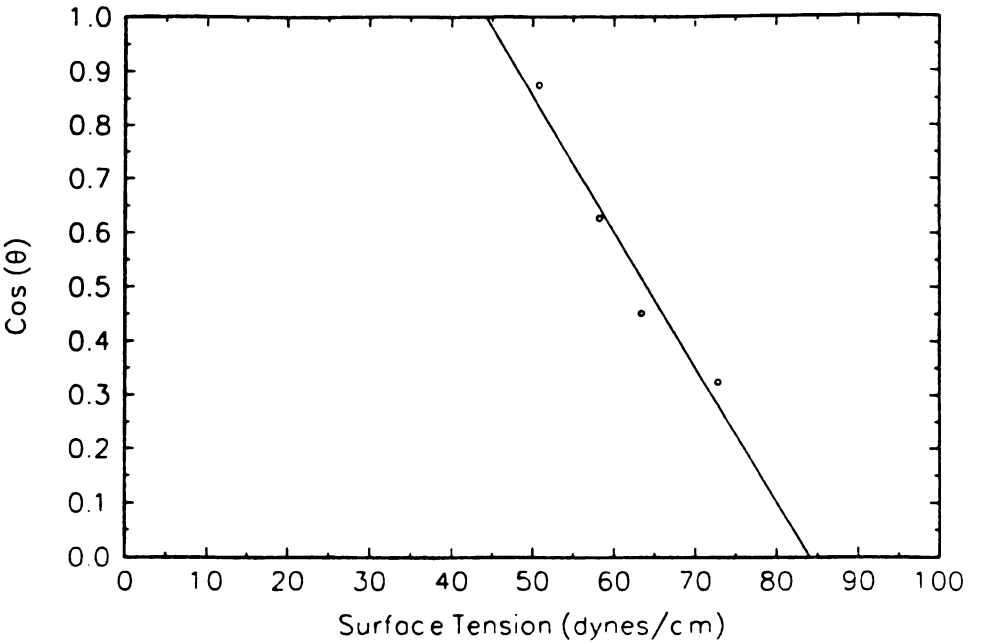

(a)

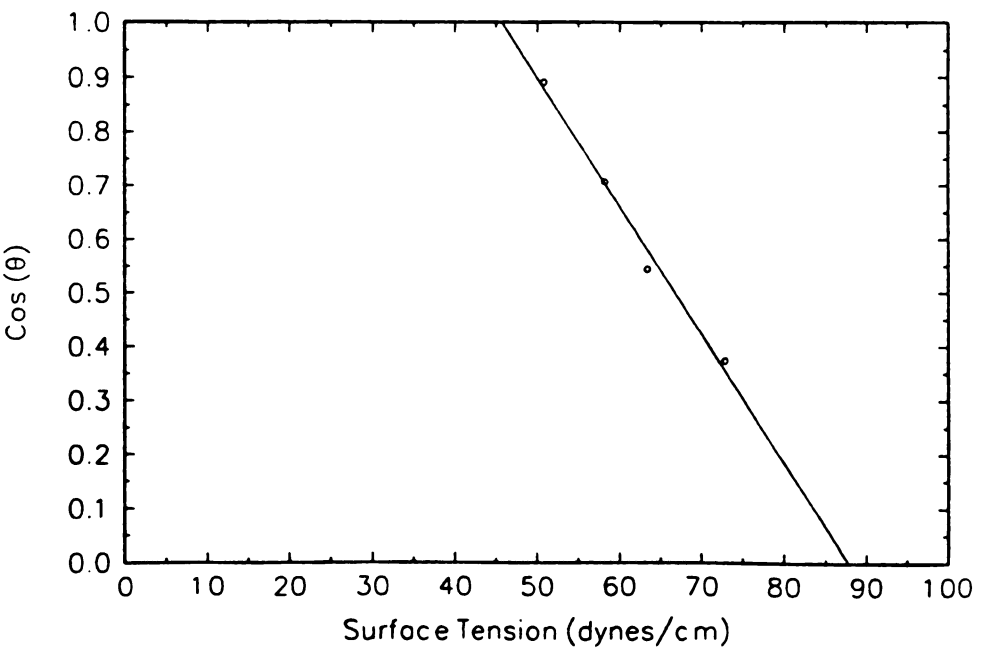

(b)

FIGURE 5.1 Zisman Plots of (a) 1C Polyurethane Sample with 46.7 wt. % Hard Segment and (b) HS Polyurethane Sample with 100% Hard Segment

TABLE 5.4

Observed Surface Free Energies of the Polyurethanes
Based on Contact Angle Measurements

Samples	Surface Free Energy (dynes/cm)			
	γ_c	γ^P	γ^D	$\gamma_U = (\gamma^P + \gamma^D)$
10A	44.4	6.83	33.64	40.47
10B	44.0	6.50	34.20	40.70
10C	44.6	10.55	30.58	41.13
10D	44.3	13.55	30.49	44.04
10E	42.2	14.97	30.25	45.22
1C	41.83	7.72	34.22	41.94
1D	42.46	10.72	32.49	43.21
1E	42.76	11.11	32.49	43.60
HS	43.64	8.73	35.76	44.49
Glass	-	37.59	19.18	56.77

can be represented by the sum of two components, namely a dispersion (γ^D) and a polar component (γ^P).

$$\gamma = \gamma^D + \gamma^P \tag{5.10}$$

By using this and the expressions derived for interfacial free energy by Fowkes (Fowkes, 1967), Owens and Wendt (Owens and Wendt, 1969) and Kaelble and Uy (Kaelble and Uy, 1970), the interfacial free energy between the polyurethanes and the liquids can be expressed as:

$$\gamma_{UL} = \gamma_U + \gamma_L - 2\,(\gamma_U^D\,\gamma_L^D)^{1/2} - 2\,(\gamma_U^P\,\gamma_L^P)^{1/2} \tag{5.11}$$

Combining this with the Young's equation

$$\gamma_U = \gamma_{UL} + \gamma_L \mathrm{Cos}\theta, \text{ we get} \tag{5.12}$$

$$1 + Cos\ \theta = \frac{2(\gamma_U^D\ \gamma_L^D)^{1/2}}{\gamma_L} + \frac{2(\gamma_U^P\ \gamma_L^P)^{1/2}}{\gamma_L} \tag{5.13}$$

or

$$\frac{\gamma_L(1+Cos\,\theta)}{2(\gamma_L^D)^{1/2}} = (\gamma_U^D) + \left(\frac{\gamma_L^P}{\gamma_L^D}\right)^{1/2} (\gamma_U^P)^{1/2} \tag{5.14}$$

The $\left(\frac{\gamma_L^P}{\gamma_L^D}\right)^{1/2}$ and $\frac{\gamma_L(1+Cos\,\theta)}{2(\gamma_L^D)^{1/2}}$ values for the various polyurethanes were plotted and $(\gamma_U^P)^{1/2}$ and $(\gamma_U^D)^{1/2}$ values were obtained from the slope and the intercept of the linear regression fit lines through the experimental data points. One such plot for Tone 0310 based polyurethanes is shown in Figure 5.2. From the graph, we see

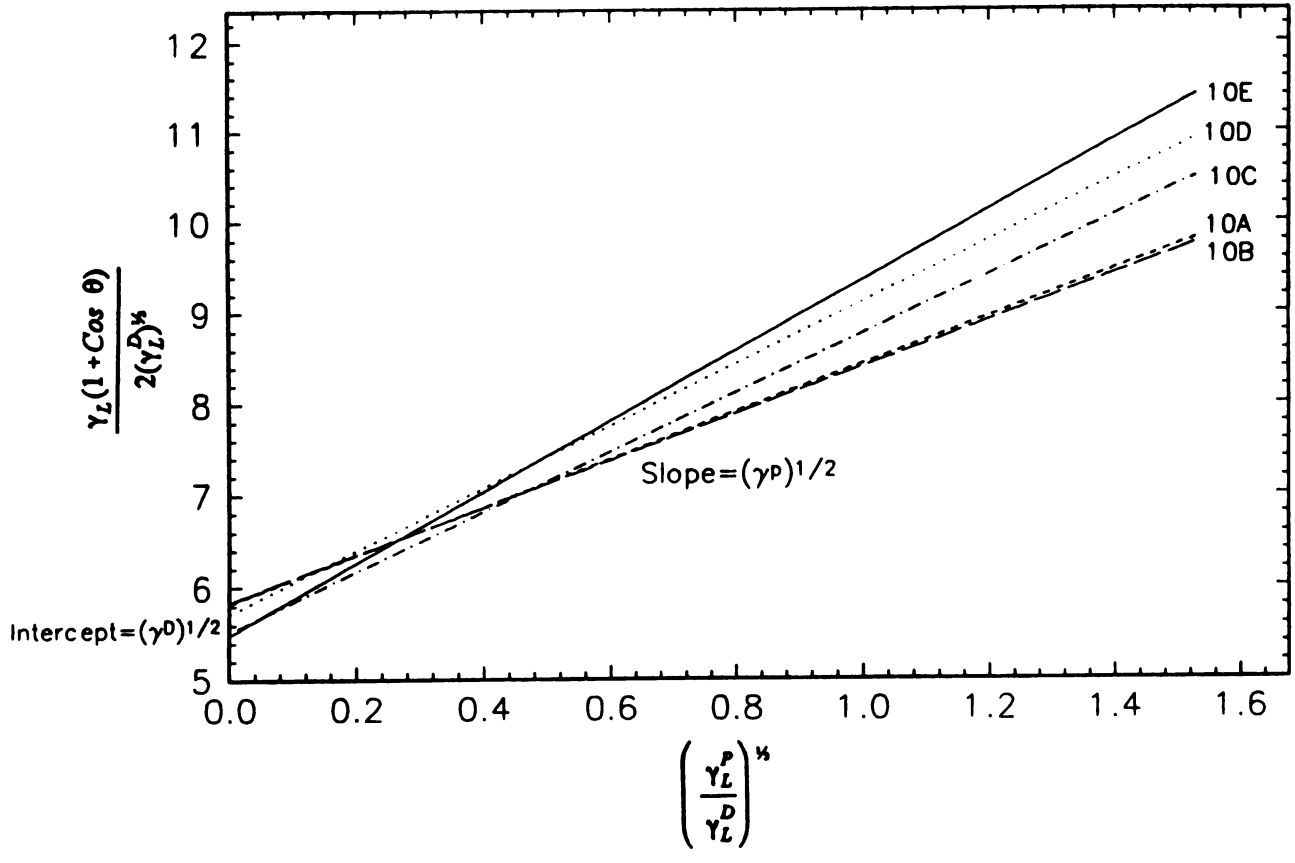

FIGURE 5. 2 $\left(\frac{\gamma_L^P}{\gamma_L^D}\right)^{1/2}$ vs. $\frac{\gamma_L(1+Cos\ \theta)}{2(\gamma_L^D)^{1/2}}$ plot for Tone 0310 Based Polyurethanes with Different Hard Segment Contents.

that as the hard segment content increases in these samples, their slopes also increase. This indicates that with as the hard segment content increases, the polar component of the urethane surface free energy also increases. The γ^P and γ^D values obtained from these graphs are shown in Table 5.4. The last column in Table 5.4 also shows the overall surface free energy of these polyurethanes (γ_U) which is the sum of the γ^P and γ^D values.

Figure 5.3 shows the graph of the measured γ_U values versus the hard segment content in the Tone 0310 based polyurethanes. Also shown are the graphs of the theoretically predicted γ_U values for these polyurethanes. Both the theoretical and experimental graphs show the same trend that the surface tension increases with the increasing hard segment content. The theoretically predicted values are in very good agreement with the experimental values. They are higher than the experimental values by only 3-4 dynes/cm and the difference is less for the higher hard segment content samples (10D, 10E, etc.) which are phase separated polyurethane systems (Agrawal and Drzal, I and II, 1994). This small amount of difference could be due to the assumption made in the theoretical prediction regarding the surface composition being the same as the bulk composition. The experimental γ_U curve shows an increase in the value after the sample 10C and then maintains the high γ_U values for the samples 10D, 10E, and HS. This sharp rise in γ_U values could be due to the phase separation in these samples leading to the surface enrichment in high surface energy species. This is further explored by plotting the polar component of the surface free energy for these samples.

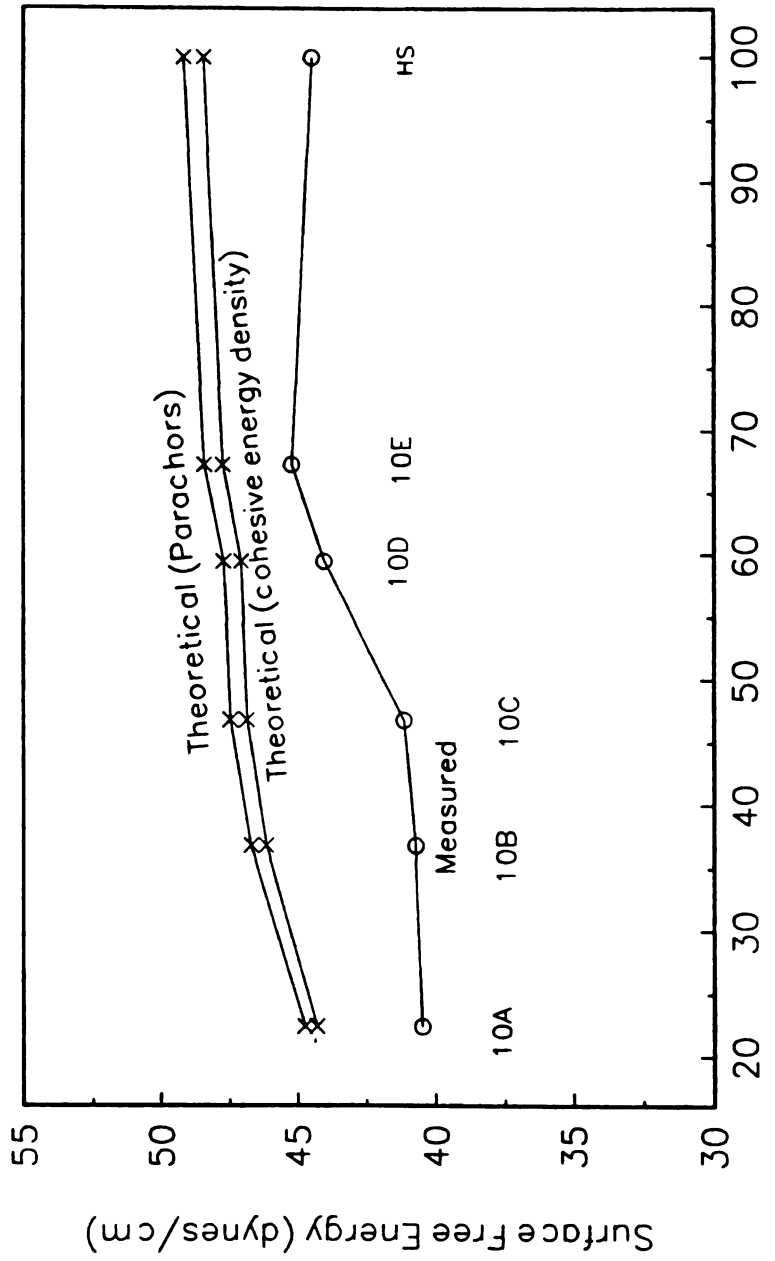

FIGURE 5.3 Theoretical (X) and Measured (O) Surface Free Energy Values for Tone 0310 Based Polyurethanes at Different Hard Segment Contents

Figure 5.4 shows the γ^P versus hard segment content for Tone 0301 and Tone 0310 based polyurethanes. Also shown is the data point HS for the 100% hard segment content polyurethane (contains only BDO and TDI). The data shows that the γ^P values increase with increasing hard segment content in both the 1 and 10 series polyurethane samples. The γ^P values for the 1 series are in general lower than that for the 10 series for the same hard segment contents. A sharp increase in the γ^P value of sample 10C is also served and the trend continues with the samples 10D and 10E. This observation can be explained by noting that with increasing hard segment content, phase separation increases in higher molecular weight polyol (Tone 0310) based polyurethanes (Agrawal and Drzal, I and II, 1994). The phase separation in the lower molecular weight polyol (Tone 0301) based polyurethanes is not as significant and thus the γ^P values for these polyurethanes are lower than 10 series polyurethanes. The γ^P value for the 100% hard segment content polyurethane is 8.73 dynes/cm which is lower than the γ^P values for the samples 10C, 10E, and 10E; all of which have lower hard segment content. The higher γ^P values for 10C, 10D, and 10E suggests that the surfaces of these polyurethanes are not rich in the hard segment. Further, the higher γ^P values can be explained by the phase separation in these polyurethanes. In our previous studies (Agrawal and Drzal, I and II, 1994), we have discussed phase separation in these polyurethanes and have shown that due to phase separation, the surface composition in these polyurethanes tend to be rich in hydroxyl containing species and deficient in nitrogen containing groups when compared with the stoichiometric composition. The two hydroxyl containing species in these polyurethanes are the polyols and the chain extender (BDO). Due to the lower molecular weight of the chain extender, BDO is more likely to come to the surface (Agrawal and Drzal, II, 1994).

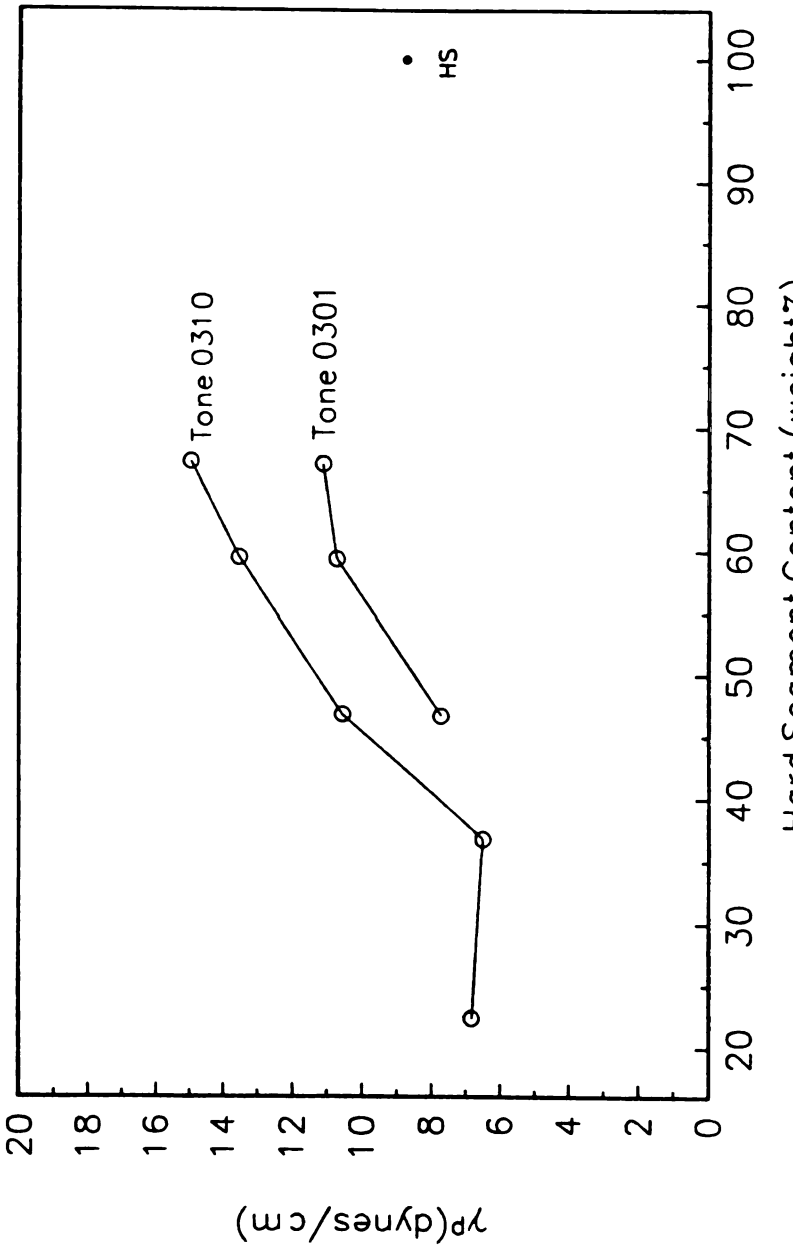

FIGURE 5.4 Polar Surface Free Energy Component of Various Polyurethanes at Different Hard Segment Contents

This is also supported by the γ^P values observed here. The lower γ^P value samples 10A, 1C, and 10B have no or very small BDO content and also poor phase separation and thus their surfaces are not rich in BDO. On the other hand, in the samples 10D and 10E, BDO segregates to the surface and results in higher γ^P values. The surface free energy values for BDO are (Brandrup and Immergut, 1989):

$\gamma^P = 14.6$ dynes/cm

$\gamma^D = 29.6$ dynes/cm

$\gamma = 44.2$ dynes/cm

The γ^P of polyol is expected to be less than 14.6 due to higher hydrocarbon content and this further supports the conclusion that the surfaces of these polyurethanes are rich in BDO.

The adhesion values of these polyurethanes to soda-lime glass surface were determined previously (Agrawal and Drzal, I, 1994) and are shown in Table 5.5. We had shown that the polyurethane to the glass adhesion improved with phase separation in the matrix and also with the modulus of the matrix. A plot of the adhesion values as a function of γ^P is shown in Figure 5.5. A linear relationship can be seen between the γ^P and the adhesion values.

The above observations suggest that in the samples exhibiting good adhesion to the glass, the interphase region between the polyurethane matrix and the glass surface (Agrawal and Drzal, II, 1994) consists of a larger concentration of higher polar free energy components than the bulk and the components are butanediol type species.

TABLE 5.5

Thermodynamic Work of Adhesion Between the Polyurethanes and the Glass Surface

Samples	W_{adh} (dynes/cm)	Shear Adhesion (Psi) (Agrawal and Drzal, I, 1994)
10A	83	706 ± 4
10B	83	1590 ± 30
10C	88	2690 ± 60
10D	92	4640 ± 80
10E	96	5370 ± 300
1C	85	825 ± 340
1D	90	2120 ± 530
1E	91	3020 ± 1360
HS	89	-

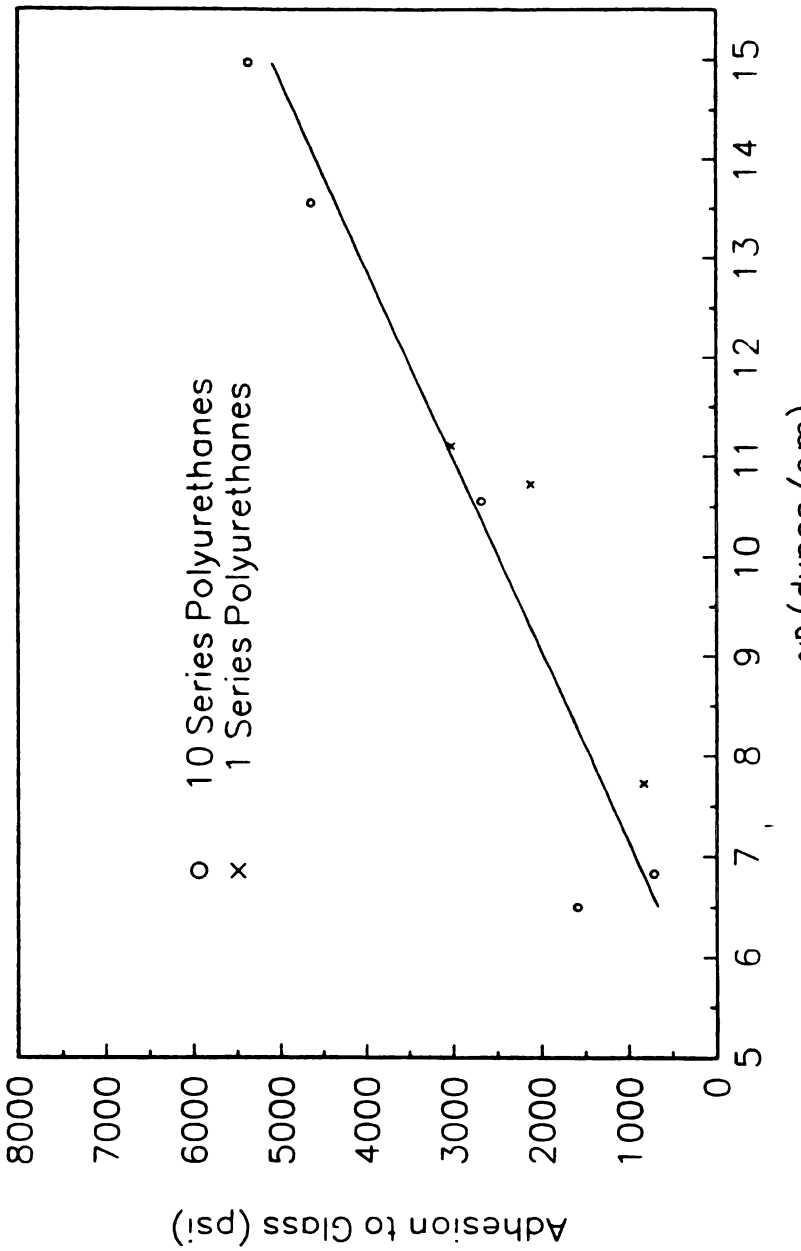

FIGURE 5.5 Adhesion to Glass Versus Polar Component of the Surface Free Energy for Various Polyurethane Systems

The polar forces on the surface arise from the orientation of permanent electric dipoles and the induction effect of permanent dipoles on polarizable molecules. In the case of polyurethanes, these molecules would include 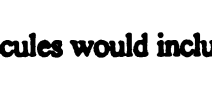 and 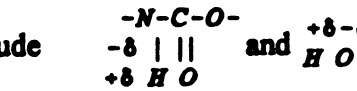 type species and especially the  due to their preferential segregation to the surface. These dipoles can create hydrogen bonds (permanent dipole-dipole interactions), other dipole-dipole bonds (excluding hydrogen) and dipole-induced dipole interactions with the hydroxyl rich glass surfaces (Kinloch, 1987).

To further explore the role of the hydrogen bonding and other polar interactions between the polyurethane surface and the glass surface, an additional adhesion experiment was conducted. In this experiment, selected polyurethanes with varying surface γ^P values (and thus with varying surface BDO content) were bonded to the bare soda-lime glass plaques and to glass plaques coated with 2% (weight) layer of BDO from acetone. The samples were tested for adhesion values in a shear mode (details of adhesion testing are discussed in Agrawal and Drzal, I, 1994) and the data is shown in Table 5.6. The data reveals that the adhesion values of the polyurethanes with low γ^P values can be significantly improved by coating the glass surface with BDO, or in other words, by making their surface rich in higher γ^P component BDO.

The failed glass surfaces after the adhesion testing were analyzed using XPS. Figure 5.6 shows the curve fitted C 1s spectra of sample 1D and Sample 1D with the glass surface coated with BDO, taken at 15° photoelectron take-off angle. These spectra have been charge corrected with the C-C peak referenced to 285.0 eV. A cursory look at the spectra

TABLE 5.6

Adhesion Values (Psi) of Various Polyurethanes to Bare Glass Surface and to 1,4 Butanediol Coated Glass Surface

Samples	2% Secant Shear Modulus (Psi) Iosipescu Testing Ref. 9	γ^p (dynes/cm)	Relative BDO Concentration on the Surface (Arbitrary Units)	Adhesion to Bare Glass Surface (Psi)	Adhesion to 1, 4 Butanediol Coated Glass Surface (Psi)
10D	150,653	13.6	+++	4640 ± 80	4550 ± 80
1D	184,962	10.7	++	2120 ± 530	4980 ± 850
1C	176,060	7.7	+	825 ± 340	4120 ± 130
10B	1400*	6.5		1590 ± 30	1510 ± 50

*Tensile Modulus, sample was too soft for Iosipescu testing

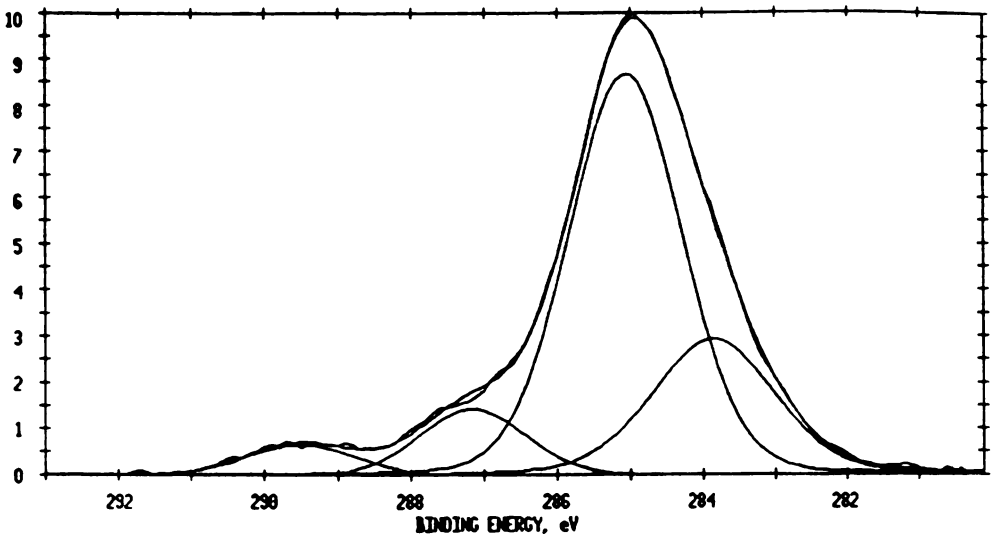

(a)

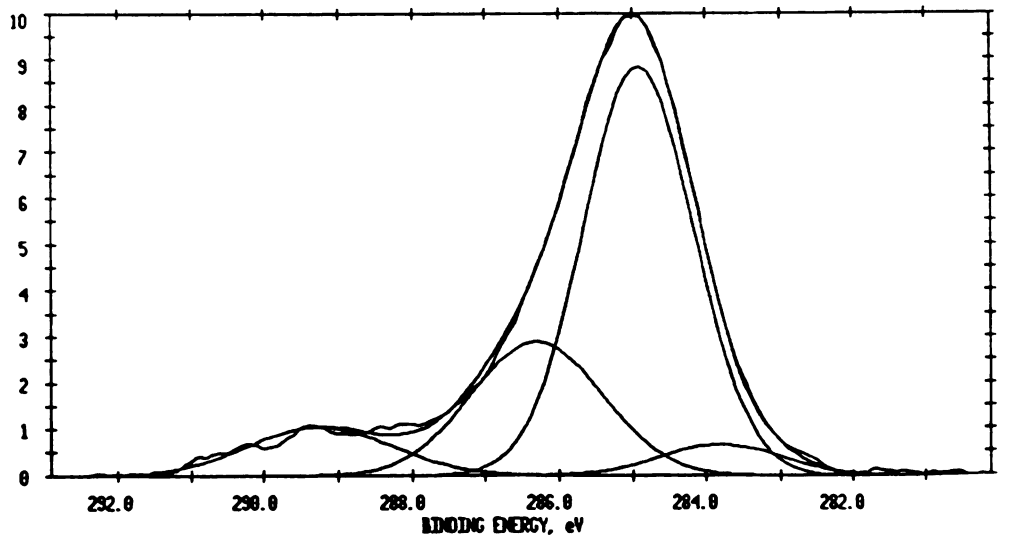

(b)

FIGURE 5.6 Curve Fitted C 1s Spectra of Failed Glass Surfaces Taken at 15° Photoelectron Take-Off Angle (a) Sample 1D (b) Sample 1D with BDO Coated Glass

reveals that there are several binding states of carbon present on the samples, both at higher and at lower binding energies of C-C bonds (285.0 eV). The C 1s peak binding energies and the relative peak areas are shown in Table 5.7. The peak at ~289.5 eV can be associated with urethane linkage (Agrawal and Drzal, II, 1994) and its presence indicates cohesive mode of failure in both the samples. The higher urethane peak area in the BDO coated glass surface indicates urethane richer surface than the 1D glass surface without BDO coating. The peak ~286.5 eV can be due to the unreacted free hydroxyls C-OH from the polyol and BDO. The significantly higher area fraction for this peak in BDO coated adhesion sample as compared to the uncoated adhesion sample, suggests the presence of partially or completely unreacted BDO on the surface. Thus we can conclude that some BDO molecules from the coating react with isocyanates to form urethane linkages and integrate in the matrix while others remain unreacted.

It is conceivable that the unreacted BDO molecules present in the interphase region of BDO coated glass adhesion samples can lead to localized change in the mechanical properties of the interphase region. The modulus of the modified interphase region could influence the adhesion of the matrix in addition to the hydrogen bonding mentioned earlier. To understand the mechanical properties of the butanediol rich interphase region, polyurethane rectangular bars were prepared with 5% and 15% (by total weight) excess of 1,4 butanediol. The excess BDO was incorporated into the urethane composition. Excess BDO was added to a homogeneous stoichiometric mixture of polyol, BDO, and isocyanate. It is expected that the urethane produced would closely represent the interphase formation process in the experimental samples used in this study. The samples

TABLE 5.7

C 1s Peak Binding Energies and Relative Peak Areas
of Carbon Chemical States on Failed Glass Samples

Sample	Peak I		Peak II		Peak III		Peak IV	
	B.E. (eV)	Area (%)	B.E. (eV)	Area (%)	B.E. (eV)	Area (%)	B.E. (eV)	Area (%)
1D	283.76	23.90	285.13	62.81	286.98	9.11	289.46	4.17
1D with BDO Coating on Glass	283.80	5.07	284.91	61.57	286.3	23.87	289.24	9.48

with 15% excess butanediol did not cure well, and the samples were either tacky and "putty-like" or very brittle with poor tensile properties. These samples could not be tested for mechanical properties. The samples with 5% excess butanediol were tested for elastic storage modulus using Dynamic Mechanical Analysis and the data is shown in Table 5.8. Also shown in Table 5.8 is the elastic storage modulus for the corresponding polyurethane with stoichiometric formulation.

The data indicates that the elastic storage modulus of polyurethane 1D with 5% BDO is about 10%-12% higher than for the stoichiometric composition 1D. Since the interphase formation in BDO coated glass plaques is expected to be simulated by this method, we can conclude that the localized interphase modulus in BDO coated 1D adhesion sample is higher than that of in the 1D adhesion sample without any coating. Based on the observations from our previous study (Agrawal and Drzal, I, 1994), the higher interphase modulus should result in higher adhesion values which is in agreement with the adhesion data obtained with BDO coated glass plaques. This observation suggests that the preferential segregation of BDO type species to the interphase region in polyurethane/glass samples influences its adhesion not only through increased polar interactions and hydrogen bonding but also by increasing the modulus of the interphase region.

The thermodynamic work of adhesion due to the polar and the dispersive interactions was also calculated for the various polyurethanes/glass systems using Kaelble's expression. Kaelble (Kaelble, 1971) has modified the expression originally developed by Good (Good,

TABLE 5.8

Elastic Storage Modulus of Various Polyurethanes
at Different Temperatures

Temperature (°C)	Elastic Storage Modulus (Psi)	
	1D	1D with 5% Excess BDO
10	390,000	438,000
15	381,000	438,000
20	381,000	428,000
25	381,000	418,000
30	373,000	418,000
35	364,000	399,000
40	356,000	390,000
45	348,000	373,000
50	348,000	356,000

1967) and Fowkes (Fowkes, 1967) and has represented it as the sum of the work due to the dispersion and the polar components.

$$W_{adh} = W_{adh}^{D} + W_{adh}^{P} \tag{5.15}$$

Using the geometric mean relation to predict the interactions,

$$W_{adh} = 2\,[(\gamma_U^{D}\,\gamma_G^{D})^{1/2} + (\gamma_U^{P}\,\gamma_G^{P})^{1/2}] \tag{5.16}$$

The W_{adh} values for the polyurethane/glass systems are shown in Table 5.5. A quantitative comparison between the calculated work of adhesion and the measured adhesion values in terms of the load required to induce bond failure is not relevant but, a qualitative comparison of the trends in the data can provide valuable information. The data shows that the W_{adh} increases slightly with increasing hard segment content but not to the extent observed in the experimental adhesion data. The shear adhesion data increases from 706 psi for Sample 10A, with 22 weight percent hard segment content to 5370 psi for ssample 10D, with 67 weight percent hard segment content. The lack of agreement between the calculated W_{adh} and the experimental adhesion data may be explained by the recent observations made by Fowkes et al (Fowkes et al, 1990) that the geometric mean relation to predict polar interactions may not include the effects of hydrogen bonding at the interface which might be an important factor in the polyurethane/glass systems. Another reason for this discrepancy can be the fact that the W_{adh} calculation does not take into consideration the modulus of the polyurethane matrix. In the adhesion experiment, the matrix modulus affects the energy less going into the deformation of the matrix prior to the bond failure.

5.5.2 Chemical Interactions

Glass surfaces are known to be rich in isolated, vicinal, and geminal silanol groups. In addition to the physical interactions between the surface silanols and the urethane matrix, there could be various chemical interactions. To investigate the chemical interactions such as covalent and ionic bonding, the glass surfaces were pretreated with two different silane coupling agents. A 2% (by weight) solution of prehydrolyzed methyltrimethoxysilane and a 2% (by weight) solution of trimethyl chlorosilane in tetrahydrofuran were used to pretreat glass surfaces prior to the adhesion testing. The purpose of the silane treatment was to make the otherwise hydroxylated glass surface chemically inert towards any subsequent covalent bond formation with polyurethanes. Another function of the silane coating was to provide a barrier layer between the glass and the urethane matrix to avoid any possibility of ionic bond formation between the Na^+, K^+, and Ca^{++} ions and the urethane matrix. On the other hand, the silane coatings could also influence wettability of the various polyurethanes by providing lower energy surfaces. However, Plueddemann (Plueddemann, 1982) had shown that little correlation existed between the surface energy of silanes and their effectiveness as coupling agents between glass and polymeric matrices. The polyurethanes of this study showed adequate wetting to the silane treated glass surfaces. Shown in Figure 5.7a and 5.7b are the idealized monolayers of the condensed methyltrimethoxysilane and trimethyl chlorosilane on glass surfaces respectively.

The methyltrimethoxysilane treated glass surface was analyzed using XPS. The atomic concentrations determined from the XPS analysis did not show the presence of Na^+ ions which indicated that the glass surface was covered completely with the silane layer.

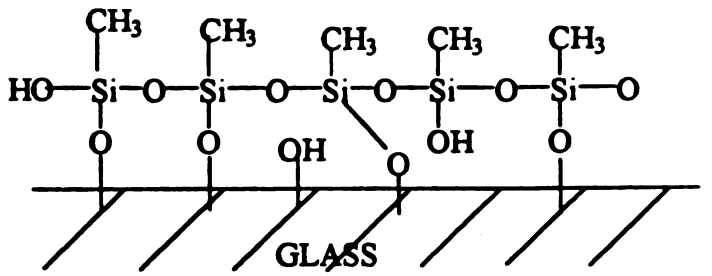

(a)

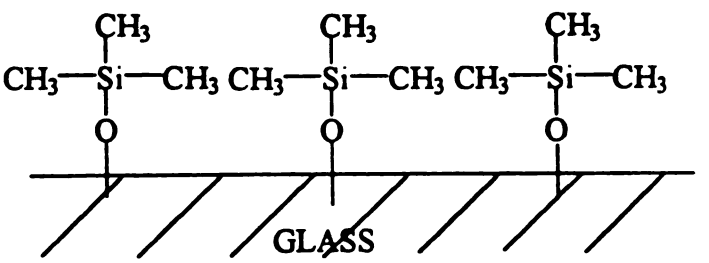

(b)

FIGURE 5.7 Idealized Monolayer of Condensed (a) Methyltrimethoxysilane (b) Trimethylchlorosilane on Glass Surface

Figure 5.8 shows the curve fitted C-1s spectrum of the silane treated glass surface at 45° photoelectron take-off angle. The curve fit spectra reveals that the major portion of the carbon is Si-CH_3 type carbon (75.74%) followed by a C-O type linkage (23.23%). The presence of this ether linkage indicates that there might be some unhydrolyzed methoxy groups (Si-O-CH_3) present in the silane layer. This type of methoxy group will not be present on the trimethyl chlorosilane treated glass surfaces. The adhesion data from these glass surfaces will not be influenced by the methoxy groups presence as might be the case in the methyltrimethoxysilane treated glass surfaces.

Blocks of several polyurethanes were cast on the silane treated glass surfaces and were cured in the same manner as reported previously. These samples were tested for adhesion values and the data is shown in Table 5.9. A comparison of this data on glass surfaces completely blocked by the silane with adhesion data for the bare glass surface (Agrawal and Drzal, I, 1994) reveals that the methyltrimethoxysilane coating on the glass surface had little influence on the adhesion values within experimental error. Similar adhesion data is obtained from the trimethyl chlorosilane treated glass surfaces. Both these data suggest that the adhesion mechanism of the polyurethanes to the glass surface is probably not due to covalent or ionic bonding in the interphase region.

The failed glass surface of the sample 10D from the methyltrimethoxysilane adhesion test was also analyzed using the XPS to determine the locus of failure. Table 5.10 shows the atomic concentrations of N,O,C and Si at three different photoelectron take-off angles 15°, 45°, and 90°. The presence of nitrogen reveals that nitrogen containing species such

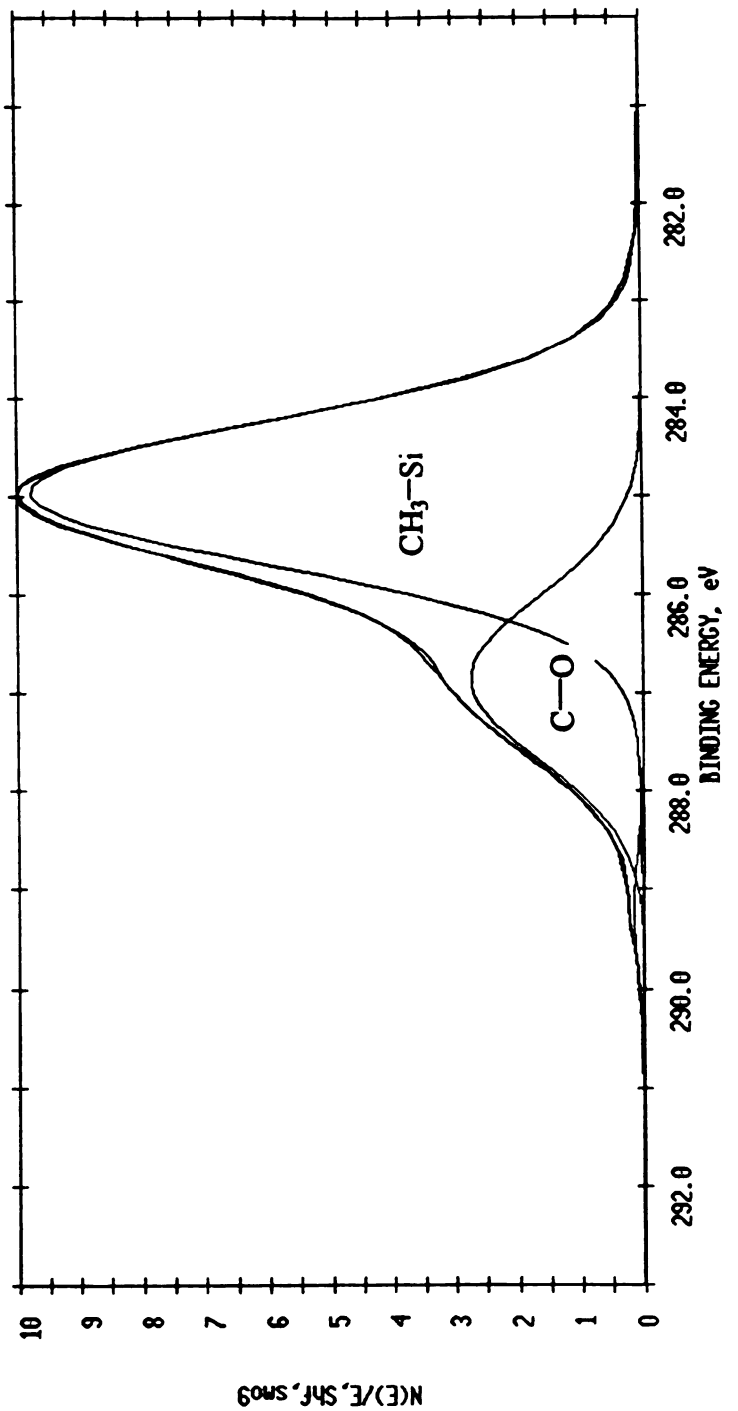

FIGURE 5.8 Curve Fitted C 1s Spectrum of Methyltrimethoxysilane Treated Glass Surface at 45° Photoelectron Take-Off Angle

TABLE 5.9

Adhesive Values (Psi) of Various Polyurethanes to SilaneTreated Glass Surfaces

Samples	Adhesion to Bare Glass Surface (Ref. 9)	Adhesion to Methyltrimethoxysilane Treated Glass Surface	Adhesion to Trimethyl Chlorosilane Treated Glass Surface
10D	4640 ± 80	4940 ± 390	4290 ± 310
5D	5240± 220	4790 ± 450	4740 ± 560
1D	2120 ± 530	2480 ± 440	2380 ± 550
10B	1590 ± 30	1470 ± 170	1370 ± 140

TABLE 5.10

O 1s, N 1s, C 1s, and Si 2p Atomic Percent Concentrations at Different Photoelectron Take-Off Angles for the Adhesion Failed 10D Glass Sample Coated with Methyltrimethoxysilane

Elements	Photoelectron Take-Off Angle		
	15°	45°	90°
O	36.44	40.19	44.30
N	0.93	1.62	2.17
C	45.40	40.01	34.69
Si	17.23	18.19	18.84

as TDI and/or urethane linkages were present on the surface. Figure 5.9 shows the curve fitted C-1s spectra at 15°, 45°, and 90° photoelectron take-off angles. The peak at ~289.5 eV indicates that nitrogen is coming from the polyurethane linkages rather than from the TDI. The nitrogen concentration gradient increases with the sampling depth. This indicates that interdiffusion might have taken place between the silane layer and the urethane matrix resulting in an interphase region. The locus of failure seems to be between the silane layer and the urethane matrix, through the interphase region. This interphase region observation is consistent with the previously made observations regarding interphase formation in the polyurethane/glass systems (Agrawal and Drzal, II, 1994).

5.5.3 Adhesion Mechanisms

Based on our previous studies regarding; the structure-property relationships in polyurethanes and their effects on adhesion; the phase separation in polyurethane and the formation of an interphase region between the polyurethanes and the glass surface (Agrawal and Drzal, I and II, 1994); and the observations made in this study regarding the role of physico-chemical interactions in the interphase region, it can be inferred that the reversible physical interactions and not covalent chemical interactions in the interphase region play a key role in determining adhesion of the polyurethanes of this study to the soda-lime glass surfaces. The permanent dipole-dipole interactions and especially the hydrogen bonding between the urethane surface and glass surface appear to be very important for the overall adhesion. Phase separation in the matrix tends to cause a preferential segregation of BDO type species in the interphase region. Based on the linear

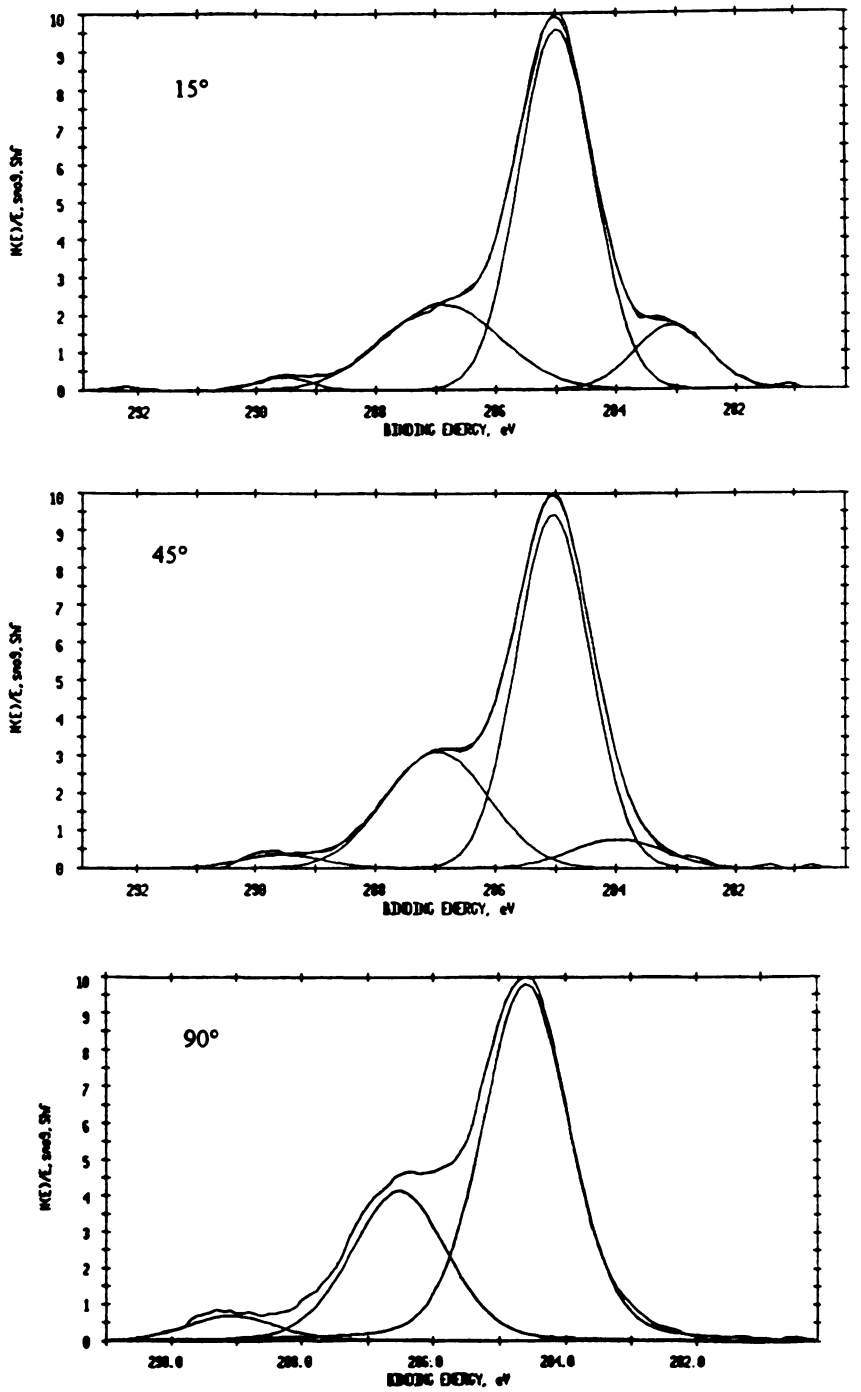

FIGURE 5.9 Curve Fitted C 1s Spectra of Adhesion Failed 10D Glass Samples Precoated with Methyltrimethoxysilane Taken at 15°, 45°, and 90° Photoelectron Take-Off Angles

relationship between the polar surface free energy (γ^p) and the matrix adhesion, and the findings of the adhesion experiments with BDO coated glass plaques, it can further be inferred that the presence of excess BDO in the interphase region influences matrix adhesion by increasing the modulus of the interphase region and by increasing the polar interactions with the glass surface.

To explore the roles of the increased interphase modulus and the increased polar interactions (hydrogen bonding) on adhesion, another experiment was conducted. In this experiment, the air sides of soda-lime glass plaques were coated with 2% (by weight) solution of trimethyl chlorosilane in tetrahydrofuran solvent. After 30 minutes of air drying, some of the glass plaques were rinsed with tetrahydrofuran to remove any unbonded trimethyl chlorosilane from the glass surfaces. The glass plaques thus prepared were overcoated with a 2% (by weight) solution of BDO in acetone and were allowed to dry at room temperature. The glass plaques were then evaluated for adhesion with 1D polyurethane and the data is shown in Table 5.11.

The purpose of coating glass plaques with trimethyl chlorosilane was to obtain an inert surface with which the possibility of hydrogen bonding with the subsequent coating of BDO can be minimized. In the case where the trimethyl chlorosilane treated glass plaques were further rinsed with tetrahydrofuran, the possibility of any potential polar interactions between the unbonded trimethyl chlorosilane and the BDO was eliminated. In this fashion, the effect of increased interphase modulus due to excess BDO on the overall adhesion of the matrix can be studied. A comparison of the adhesion data between the

TABLE 5.11

Adhesion Values (Psi) of 1D Polyurethane to
Various Treated Glass Surfaces

Glass Treatments	Adhesion (Psi)
Bare Glass	2120 ± 530
Glass Coated with BDO	4980 ± 850
Glass Coated with Trimethyl Chlorosilane	2380 ± 550
Glass Coated with Trimethyl Chlorosilane and Rinsed	2870 ± 530
Glass Coated with Trimethyl Chlorosilane and Overcoated with BDO	1570 ± 400
Glass Coated with Trimethyl Chlorosilane and Rinsed and Overcoated with BDO	1780 ± 600

BDO coated glass plaques and the trimethyl chlorosilane/BDO coated glass plaques reveals that the adhesion value went down from 4980 psi to 1570 psi when the BDO layer was devoid of potential hydrogen bondings with the glass surface. Similar results were obtained from the glass plaques treated with trimethyl chlorosilane, rinsed and overcoated with BDO. This experiment suggests that hydrogen bonding between the excess butanediol in the interphase region and the glass surface is the prominent mechanism of adhesion for phase separated polyurethanes.

The suggested hydrogen bonding between BDO and the glass surface was further investigated using XPS. The air side of a soda-lime glass plaque was coated with a 2% (by weight) solution of BDO and was subjected to the polyurethane curing cycle (90°C for 24 hours). Afterwards, the glass plaque was rinsed several times with acetone to remove any unadsorbed BDO from the glass surface. A control sample was also subjected to the same procedure except for the BDO coating step. The curve fitted C1s spectra of the control sample and the BDO coated sample are shown in Figures 5.10a and 5.10b respectively. The bands at ~286.5 eV, associated with C-OH type species, indicate higher hydroxyl content (9.83%) on BDO treated sample as compared to the control sample (6.63%). This suggests that BDO can be adsorbed on the glass surfaces.

A schematic of the interphase region is shown in Figure 5.11 with some possible hydrogen bonding mechanisms. It is apparent that the majority of the hydrogen bonding is between the butanediol species which segregate to the polyurethane surfaces and the hydroxyl groups present on the glass surface. The hydrogen bonding in the interphase region can

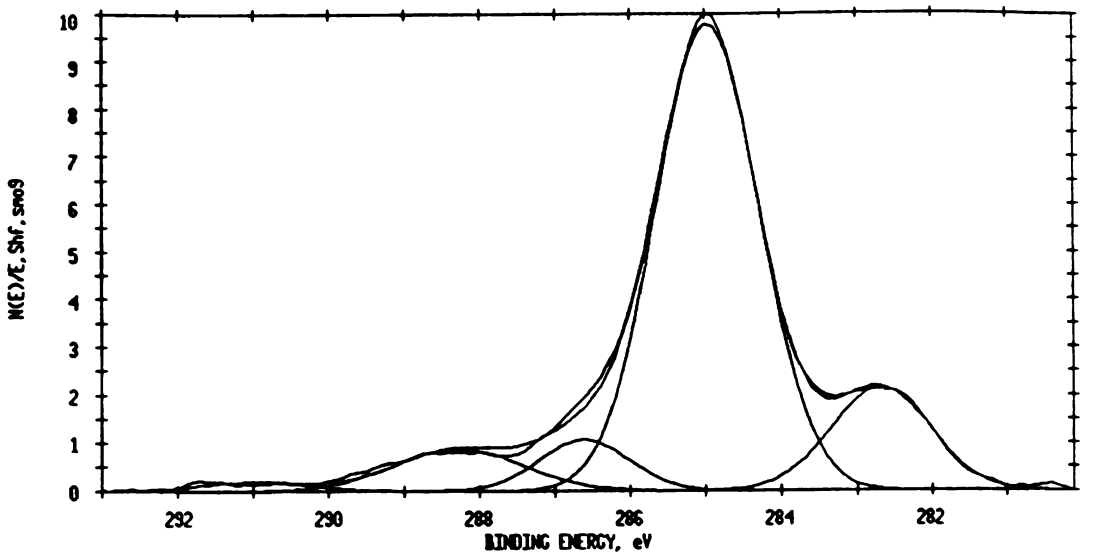

(a)

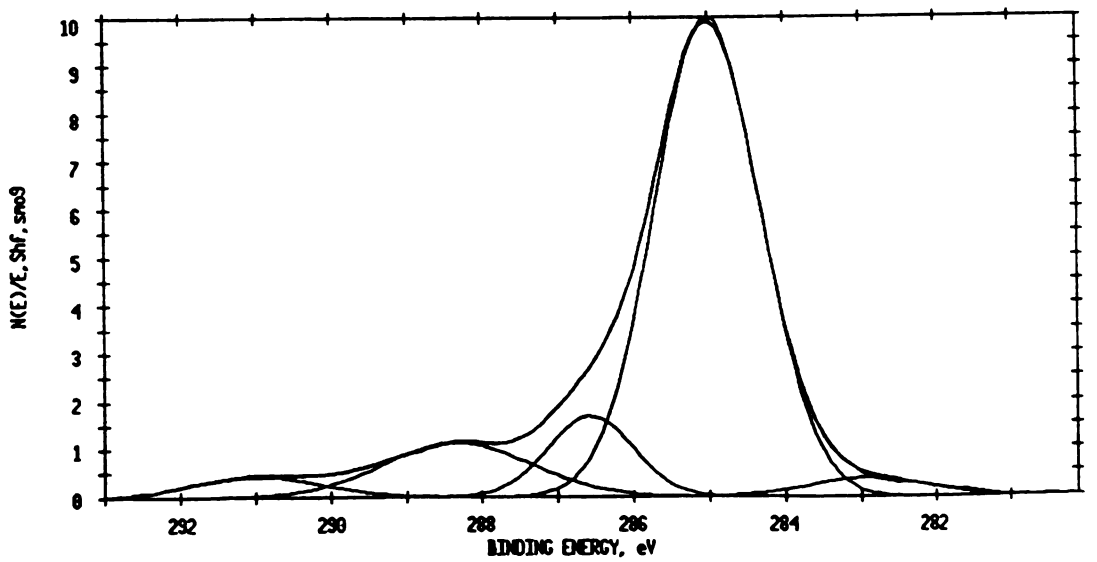

(b)

FIGURE 5.10 Curve Fitted C 1s Spectra of (a) Control Glass Sample (b) Glass Treated with BDO and Rinsed

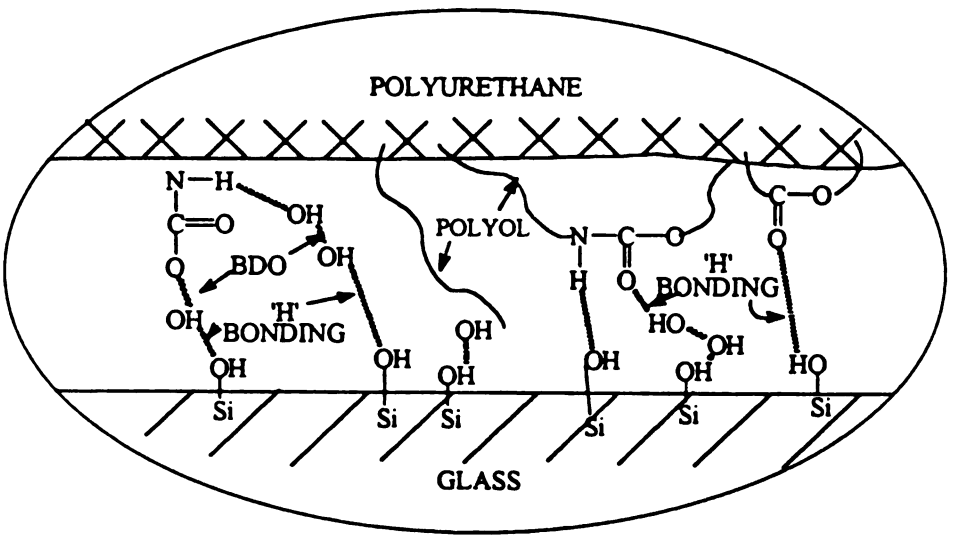

FIGURE 5.11 Schematic of Polyurethane/Glass Interphase Region with Probable Hydrogen Bonding Mechanisms

take place in numerous possible ways. One end of the butanediols can be hydrogen bonded to the $\begin{matrix}-N-\\ |\\ H\end{matrix}$ or $\begin{matrix}-C-\\ ||\\ O\end{matrix}$ linkages of the urethane groups and the other end can be hydrogen bonded with the glass surface hydroxyls. In another scenario, partially reacted butanediols will have free hydroxyl groups to hydrogen bond with the glass surface. The polyester functionalities of the polyols and also the unreacted free hydroxyl ends of the polyols can potentially hydrogen bond with the glass surface. Yet another mechanism can be the direct hydrogen bonding of the urethane groups to the glass surface either through the $\begin{matrix}-N-\\ |\\ H\end{matrix}$ or through the $\begin{matrix}-C-\\ ||\\ O\end{matrix}$ linkages of the urethane groups.

The preferential segregation of BDO at the interphase region observed in this study is not inconsistent with the previously reported studies. Hearn et al (Hearn et al, I, 1983) and Vargo et al (Vargo et al, 1991) have reported the enrichment of air/polyurethane interface in low molecular weight polyether based polyol components. The glass/polyurethane interphase of this study is expected to be different than the air/polyurethane interface studied by the above mentioned researchers. The high surface energy (56.77 dynes/cm) and especially the polar nature of the glass surface (γ^p = 37.59 dynes/cm) will have a significant influence on the interphase composition. This reasoning is further supported by the studies reported by Deng and Schreiber (Deng and Schreiber, 1991) discussing orientation phenomena at polyurethane surfaces in contact with different media.

5.6 CONCLUSIONS

In our previous studies (Agrawal and Drzal, I and II, 1994) we concluded that phase separation in polyurethanes significantly affects its adhesion to glass surfaces. It was

determined that the matrix phase separation influenced the composition and the thickness of the interphase region by causing a preferential segregation of high polar surface energy component to the interphase region. In the present study, the actual mechanism of adhesion between the interphase constituents and the glass surface was explored.

The contribution of chemical bonding in the form of covalent and ionic bonding on the overall glass/polyurethane adhesion was found to be not important. It was concluded that physical interactions are the most important factors in controlling glass/polyurethane adhesion. The polar surface free energy of the various polyurethanes correlated well with the XPS results regarding the BDO enrichment of the interphase regions in the phase separated polyurethanes. The work of adhesion calculated from the surface free energy components of the polyurethanes and the glass surface was found to be a poor predictor of the actual adhesion behavior. However, a linear relationship between the polar surface free energy and the observed adhesion values emphasized the role of polar interactions on the adhesion.

The modulus of the interphase region was found to be higher than that of the matrix due to the preferential segregation of butanediol at the interphase. This increase in modulus was determined not to be the factor for the superior adhesion performance demonstrated by the phase separated polyurethanes. It was concluded that the most important mechanism of adhesion between the polyurethanes and the glass surface of this study is through the formation of an interphase region in which hydrogen bonding between the butanediol rich interphase region and the hydroxylated glass surface plays a key role.

CHAPTER 6

CONCLUSIONS AND RECOMMENDATIONS

6.1 CONCLUSIONS

In this work, adhesion mechanisms of segmented polyurethanes to soda-lime float glass were investigated. The focus of the research was around the glass/polyurethane interphase region with emphasis on its structure/morphology, physical, mechanical, and chemical characterization to understand the underlying adhesion mechanisms. The model polyurethanes used in this study have allowed for the evaluation of phase separation, wide range of mechanical properties, different structure/morphology and varying surface energetics on their adhesion to glass surfaces, while keeping the urethane chemistry constant. This approach has simplified the experimentation and the interpretation of the results.

A model based on hard and soft segment miscibility was developed to predict phase separation in these polyurethanes. The model utilizes urethane chemistry/composition, polyol molecular weight and solubility parameter of the hard and soft segments to predict phase separation. The model predictions agreed well with the phase separation data obtained from the spectroscopic (NIR, FTIR), thermal (DSC, DMA), and mechanical (Iosipescu shear test, tensile test) characterizations.

It was found that phase separation in polyurethanes significantly affects adhesion to glass surfaces. Polyurethanes with higher modulus showed better adhesion, but among the

polyurethanes with the same modulus, phase separated samples showed better adhesion than the phase mixed samples.

SEM and XPS analyses of the fractured surfaces from the glass/polyurethanes adhesion tests revealed the formation of an interphase region, 20Å - 100Å in thickness, and a composition intermediate to that of the matrix and the glass. It was determined that matrix phase separation had significant influence on the composition, the thickness, and the mechanical properties of the interphase region. It was further determined that phase separation in the matrix along with the highly polar nature of the glass surface could cause preferential segregation of high polar surface energy component to the interphase region.

The modulus of the BDO rich interphase was found to be slightly higher than the corresponding stoichiometric composition polyurethane. However, this increased modulus interphase was found not to be contributing to the superior adhesion levels of the phase-separated polyurethanes. Through the use of unreactive silanes such as methyltrimethoxy silane and trimethyl chlorosilane on the glass surface, the role of covalent and ionic bonding between the polyurethane and the glass surface was investigated and was also found to be not important for the adhesion. It was concluded that polar interactions are the most important factors in controlling glass/polyurethane adhesion.

The polar surface free energy of the various polyurethanes correlated well with the XPS determined results regarding the BDO enrichment of the interphase regions. The work of

adhesion calculated from the surface free energy components of the polyurethanes and the glass surface was found to be a poor predictor of the actual adhesion behavior. However, a linear relationship between the polar surface free energy and the observed adhesion values further emphasized the importance of polar interactions for adhesion.

An adhesion experiment with BDO coated glass plaques demonstrated that adhesion of polyurethanes can be significantly improved by creating a "Beneficial" interphase rich in high polar surface free energy components. It was concluded that the most important mechanism of adhesion between the polyurethanes and the glass surface of this study is through the formation of an interphase region in which hydrogen bonding between the butanediol rich interphase region and the hydroxylated glass surface plays a key role.

6.2 RECOMMENDATIONS FOR FUTURE WORK

While the main objectives of this project have been met, still more work is needed to completely understand the adhesion mechanisms of polyurethanes in an actual reaction injection molding process. This work did not examine catalysts, which may play a very important role in the overall adhesion scheme by controlling reaction and phase separation kinetics.

The experimental work of this project can be extended to include other glass substrates such as glass fibers and glass mats. The majority of commercial glass fibers have some sort of sizing on them. The effects of sizing on the glass/polyurethane interphase region and on the overall adhesion add more complexity to the system and should be explored.

Only the thermoset polyurethane matrix was studied in this work. The experimental and theoretical work can be extended to include thermoplastic polyurethanes which generally have better phase separation than thermoset polyurethanes. Also, some of the polyurethane constituents can be tagged to study their preferential segregation to the surface or to the interphase region. Finally, the durability of the glass-polyurethane bond was not addressed in this study. The durability of these bonds in hot and humid environments has specific significance, especially in the automotive industry where these glass-polyurethane bonds must survive over a period of at least 10 years.

APPENDICES

APPENDIX A

GROUP CONTRIBUTIONS TO SOLUBILITY PARAMETER (δ_H) OF THE HARD SEGMENT BASED ON TOLUENE DIISOCYANATE AND BUTANEDIOL.

Groups	No.	$E_{cohesive}$ (J/mol) Bunn, (Van Krevelen, 1990)	$E_{cohesive}$ (J/mol) Fedor, (Van Krevelen, 1990)	Molar Attraction Constant, F Van Krevelen, (Van Krevelen, 1990)	Molor Volume (cm^3/mol) (Van Krevelen, 1990)
$-CH_3$	1	7120	4710	420	33.5
Phenyl (trisubstituted)	1	16340	31940	1377	33.4
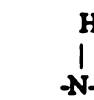	2	36620	26370	1483	18.5
$-CH_2-$	4	2850	4940	280	16.1
		ΣE_{Coh} = 108100	ΣE_{Coh} = 109150	ΣF = 5883	ΣV = 168.3

$$\delta_H = \left(\frac{E_{Coh}}{V} \right)^{1/2}$$

According to the group contribution approach,

$$\delta_H = \left(\frac{\Sigma E_{Coh}}{\Sigma V} \right)^{1/2}$$

$$\delta_{H_{Bonn}} = 25.34(J/cm_3)^{1/2} = 12.39(Cal/cm^3)^{1/2}$$

$$\delta_{H_{Fedor}} = 25.40(J/cm_3)^{1/2} = 12.45(Cal/cm^3)^{1/2}$$

According to Small's approach (26),

$$\delta_{H_{Vm}} = \frac{\rho \Sigma F}{M}$$, where M - molecular weight
ρ - specific gravity

For TDI/BDO based hard segment, M = 264, ρ = 1.1451 (based on stoichiometric calulation)

Thus,

$$\delta_{H_{Vm}} = 25.52(J/cm_3)^{1/2} = 12.47(Cal/cm^3)^{1/2}$$

Thus,

$$\delta_{H_{Avg}} = \left(\frac{\delta_{H_{Bonn}} + \delta_{H_{Fedor}} + \delta_{H_{Vm}}}{3} \right) = 12.44(Cal/cm^3)^{1/2}$$

APPENDIX B

SURFACE FREE ENERGY ESTIMATION OF THE HARD SEGMENT BY THE MOLAR PARACHORS AND THE COHESIVE ENERGY DENSITIES.

Groups	No.	P_s Sugden, (Van Krevelen, 1990)	V_w (cm^3/mol) Van der Waals Volume, (Van Krevelen, 1990)	$E_{cohesive}$ (J/mol) Fedor, (Van Krevelen, 1990)
$-CH_3$	1	56.1	13.67	4710
Phenyl (trisubstituted)	1	155.8	40.80	31940
H O | | -N-C-O-	2	94.4	18.0	26370
$-CH_2-$	4	39.0	10.23	4940
		$\Sigma P_s = 556.7$	$\Sigma V_w = 131.39$	$\Sigma E_{coh} = 109150$

$$\Sigma V = 1.6\Sigma V_w = 210.22 \text{ cm}^3/\text{mol}$$

According to the molar parachor approach,

$$\gamma_H = \left(\frac{\Sigma P_s}{\Sigma V} \right)^4$$

$$\gamma_H = \left(\frac{556.7}{210.22} \right)^4 = 49.2 \ dynes/cm$$

According to an empirical relationship between the cohesive energy density and the surface free energy,

$$\gamma_H \approx 0.75\ (e_{cohesive})^{\frac{1}{2}}$$

or

$$\gamma_H \approx 0.75 \left(\frac{\Sigma E_{cohesive}}{\Sigma V} \right)^{\frac{1}{2}} \quad (33)$$

$$\gamma_H \approx 0.75 \left(\frac{109150}{210.22} \right)^{\frac{1}{2}} = 48.5\ \textit{dynes/cm}$$

BIBLIOGRAPHY

BIBLIOGRAPHY

Agrawal, R.K., Agrawal, A., and Thomas, J., "Developments in Modular Windows for Automotive Applications", SAE Int. Cong. and Exp., Detroit, MI, Paper 910759, (1991).

Agrawal, R.K. and Drzal, L.T., "Adhesion Mechanisms of Polyurethanes to Glass Surfaces I. Structure - Property Relationship in Polyurethanes and Their Effects on Adhesion to Glass", accepted for publication in J. Adhesion, (1994).

Agrawal, R.K. and Drzal, L.T., "Adhesion Mechanisms of Polyurethanes to Glass Surfaces II. Phase Separation in Polyurethanes and Its Efects on Adhesion to Glass", submitted for publication in the J. Adhesion Science and Technology, (1994).

Agrawal, R.K., Fox, K.L., and Lynam, N.R., "Characterization of In-Mold Coatings on RIM Encapsulated Modular Windows", SAE Int. Cong. and Exp., Detroit, MI, (1991).

Benoit, H. and Hadziioannou, G., "Scattering Theory and Properties of Block Copolymers with Various Architectures in the Homogeneous Bulk State", Macromolecules, 21, 1449-1464, (1988).

Blackwell, J. and Gardner, K.H., "Structure of the Hard Segments in Polyurethane Elastomers", Polymer, 20, 13, (1979).

Bonart, R., Morbitzer, L. and Muller, E.H., "X-ray Inestigations Concerning the Physical Structure of Crosslinking in Urethane Elastomers. III. Common Structure Principles for Extensions with Aliphatic Diamines and Diols", J. Macromol. Sci., Phys., B9, 447, (1974).

Born, L., and Hespe, H., "Prediction of Polyurethane Hard Segment Structures Based on Diphenylmethane-Urethane Model Compounds", Colloid and Polmer Sci., 263, 335, (1985).

Brandrup, J. and Immergut, E.H., "Polymer Handbook", John Wiley & Sons, (1989).

Broutman, L.J., "Measurement of the Fiber-Polymer Matrix Interfacial Strength", Interfacaes in Composites, ASTM Special Technical Publication 452, American Society for Testing and Materials (1969).

Byrne, C.A., Mead, J.L., and Desper, C.R., "Structure-Property Relationships of Aliphatic Polyurethane Elastomers Prepared from CHDI", Advances in Urethane Science and Tech., Vol. 11, 68-109, Technomic Publication, Lancaster, PA, (1992).

Camargo, R.E., Macosko, C.W., Tirrell, M., and Wellinghoff, S.T., "Experimental Studies of Phase Separation in Reaction Injection Molded (RIM) Polyurethanes", Polymer Engineering and Science, Vol. 22, No. 11, (1982).

Camargo, R.E., Macosko, C.W., Tirrell, M., and Wellinghoff, S.T., "Phase Separation Studies in RIM Polyurethanes: Catalyst and Hard Segment Crystallinity Effects", Polymer, 26, 1145-1154, (1985).

Camberlin, Y. and Pascault, J.P., "Phase Segregation Kinetics in Segmented Linear Polyurethanes: Relations between Equilibrium Time and Chain Mobility and between Equilibrium Degree of Segregation and Interaction Parameter", J. Polymer Science: Polymer Physics Edition, Vol. 22, 1835-1844, (1984).

Camberlin, Y. and Pascault, J.P., "Quantitative DSC Evaluation of Phase Segregation Rate in Linear Segmented Polyurethanes and Polyurethaneureas", J. Polymer Science: Polymer Chemistry Edition, Vol. 21, 415-423, (1983).

Carleton, C.S., Waszeciak, D.P., and Alberino, L.M., "A RIM Process for Reinforced Plastics", Session 9-D, Proc. of Reinforced Plastics/Composites Inst., Soc. Plast. Ind., Atlanta, (1986).

Chang, A.L., "Processing-Marphology-Property Relationships of Polyurethanes", Ph.D. Thesis, Univ. of Minnesota, (1984).

Chang, A.L., Briber, R.M., Thomas, E.L., Zdrahala, R.J., and Critchfield, F.E., "Morphology Study of the Structure Developed During the Polymerization of a Series of Segmented Polyurethanes", Polym, 23, 1060-1065, 1982).

Chen, J.H. and Rukenstein, E., "Solvent-Stimulated Surface Rearrangement of Polyurethanes", J. Colloid Interface Sci. 135, 496, (1990).

Chen, W.P., Frisch, K.C., and Wong, S.W., "The Effect of Soft Segment on the Morphology of Polyurethane Elastomers", Advances in Urethane Science and Tech., Vol. 11, 110-136, Technomic Publication, Lancaster, PA, (1992).

Chen, Z.S., Yang, W.P., and Macosko, C.W., "Polyurea Synthesis and Properties as a Function of Hard Segment Content", Rubber Chem. and Tech., 61, 86-99, (1987).

Chiang, C.H., Ishida, H., and Koenig, J.L., "The Structure of .Gamma.-Aminopropyltriethoxysilane on Glass Surfaces", Journal of Colloid and Interface Science, Vol. 74, 396 (1980).

Cornell, M.C., Turner, R.B., and Morgan, R.E., "Amine Modified Polyol for RIM Systems", Proceed. SPI 26th Ann., (1984).

Damani, S.G. and Lee, L.J., "The Resin-Fiber Interface in Polyurethane and Polyurethane-Unsaturated Polyester Hybrid", Polymer Composites, Vol. 11, No. 3, 174-183 (1990).

Dawson, J.R. and Shortall, J.B., "The Impact Behaviour of RRIM Polyurethane Elastomers", Cellular Polymers 1, 41-51, (1982).

Deng, Z. and Schreiber, H.P., "Orientation Phenomena at Polyurethane Surfaces", J. Adhesion, Vol. 36, pp. 71-82, (1991).

Drown, E.K., Moussawi, H.A., and Drzal, L.T., "Glass Fiber Sizings and Their Role in Fiber-Matrix Adhesion", J. Adhesion Sci. Technol., Vol. 5, No. 10, 865-881 (1991).

Eberhardt, J.G., Journal of Physical Chemistry, 70, 1183, (1966).

Eckles, J.H. and Wilkinson, T.C., "Composite Manufacturing Using the Reaction Injection Molding Process", Session 9-B, Proc. of Reinforced Plastics/Composites Inst., Soc. Plast. Ind., Atlanta, (1986).

Estes, G.M. and Cooper, S.L., "Block Copolymers and Related Heterophase Elastomers", J. Macromol. Sci.-Revs. Macromol. Chem., C4 (2), 313-366, (1970).

Fielder, J.K. and Carswell, R., "Polyurethane RIM Systems for Automotive Modular Windows", SAE Int. Cong. and Exp., Detroit, MI, Paper 900515, (1990).

Fowkes, F.M., "Treatise on Adhesion and Cohesion", Vol. 1, Patrick, R.L., Ed., Marcel Dekker, p. 352, (1967).

Fowkes, F.M., Dwight, D.W., and Cole, D.A., "Acid-Base Properties of Glass Surfaces", J. Non-Crystalline Solids 120, 47-60, (1990).

Galla, E.A., Mascioli, R.L., and Bechara, I.S., "RIM Catalysis and Coating Interaction", Proceed. SPI 26th Ann. Tech. Conf., 24-31, (1981).

Galli, E., "Surface Modification for RRIM Urethanes", Plastic Compounding, January, 21-28 (1982).

Garbassi, F., Occhiello, E., Bastioli, C. and Romano, G., "A Qualitative and Quantitative Assessment of the Bonding of 3-Methacryloxypropyltrimethoxysilane to Filler Surfaces Using XPS and SSIMS (FABMS) Techniques", Journal of Colloid and Interface Science, Vol. 117, No. 1 (1987).

Garton, A., "Infrared Spectroscopy of Polymer Blends, Composites and Surfaces", Hanser Publishers, (1992).

Geer, R.P., "Poly (dicyclopentadiene): A New RIM Thermoset", Proceed, Soc. Plast. Eng., National Techn. Conf., Detroit, MI, (1983).

Gilli, Ed, "Surface Modifications of RRIM Urethanes", Plastics Compounding, 21-28, (1982).

Gillis, H.R., Hurst, A.T., Ferrarini, L.J., and Watts, A., "Liquid MDI Isocyanates: Effects of Structure on Properties of Derived Polyurethane Elastomers", SPI Polyurethane Div., 6th Intern. Tech./Marketing Conf., 375-380, (1983).

Gonzalez, V.M. and Macosko, C.W., "Properties of Mat Reinforced Reaction Injection Molded Materials", Polym. Comp. 4, 190-195, (1983).

Good, R.J., "Treatise on Adhesion and Cohesion", Vol. 1, Chapter 2, Patrick, R.L., Ed., Marcel Dekker, (1967).

Hearn, M.J., Ratner, B.D., and Briggs, D., "SIMS and XPS Studies of Polyurethane Surfaces 1. Preliminary Studies", Macromolecules, 21, 2950-2959, (1988).

Hearn, M.J., Briggs, D., Yoon, S.C., and Ratner, B.D., "SIMS and XPS Studies of Polyurethane Surfaces, 2. Polyurethanes with Fluorinated Chain Extenders", Macromolecules, 21, 2950-2959, (1988).

Hedrick, R.M., Gabbert, J.D., and Wohl, M.H., "Nylon 6 RIM", in Reaction Injectin Molding, Editor Kresta, J.E., Am. Chem. Soc. Symp. Series 270, Washington, D.C., Chapter 10, (1985).

Hepburn, C., "Polyurethane Elastomers", Elsevier Science Publication, New York, NY, (1992).

Ho, H., Tsai, M., Morton, J., and Farley, G.L., "An Experimental Procedure for the Iosipescu Composite Specimen Tested in the Modified Wyoming Fixture", J. Composites Technology and Research, 15, 1, 52-58, (1993).

Kaelble, D.H., "Physical Chemistry of Adhesion", John Wiley & Sons, (1971).

Kaelble, D.H. and Uy, K.C., "Reinterpretation of Organic Liquid-Polytetrafluoroethylene Surface Interactions", J. Adhesion, 2, 50, (1970).

Kau, C., Hiltner, A., Baer, E., and Huber, L., "Damage processes in Reinforced Reaction Injection Molded Polyurethanes", J. of Reinforced Plastics and Composites, Vol. 8, 18-39, (1989).

Kinloch, A.J., "Adhesion and Adhesives", Chapman and Hall, (1987).

Koenig, J.L. and Shih, P.T.K., "Raman Studies of the Glass Fiber-Silane-Resin Interface", Journal of Colloid and Interface Science, Vol. 36, 247 (1971).

Lassas, A., Fagerholm, L.E., Stenlund, B.G. and Nasman, J.H., "Modification of E Glass Fiber Surfaces with Polyacrylic Acid Polymers From an Aqueous Solution", Polymer Composites, Vol. 14, No. 1, (1993).

Legge, N.R., Holden, G. and Schroeder, H.E., "Thermoplastic Elastomers", Hanser Publishers, pp. 22, (1987).

Macosko, C.W., "Fundamentals of Reaction Injection Molding", Hanser Publishers, New York, NY, (1988).

Markus, S. and Priel, Z., "Chemical Bonding Between Aromatic Molecules and Glass Surfaces", Journal of Colloid and Interface Science, Vol. 82, No. 1 (1981).

Markus, S. and Priel, Z., "Chemical Bonding Between Molecules and Glass Surfaces", J. of Colloid and Interface Science, Vol. 82, No. 1, (1981).

McGarry, F.J. and Fyiwara, M., Modern Plastics, 45, 143, (1968).

McWilliams, D.E., Killmeyer, C.W., and Eilerman, G.E., "Glass Fiber Size of Curable Blocked Polyurethane Emulsion with Amino Silane", U.S. Patent 3,803,069 (1974).

Miller, C.E., "Near-Infrared Spectroscopy of Synthetic Polymers", Applied Spectroscopy Reviews, 26 (4), 277-339, (1991).

Miller, C.E., Edelman, P.G., Ratner, B.D. and Eichinger, B.E., "Near-Infrared Spectroscopic Analyses of Poly (ether urethane urea) Block Copolymers. Part I. Bulk Composition", Applied Spectroscopy, Vol. 44, No. 4, (1990).

Miller, C.E., Edelman, P.G., Ratner, B.D. and Eichinger, B.E., "Near-Infrared Spectroscopic Analyses of Poly (ether urethane urea) Block Copolymers. Part II. Phase Separation", Applied Spectroscopy, Vol. 44, No. 4, (1990).

Mohai, M., Bertoti, I. and Revesz, M., "XPS Study of the State of Oxygen on a Chemically Treated Glass Surface", Surface and Interface Analysis, Vol. 15, pp. 364-368, (1990).

Oertel, G., "Polyurethane Handbook", Hanser Publishers, (1993).

Otaigbe, J.U., "Effect of Coupling Agent and Absorbed Moisture on the Tensile Properties of a Thermoplastic RRIM Composite", Journal of Applied Polymer Science, Vol. 45, 1213-1221 (1992).

Owens, D.K. and Wendt, R.C., "Estimation of the Surface Free Energy of Polymers", Journal of Applied Polymer Science, 13, 1740, (1969).

Pannone, M.C. and Macosko, "Reaction Kinetics of a Polyurea Reaction Injection Molding System", Polym. Eng. and Sci., 28, 660-669, (1988).

Pantano, C.G., "Surface and In-Depth Analysis of Glass and Ceramics", Ceramic Bulletin, Vol. 60, No. 11, (1981).

Plueddemann, E.P., "Silane Coupling Agents", Plenum Press, (1982).

Rao, V. and Drzal, L.T., "The Dependence of Interfacial Shear Strength on Matrix and Interphase Properties", Polymer Composites, Vol. 12, No. 1, 48-56, (1991).

Rao, V. and Drzal, L.T., "The Temperature Dependence of Interfacial Shear Strength for Various Polymeric Matrices Reinforced with Carbon Fibers", J. Adhesion, Vol. 37, 83-95, (1992).

Reilly, Albert F. and Sanok, John L., "Method and Apparatus for Making Molded Window Gasket", U.S. Patent 4,755,339, (1988).

Ryan, A.J., Stanford, J.L., and Still, R.H., "Calculation of Solubility Parameters of Typical Structural Units Present in Segmented Polyurethanes, Poly (urethane ureas) and Polyureas Formed by Reaction Injection Moulding", Polymer Communications, Vol. 29, (1988).

Saunders, J.H. and Frisch, K.C., "Polyurethanes Chemistry and Technology, Part 1", John Wiley and Sons Inc, (1983).

Schneider, N.S., Desper, C.R., Illinger, J.L., King, A.O., and Barr, D., "Structural Studies of Crystalline MDI-Based Polyurethanes", J. Macromol. Sci-Phys., B11 (4), 527-552, (1975).

Schultz, J., Tsutsumi, K. and Donnet, J.B., "Surface Properties of High-Energy Solids. II. Determination of the Nondispersive Component of the Surface Free Energy of Mica and Its Energy of Adhesion to Polar Liquids", J. Colloidal Interfacial Science, 59, 277, (1977).

Schwarz, E.G., Critchfield, F.E., Tackett, L.P., and Tarin, P.M., "Silane Effects and Machine Processing in Reinforced High Modulus RIM Urethanea Composites", Journal of Elastomers and Plastics, Vol 11, p. 280, (1979).

Sengupta, A. and Schreiber, H.P., "Surface Characteristics of Polyurethane Adhesive Formulations", J. Adhesion Science and Technology, Vol. 5, No. 11, pp. 947-957, (1991).

Speckhard, T.A. and Cooper, S.L., "Ultimate Tensile Properties of Segmented Polyurethane Elastomers: Factors Leading to Reduced Properties for Polyurethantes Based on Nonpolar Soft Segments", Rubber Chem. and Tech., 59, 405-431, (1986).

Sugden, S., J. Chem. Soc., 125, 1177, (1924).

Trivosono, N.M., Lee, L.H., and Schriner, S.M., Ind. Eng. Chem. 50, 912 (1958).

Uhlmann, D.R. and Kreidl, N.J., "Glass: Science and Technology", Vol. 1, Academic Press, (1983).

Van Krevelen, D.W., "Properties of Polymers", Elsevier Science Publishers, 3rd Ed., (1990).

Vargo, T.G., Hook, D.J., Gardella Jr., J.A., Eberhardt, M.A., Meyer, A.E., and Baier, R.E., "A Surface Spectroscopic and Wettability Study of a Segmented Block Copolymer Poly (ether urethane)", Applied Spectroscopy, Vol. 45, No. 3, (1991).

Vaughan, D.J. and Peek Jr., R.C., "The Use of ESCA in the Study of the Surface Chemistry of Commercial Glass Fibers", The Society of Plastics Industry, Inc., 29th Annual Tech. Conf., The Society of Plastics Industry, Sec. 13-D, 1-4 (1974).

Westley, S.A., "Some Recent Developments in Bonding RIM Urethane Automotive Modular Glass", SAE Int. Cong. and Exp., Detroit, MI, (1991).

Wongkamolsesh, K. and Kresta, J.E., "Organotin Catalysis in Urethane Systems", Reaction Injection Molding - Poly. Chem. and Eng., Editor Kresta, J.E., 111-133, (1985).

Yang, P.C. and Lee, W.M., "Fracture Mechanism Study of Flake Glass Filled RIM Urethane Systems", J. of Elastomers and Plastics, Vol. 19, 120-146, (1987).

Yoon, S.C. and Ratner, B.D., "Surface Structure of Segmented Poly (Ether Urethanes) and Poly (Ether Urethane Ureas) with Various Perfluoro Chain Extenders. An X-ray Photoelectron Spectroscopic Investigation", Macromol., 19, 1068, (1986).

Yoon, S.C. and Ratner, B.D., "Surface and Bulk Structure of Segmented Poly (ether urethanes) with Perfluoro Chain Extenders. 2. FTIR, DSC, and X-ray Photoelectron Spectroscopic Studies", Macromol., 21, 2392-2400, (1988).

Zdrahala, R.J., Gerkin, R.M., Hager, S.L., and Critchfield, F.E., "Polyether-Based Thermoplastic Polyurethanes. I. Effect of the Hard-Segment Content", J. Applied Polymer Science, 24, 2041-2050 (1979).

Zisman, W.A., "Relation of the Equilibrium Contact Angle to Liquid and Solid Constitution", Contact Angle, Wettability and Adhesion, Advances in Chemistry Symposium Series 43, Gould, R.F., Ed., ACS, (1964).